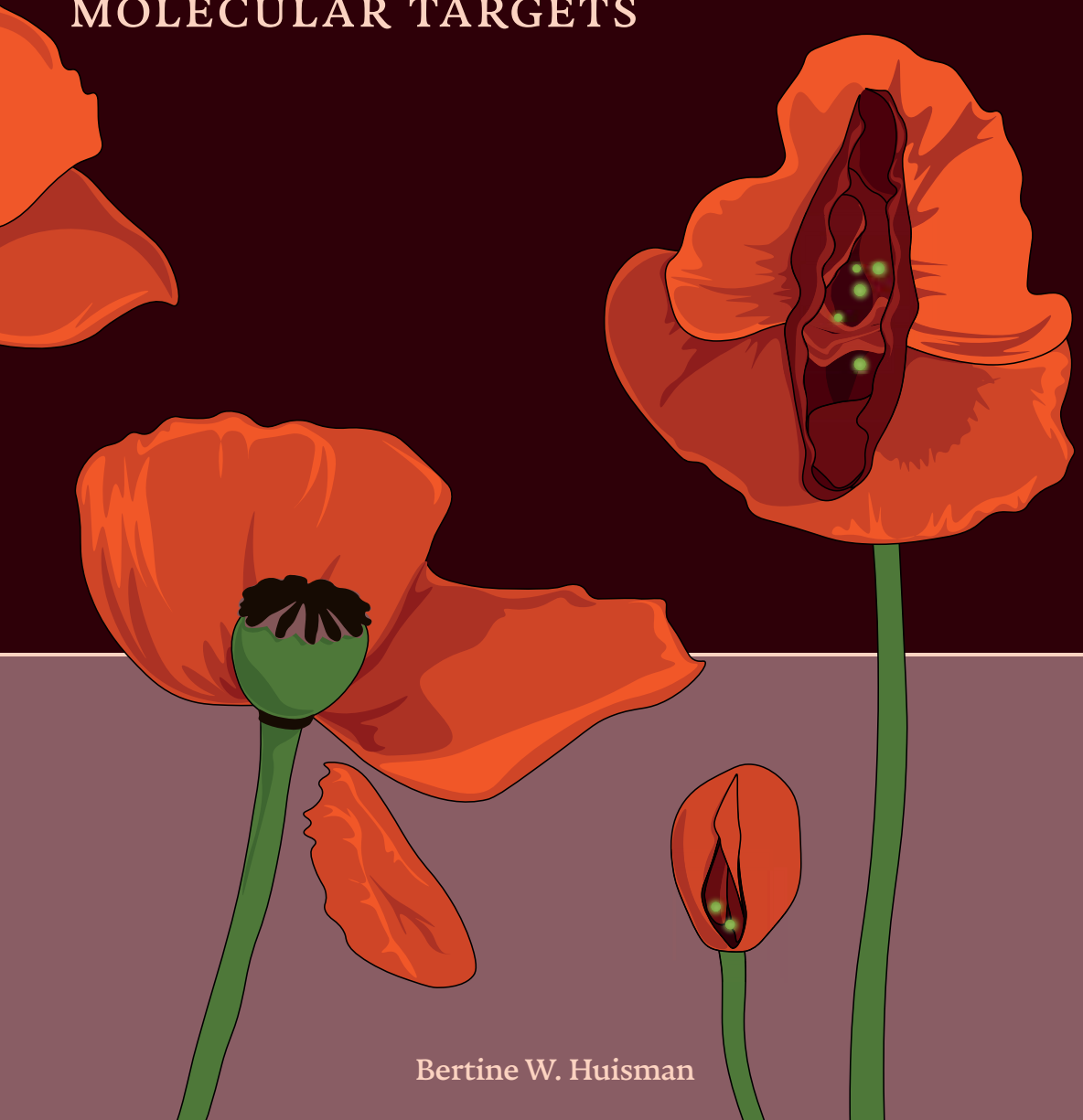


CHARACTERIZATION OF VULVAR DISEASES

NOVEL IMAGING TOOLS, MODELS AND MOLECULAR TARGETS



Bertine W. Huisman

CHARACTERIZATION OF VULVAR DISEASES
NOVEL IMAGING TOOLS, MODELS AND MOLECULAR TARGETS

**CHARACTERIZATION
OF VULVAR DISEASES**
*NOVEL IMAGING TOOLS, MODELS
AND MOLECULAR TARGETS*

Proefschrift

ter verkrijging van
de graad van doctor aan de Universiteit Leiden,
op gezag van rector magnificus prof.dr.ir. H. Bijl,
volgens besluit van het college voor promoties
te verdedigen op donderdag 20 april 2023
klokke 10:00 uur

door

Bertha Woutrina de Glint-Huisman
Geboren te Ermelo
in 1992

© Bertine de Glint-Huisman

Design: Caroline Lint, Den Haag (caro@delint.nl)

Cover image: Jette Smedema (ja@smedema.pro)

*All rights reserved. No part from this thesis may be reproduced, distributed
or transmitted in any form or by any means, without prior written permission
of the author.*

Publication of this thesis was financially supported by the foundation
Centre for Human Drug Research (CHDR), Leiden, the Netherlands

PROMOTOR

Prof. dr. J. Burggraaf

CO-PROMOTORES

Dr. M.I.E. van Poelgeest

Dr. C.F.M. Sier

LEDEN PROMOTIECOMMISSIE

Prof. Dr. V.T.H.B.M. Smit

Prof. Dr. E.H.J. van den Bogaard (*Radboud Universitair Medisch Centrum*)

Prof. Dr. R.G.H. Beets-Tan (*Antoni v Leeuwenhoek, Nederlands Kanker Instituut*)

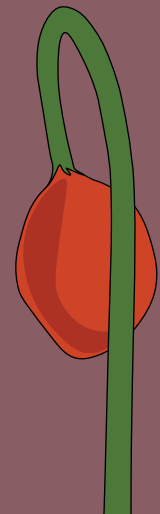
dr. A. I. Vahrmeijer

	I	General introduction and thesis outline	7
SECTION I		NON-INVASIVE CLINICAL TOOLS TO DISCOVER VULVAR SKIN BIOMARKERS	
	II	Dermatoscopy and dynamic optical coherence tomography in vulvar HSIL and lichen sclerosus: a prospective feasibility study	25
	III	Reflectance confocal microscopy as a non-invasive imaging tool in vulvar high grade squamous intraepithelial lesions and lichen sclerosus: a descriptive morphological study in patients and healthy volunteers	43
SECTION II		DEVELOPMENT OF HEALTHY AND DISEASED IN VITRO VULVAR MODELS	
	IV	Development of healthy and tumorous vulvar organotypic 3D models as a novel tool to study tumour-stroma interaction and assist nonclinical drug evaluation	65
SECTION III		MOLECULAR TARGET IDENTIFICATION OF VULVAR CARCINOMAS	
	V	Potential targets for tumor-specific imaging of vulvar squamous cell carcinoma: a systematic review of candidate biomarkers	89
	VI	Integrin $\alpha v \beta 6$ as a target for tumor-specific imaging of vulvar squamous cell carcinoma and adjacent premalignant lesions	111
	VII	General Discussion	137
APPENDICES		Nederlandse Samenvatting	151
		Curriculum Vitae	165
		Publication list	166

CHAPTER 1

General introduction and thesis outline

All mentioned supplementary figures and tables in this thesis can be found on their corresponding websites (see chapter-references).



Vulvar cancer is a rare gynecological malignancy with a tremendous disease burden. Vulvar squamous cell carcinoma (vSCC) is the most common histologic type of vulvar cancer and constitutes 80–90% of all vulvar cancers.^{1–4} Other histological subtypes include melanoma, basal cell carcinoma, Bartholin gland adenocarcinoma, sarcoma, and Paget disease.⁵ The cornerstone of treatment for vSCC consists of surgery with or without radiochemotherapy. In addition, precursors of vSCC often require surgical or medical intervention as well.⁶ Treatment of vulvar (pre)malignancies is a challenging balance act, as on the one hand clearance of all lesions is desired, while on the other hand normal vulvar anatomy and function must be preserved as best as possible. Utilizing the current treatment interventions, recurrence occurs in up to 40% of vSCC patients and no major improvements in 5-year survival rates were observed in the last decades.^{1,7,8} Additionally, most treatments are accompanied by bothersome side-effects such as disfigurement, sexual dysfunction, and psychological problems in more than half of the patients.^{9,10} This is partly caused by the difficulty to recognize vulvar (pre)malignant lesions for the medical specialist, either macroscopically or pathologically.^{11,12} This highlights the high unmet medical need for preferably non-invasive and accurate diagnostics for vulvar (pre)malignancies. Further, effective therapies are needed with a favorable safety profile that encompass complete reduction of the affected tissue. Therefore, the aim of this thesis has been to search for disease-specific biomarkers to improve the clinical management of vulvar (pre)malignancies. This first chapter of this thesis summarizes the pathophysiology and current treatments of vulvar (pre)malignancies. In the subsequent chapters, the multimodal profiling approach to evaluate novel techniques for diagnosis and treatment evaluation of the affected vulvar area is introduced. Finally, the aims and outlines of this thesis are discussed.

PATHOPHYSIOLOGY AND CURRENT TREATMENTS OF VULVAR (PRE)MALIGNANCIES

The vulva is the outer female genital. The vulvar area is bordered by the mons pubis, the groins and the anus. It includes the clitoris, urethral meatus, labia majora and minora and the introitus of the vagina (Figure 1).¹³ The vulva is important in many aspects of female life, as the entrance to the interval environment via the vagina, for urinating, sexual functioning and childbearing. Unfortunately, several diseases can occur in this area which may affect all these different domains of vulvar functioning.¹⁴

The studies included in this thesis are focusing on four diseases of the vulva

- vulvar squamous cell carcinoma (vSCC)¹⁴;
- precursors vulvar intraepithelial neoplasia (VIN) consisting of
 - a. vulvar high grade squamous intraepithelial lesion (vHSIL)
 - b. differentiated vulvar intraepithelial lesion (dVIN)¹⁵;
- genital lichen sclerosus (LS)¹⁶ (Table 1).

Table 1 Key characteristics of vulvar (pre)malignancies.

	vSCC ^{1,2}	vHSIL ^{15,17}	dVIN ^{15,17}	LS ^{16,18,19}
Incidence	2.6 : 100.000	3.3 : 100.000	0.08 : 100.000	10-20 : 100.000
Gradation	malignant	pre-malignant	pre-malignant	benign
Relative proportion of VIN-	-	95%	5%	-
Risk of malignant progression	-	9% (if treated)	33-86%	3-6%
Time to progression	-	41 months	9-23 months	unknown
Current treatment(s)	surgical excision, adjuvant (chemo) radiotherapy	surgical excision, ablative therapy and topical treatment	surgical excision	topical corticosteroids
Average age at diagnosis	68 years	30-50 years	60-80 years	69 years
Etiology	HPV infection/ unknown, TP-53 mutation early observed	HPV infection	unknown, TP-53 mutation early observed	unknown, an overactive immune system or an imbalance of hormones may play a role
Recurrence	up to 40%	common	13-32 months, less common	NA

vSCC=vulvar squamous cell carcinoma, vHSIL=vulvar high grade squamous intraepithelial lesion, dVIN=differentiated vulvar intraepithelial lesion, HPV=human papilloma virus, NA=not applicable

VULVAR SQUAMOUS CELL CARCINOMA Vulvar cancer is rare with an incidence of 2.6 per 100,000 women per year and only accounts for an estimated 0.4% of all cancers and 5% of gynecologic cancers.¹ As mentioned, of all vulvar cancer types, vSCC is the most common histologic type and focus of this thesis is on this subgroup. The average age at diagnosis is 68 years for vSCC patients. Remarkably, especially in younger women the incidence is rising.^{7,21} There are two different pathophysiological pathways for vSCC: (I) an human papilloma virus (HPV)-independent type, accounting for 70% of all vSCC's, which is frequently associated with LS and/or dVIN and therefore mostly observed in older women and (II) a HPV-dependent type, accounting for 30% of all vSCC's, which is often associated with vHSIL and occurs mostly

in younger women.^{16,22-25} Surgery with or without adjuvant (chemo)radiotherapy is the cornerstone of treatment for vSCC.^{26,27} Positive surgical margins are associated with high local recurrence rates up to 40% and a corresponding poor 5-year survival of 25-50%.^{28,29} In addition, difficult to identify precursor lesions as vHSIL and dVIN are often found adjacent to the tumor. Incomplete resection of these lesions may contribute to earlier recurrence of disease.³⁰

VULVAR INTRA-EPITHELIAL NEOPLASIAS: vHSIL AND dVIN Vulvar intra-epithelial neoplasias are etiologically categorized into a HPV-dependent and HPV-independent variant (vHSIL and dVIN respectively).²⁵ 95% of all VIN cases concern vHSIL.¹⁶ Both premalignant conditions have a distinct etiology and pathways towards vSCC.²³ vHSIL is caused by a persistent high-risk HPV infection, which in 90% of cases is identified as HPV 16. These HPV-dependent lesions are more frequently observed in premenopausal patients. vHSIL lesions are typically multifocal, can appear as a visible lesion and/or a palpable abnormality and diagnosis is confirmed by histological review of a lesional biopsy. Microscopic characteristics include loss of maturation of the squamous epithelium. This phenomenon is mainly observed in the middle and upper third layer of the epithelium to full thickness (formerly termed VIN 2 or 3). If minimized to basal atypia, the lesion is classified as vulvar low-grade squamous intraepithelial lesion (vLSIL, formerly termed VIN 1). vHSIL is subdivided in a basaloid and warty subtype, based on the morphologic and histologic features.⁶ The main goals for treatment are to prevent progression towards vSCC and to relieve symptoms. The risk of malignant transformation in untreated vHSIL is estimated to be as high as 9%.^{16,31} Symptoms include vulvar pruritis, pain and dyspareunia which lead to a substantial burden for the patient. Currently the choice of treatment for vHSIL depends on the level of invasiveness, prior treatments, and the location of the lesion(s).^{11,32} Treatment options include surgical excision, ablative therapy and topical pharmacological treatment with e.g. imiquimod.^{32,33} The pathogenesis of dVIN is less understood compared to vHSIL and mostly observed in postmenopausal women. dVIN is usually found as an unifocal and unicentric lesion developed in the background of lichen sclerosis or adjacent to vSCC. Lesions appear generally as grey-white discolorations with a rough surface, elevated nodules or white plaques. Identification is difficult due to lack of accurate and reproducible diagnostic criteria.³⁴ If left untreated, dVIN

has a high absolute risk of 33-86% malignant progression.¹² As a result, dVIN is rarely identified in advance of a diagnosis of invasive malignancy, despite being the precursor lesion of approximately 80% of vSCC's.³⁵ Symptoms of dVIN are similar as described for vHSIL. Primary treatment for dVIN patients consists of surgical excision.

LICHEN SCLEROSUS LS is a chronic, progressive, mutilating disease with a high impact on quality of life. It occurs mainly (85-98 % of all cases) in the anogenital region but can theoretically develop on any skin surface. Severe cases of vulvar LS can show scarring and narrowing of the vaginal introitus, along with disappearance of the labia minora and clitoris. This is all accompanied by severe itch and pain independent of disease severity. The cause of LS is unknown.¹⁷ A genetic and autoimmune role has been suggested, as up to 12% of the patients report LS in their family history.³⁶ Histologically, LS is characterized by marked inflammation and epithelial thinning. LS treatment comprises of patient education and life-long intermittent ultrapotent topical corticosteroid application.³⁵ Disadvantages of this treatment consist of a burning or irritated sensation of the vulva. And if continuously applied, atrophy of the skin can occur, further worsening the effects of epithelial thinning. Daily use of topical emollients may help to relief symptoms or be used as vaginal lubricant for dyspareunia.¹⁷ The risk of development of vSCC in patients with LS is up to 5 percent.^{17,37} There is prospective evidence that proactive management of LS may lead to a reduction in risk of the development of squamous cell carcinoma.³⁸

MULTIMODAL CHARACTERIZATION WITH BIOMARKERS FOR VULVAR HEALTHY AND DISEASED SKIN

At present, identification of vSCC, vHSIL, dVIN and LS is mainly based on visual and tactile skills of the medical specialist. No universal objective clinical scoring systems are present to guide these diagnostics. The current 'golden standard' used for confirmation of clinically suspected vulvar tissue is by histological examination of a biopsy. However, biopsies are invasive and uncomfortable. In addition, when dVIN is suspected, it is sometimes difficult to demonstrate the presence or absence of dysplasia. The difficulties faced during this convoluted diagnostic process can lead to delayed or incorrect vulvar tissue classification.^{15,39} Accompanying consequences are re-excisions, local recurrences, regional metastases and associated

worse prognosis. Altogether a decreased quality of life often ensues patients with vulvar diseases. This underlines the high unmet medical need to preferably non-invasively and real-time discriminate vulvar abnormalities and improve therapeutic options. Disease specific biomarkers could aid for those needs. Biomarkers are quantifiable measurements of a biological process that can contribute to diagnosis, prognosis and therapy of diseases.⁴⁰ A valuable biomarker discriminates correctly normal and pathological conditions and/or the pharmaceutical response to a therapeutic intervention.^{41,42}

A multimodal approach has been applied within this thesis to identify novel biomarkers and methods for vulvar disease characterization. The multimodal research approach included different domains: imaging, molecular and cellular complemented by patient reported outcomes and physician-based input. (Figure 2). The focus of this thesis was specifically on the molecular and imaging domains. The composition of this approach is based on the most important aspects of the blueprint for early phase clinical pharmacology studies in the field of clinical pharmacodermatology.^{43,44} With this multimodal approach we aim to obtain a more complete patient profile regarding vulvar skin disease.

The following principles of this multimodal approach are described below in more detail:

- **Non-invasive clinical tools to discover vulvar biomarkers**, focusing on discrimination of aberrant vulvar tissue (Figure 1, all domains except drug development);
- **Development of healthy and diseased *in vitro* vulvar models**, to increase pathophysiologic knowledge and improve drug development (Figure 1, cellular domain);
- **Molecular target identification of vulvar carcinomas**, to guide staging and surgery with real time optical imaging (Figure 1, molecular and imaging domain).

SECTION I NON-INVASIVE CLINICAL TOOLS TO DISCOVER VULVAR SKIN BIOMARKERS

In the field of clinical (pharmaco)dermatology several non-invasive imaging tools are successfully applied to detect cutaneous biomarkers.^{43,44} These biomarkers could potentially be translated to vulvar skin research.

Therefore, discriminatory properties of several imaging tools are examined on the vulvar area in a clinical trial. Lesional tissue of vulvar HSIL and LS patients was compared to vulvar skin of healthy controls using the techniques described below.

A *dermatoscope* is used as an imaging tool to better visualize subsurface structures and identify patterns that help improve diagnostics for a wide range of dermatologic skin diseases.⁴⁶ The dermatoscope is a handheld device that functions as a magnifier and is routinely applied by dermatologists to enhance diagnosis of melanoma, basal cell carcinoma and other cutaneous disorders.⁴⁶ However, its application on the vulvar area is currently limited to vulvar pigmented lesions.⁴⁷

Optical coherence tomography (OCT) is a non-invasive imaging technique that provides real-time cross-sectional images of biologic structures, based on differences in tissue optical properties. OCT can determine epidermal thickness, skin roughness and blood flow parameters based on algorithms. These algorithms use visual information to determine numerical values. OCT has been incorporated in the daily practice of ophthalmology for the visualization and diagnosis of retinal diseases.⁴⁸ In addition, OCT is an established research tool in dermatology, mostly for recognition of non-melanoma skin cancer. In this setting, it has shown potential to reduce biopsy frequency in basal cell carcinomas.⁴⁹ OCT is not an established tool in the gynecologic clinic yet, but a handful of clinical and *ex vivo* studies in cervical, vulvar and ovarian tissue suggest potential for differentiation between healthy and (pre)malignant tissue of epithelial origin.^{50,51}

A *reflectance confocal microscope* (RCM) is an *in vivo* confocal imaging tool that uses a low powered laser to provide non-invasive and real-time visualization of the epidermis and superficial collagen layers at a cellular level up to a depth of 250 μm .⁵² This results in optical transversal sectioning of unstained epithelium and stroma. This technique has been applied for early and accurate diagnosis of skin diseases, including basal cell carcinoma, and reportedly may reduce unnecessary biopsies for the diagnosis of melanocytic lesions.^{53,54} Despite these technological and clinical advancements in the improvement of diagnostic accuracy, RCM imaging has only sparingly been applied on the vulvar area.⁵⁵⁻⁵⁷

Mobile e-diary application for monitoring of patient-reported outcomes and treatment adherence has been successfully applied in interventional studies in several skin diseases.⁴⁵

This method is convenient for both the patient and the investigator. Data can be digitally stored in a safe environment. This e-diary tool is therefore assessed in this clinical study to monitor symptoms and treatment adherence.

SECTION II DEVELOPMENT OF HEALTHY AND DISEASED IN VITRO VULVAR MODELS

Besides the importance of biomarkers for monitoring of disease status, focus should also be on novel drug development in the vulvar field. Prior to *in vivo* testing of novel drugs in human clinical trials, *ex vivo* testing in (animal) models is used to study e.g. toxicity, to define novel drug sensitivity, predict human safety and provide reliable toxicokinetic evidence. Unfortunately, no well-established experimental models are available that mimic human healthy skin or vSCC.⁵⁸

Most vulvar cancer research and drug screening programs are performed on tumor biopsies or (transgenic) animal models.^{59,60} However, animal models are time intensive, expensive, and obtained data are often difficult to extrapolate to the human situation. Human skin equivalents (HSE'S) are *in vitro* 3D reconstructions which may form a solution for the lack of experimental models (Figure 4).⁶¹⁻⁶³ HSE'S are tools that can be used to study biological processes in the skin including healthy and disease conditions.⁶⁴ In addition, these models can serve as a prediction model to determine the penetration profile of compounds/drugs across the skin. To mimic a vSCC *in vitro*, general knowledge of squamous cell carcinomas (SCC's) is essential and especially of the crucial tumor microenvironment.⁶⁵ In SCC's, the epidermal homeostasis gets disrupted by interactions between epidermal cancer cells and underlying stroma, allowing epidermal cells to invade into the stroma.⁶⁶ Stroma consists of basement membrane, immune cells, fibroblasts and extracellular matrix. It has been proven that papillary and reticular fibroblasts (PF's and RF's, respectively) are important for both epidermal and dermal homeostasis in cutaneous models.^{67,68}

In addition, cancer associated fibroblasts (CAF'S) are key players in cutaneous squamous cell carcinoma (CSCC), as demonstrated in previous work with dermatologic skin models.⁶⁹ (Wu et al., submitted) CAF'S are part of the tumor microenvironment (TME) and contribute functionally to the process of SCC progression (Figure 4).^{58,70} While increasing knowledge on pathogenesis and drug development is obtained using cutaneous 3D models, these models are still lacking for healthy vulvar skin and vSCC.

SECTION III MOLECULAR TARGET IDENTIFICATION OF VULVAR CARCINOMAS

Along with development of the diagnostic process and drug intervention studies for vulvar (pre)malignancies, we have explored vSCC-specific targets that in the future might be used for real-time optical imaging. It has been shown in other oncological fields that real-time intraoperative guidance is of added value during surgery for complete and safe tumor resection.^{71,72} Molecular imaging integrates advanced imaging modalities with probes targeting molecular biomarkers of interest.⁷³ An imaging probe consists partly of a contrast label, such as radionuclides for nuclear based imaging, paramagnetic or electron opaque substances for radiological techniques, or bioluminescent or fluorescent molecules for fluorescence guided imaging (Figure 5). This contrast label is conjugated to a molecular imaging agent with high affinity for a biomarker selectively expressed at the surface of tumor(-associated) cells (Figure 4A). Small molecules, peptides, aptamers, antibodies, protein fragments and nanoparticles have been used as molecular imaging agents.⁷⁴ After administration of an imaging probe to a cancer patient, real-time images of the tissue of interest can be obtained by a suitable camera system that generates optical contrast between tumor and surrounding healthy tissue. Optical imaging is a discipline within the molecular imaging field. Imaging agents applicable for optical imaging benefit of their high-spatial resolution and real-time localization. An example of optical imaging coupled with image-guided surgery is fluorescent guided surgery (FGS), which has been widely explored in the last decade (Figure 4B). Particularly, the use of near-infrared (NIR) fluorescence dyes can provide sufficient tissue penetration for vulvar carcinomas with up to 1cm in-growth.⁷² In this manner, FGS is a promising technique for real-time detection of occult tumor lesions and localization of cancer margins. Proper identification of tumor-specific targets for molecular imaging is the key to the success of FGS. The following characteristics define a potential protein marker for targeted imaging: extracellular biomarker localization, expression pattern, tumor-to-healthy tissue ratio, percentage and distribution of positive cells, and previous use of the biomarker for *in vivo* targeted imaging.^{71,74,75} Although this technique is very promising, it is never generally explored for vulvar (pre)malignancies yet.

AIMS AND OUTLINE OF THIS THESIS

This thesis describes studies performed within a multimodal characterization approach of vulvar healthy and (pre)malignant skin. The focus is on the *physician, patient, cellular, molecular, and imaging* domains with the aim to find disease-specific biomarkers to improve the clinical management of vulvar (pre)malignancies. This thesis is divided into three sections:

Section I of this thesis discusses the evaluation of several non-invasive clinical tools on the vulvar healthy and diseased skin. **Chapter 2** covers the domains *physician- and patient reported outcomes and imaging*. A mobile e-diary application for monitoring of *patient-reported outcomes* and treatment adherence has been applied. Within the *imaging* domain, we investigated if outcome measures of the non-invasive imaging methods dermatoscopy and optical coherence tomography (OCT) could serve as biomarkers for vulvar diseased skin. Next, in **Chapter 3** reflectance confocal microscopy (RCM) has been assessed on the vulvar skin of healthy and diseased patients as part of the *imaging* domain. RCM shows great potential in other clinical fields, but has sparingly been applied on the vulvar area. The primary objective is to explore feasibility and tolerability of RCM imaging on premalignant vulvar skin. The *cellular* domain is discussed in **Section II**. **Chapter 4** describes how the experience with 3D human skin equivalents (HSE'S) in dermatologic research has been used to set-up vulvar healthy and diseased 3D-HSE'S. The cancer models were thereafter used to test the effect of standard-of care chemotherapeutics on the acquired tumors. In **Section III** the focus is on the *molecular* domain. In **Chapter 5** a systematic review is presented, elaborating on the search for potential molecular targets for fluorescence guided surgery (FGS) for vulvar cancer. Subsequently, in **Chapter 6** potential targets for FGS in VSCC are evaluated using immunohistochemistry on healthy and (pre)malignant vulvar tissue sections. The expression of each marker has been quantified using digital image analysis and expression scores are compared for all cohorts included. **Chapter 7** summarizes the results of all these chapters and highlights future perspectives.

Figure 1 Anatomy of the vulva.

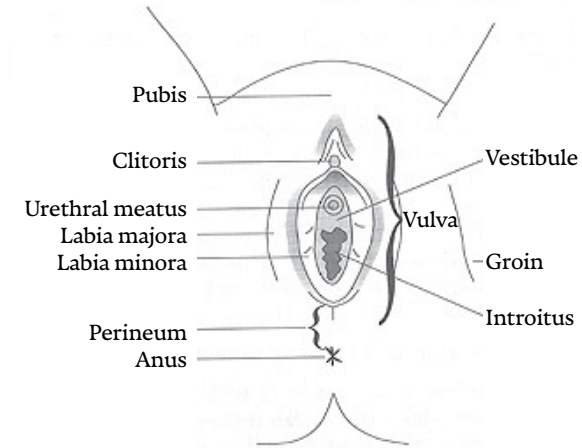


Figure 2 Multimodal profiling of vulvar healthy and diseased skin, to improve diagnostics and drug development.^{41,42} Five domains are studied: physician, patient, molecular, cellular and imaging. Section numbering indicates the location in this thesis where a specific method is discussed.

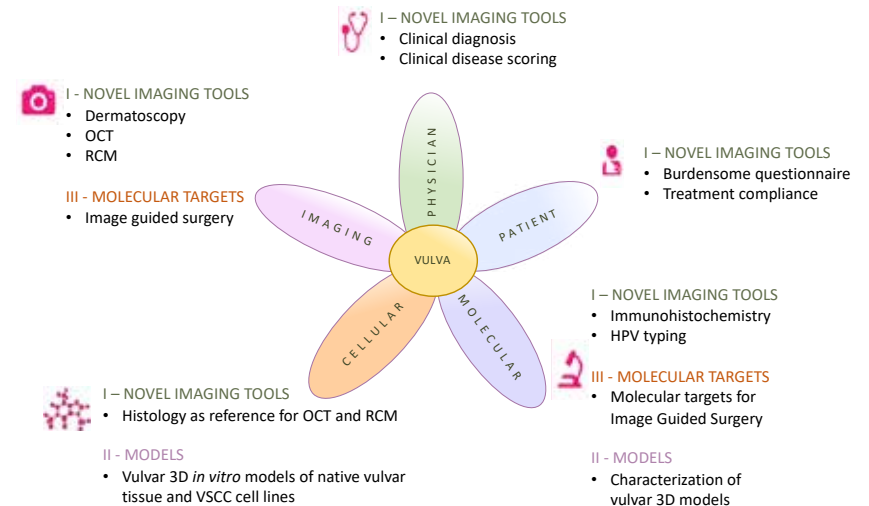
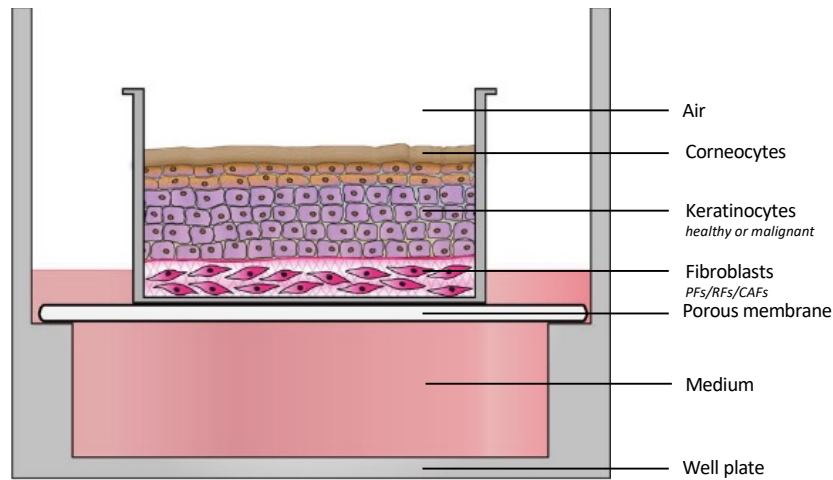


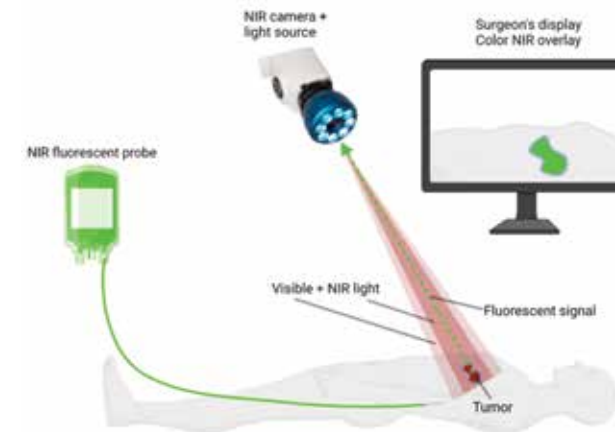
Figure 3 Cross-sectional view of a human skin equivalent (HSE) in an air-liquid well plate. Isolated healthy or squamous cell keratinocytes can grow on different type of fibroblasts. These HSE models shows an epidermis that includes all dermal layers observed in freshly obtained skin.



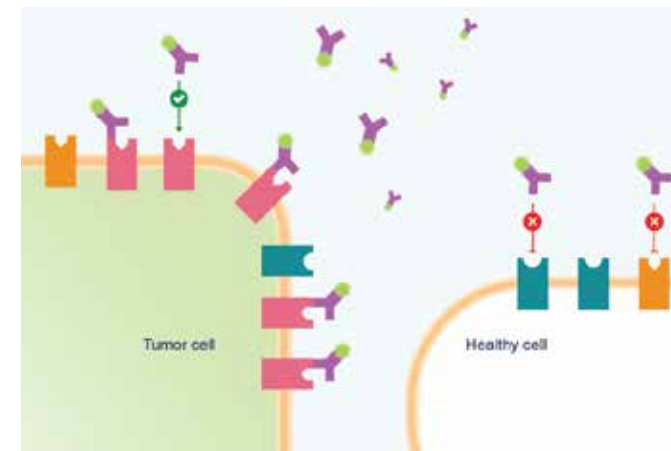
HSE=human skin equivalent, PF=papillary fibroblasts, RF=reticular fibroblasts, CAF'S=cancer associated fibroblasts

Figure 4 Image guided surgery using near-infrared (NIR) fluorescence.

A A NIR fluorescent contrast agent is administered e.g. intravenously or topically to a cancer patient. During surgery, the agent is visualized using a NIR fluorescence imaging system. This system must have adequate NIR excitation light, collection optics and filtration, and a camera sensitive to NIR fluorescence emission light. An optimal imaging system includes simultaneous visible (i.e., white) light illumination of the surgical field, which can be merged with NIR fluorescence images. The surgeon may see the camera records on a computer monitor, goggles, or a wall projector (monitor form factor shown).



B Graphical overview of binding of a probe, here an antibody (purple) conjugated to fluorescent label (fluorescent green), specifically to a target present at tumor cells and absent at healthy cells.



REFERENCES

- 1 Vulvar Cancer — Cancer Stat Facts. <https://seer.cancer.gov/statfacts/html/vulva.html>.
- 2 Alkatout, I. *et al.* Vulvar cancer: epidemiology, clinical presentation, and management options. *Int. J. Womens. Health* 7, 305–313 (2015).
- 3 Weinberg, D. & Gomez-Martinez, R. A. Vulvar Cancer. *Obstet. Gynecol. Clin. North Am.* 46, 125–135 (2019).
- 4 Olawaiye, A. B., Cuello, M. A. & Rogers, L. J. Cancer of the vulva: 2021 update. *Int. J. Gynaecol. Obstet.* 155 Suppl 1, 7–18 (2021).
- 5 D, W. & RA, G.-M. Vulvar Cancer. *Obstet. Gynecol. Clin. North Am.* 46, 125–135 (2019).
- 6 Singh, N. & Gilks, C. B. Vulvar squamous cell carcinoma and its precursors. *Histopathology* 76, 128–138 (2020).
- 7 Schuurman, M. S. *et al.* Trends in incidence and survival of Dutch women with vulvar squamous cell carcinoma. *Eur. J. Cancer* 49, 3872–3880 (2013).
- 8 Akhtar-Danesh, N., Elit, L. & Lytwyn, A. Trends in incidence and survival of women with invasive vulvar cancer in the United States and Canada: a population-based study. *Gynecol. Oncol.* 134, 314–318 (2014).
- 9 Gaarenstroom, K. N. *et al.* Postoperative complications after vulvectomy and inguinofemoral lymphadenectomy using separate groin incisions. *Int. J. Gynecol. Cancer* 13, 522–527 (2003).
- 10 Malandrone, F. *et al.* The Impact of Vulvar Cancer on Psychosocial and Sexual Functioning: A Literature Review. *Cancers (Basel)*, 14, (2021).
- 11 Preti, M., Van Seters, M., Sideri, M. & Van Beurden, M. Squamous vulvar intraepithelial neoplasia. *Clin. Obstet. Gynecol.* 48, 845–861 (2005).
- 12 Muigai, J., Jacob, L., Dinas, K., Kostev, K. & Kalder, M. Potential delay in the diagnosis of vulvar cancer and associated risk factors in women treated in German gynecological practices. *Oncotarget* 9, 8725 (2018).
- 13 Yeung, J. & Pauls, R. N. Anatomy of the Vulva and the Female Sexual Response. *Obstet. Gynecol. Clin. North Am.* 43, 27–44 (2016).
- 14 Wohlmut, C. & Wohlmut-Wieser, I. Vulvar malignancies: an interdisciplinary perspective. *J. Dtsch. Dermatol. Ges.* 17, 1257–1276 (2019).
- 15 Tan, A., Bieber, A. K., Stein, J. A. & Pomeranz, M. K. Diagnosis and management of vulvar cancer: A review. *J. Am. Acad. Dermatol.* 81, 1387–1396 (2019).
- 16 Thuijs, N. B. *et al.* Vulvar intraepithelial neoplasia: Incidence and long-term risk of vulvar squamous cell carcinoma. *Int. J. Cancer* 148, 90–98 (2021).
- 17 Corazza, M., Schettini, N., Zedde, P. & Borghi, A. Vulvar Lichen Sclerosus from Pathophysiology to Therapeutic Approaches: Evidence and Prospects. *Biomedicine* 9, (2021).
- 18 Lebreton, M. *et al.* Vulvar intraepithelial neoplasia: Classification, epidemiology, diagnosis, and management. *J. Gynecol. Obstet. Hum. Reprod.* 49, (2020).
- 19 Halonen, P., Jakobsson, M., Heikinheimo, O., Gissler, M. & Pukkala, E. Incidence of lichen sclerosus and subsequent causes of death: a nationwide Finnish register study. *BJOG* 127, 814–819 (2020).
- 20 Fergus, K. B. *et al.* Pathophysiology, Clinical Manifestations, and Treatment of Lichen Sclerosus: A Systematic Review. *Urology* 135, 11–19 (2020).
- 21 Tan, A., Bieber, A. K., Stein, J. A. & Pomeranz, M. K. Diagnosis and management of vulvar cancer: A review. *J. Am. Acad. Dermatol.* 81, 1387–1396 (2019).
- 22 Eva, L. J. *et al.* Trends in HPV-dependent and HPV-independent vulvar cancers: The changing face of vulvar squamous cell carcinoma. *Gynecol. Oncol.* 157, 450–455 (2020).
- 23 Hinten, F. *et al.* Vulvar cancer: Two pathways with different localization and prognosis. *Gynecol. Oncol.* 149, 310–317 (2018).
- 24 McAlpine, J. N. *et al.* HPV-independent Differentiated Vulvar Intraepithelial Neoplasia (dVIN) is Associated with an Aggressive Clinical Course. *Int. J. Gynecol. Pathol.* 36, 507–516 (2017).
- 25 Bornstein, J. *et al.* The 2015 International Society for the Study of Vulvovaginal Disease (ISSVD) Terminology of Vulvar Squamous Intraepithelial Lesions. *J. Low. Genit. Tract Dis.* 20, 11–14 (2016).
- 26 Oonk, M. H. M. *et al.* European society of gynaecological oncology guidelines for the management of patients with Vulvar cancer. *Int. J. Gynecol. Cancer* 27, 832–837 (2017).
- 27 Dellinger, T. H. *et al.* Surgical management of vulvar cancer. *JNCCN Journal of the National Comprehensive Cancer Network* (2017) doi:10.6004/jnccn.2017.0009.
- 28 Nooij, L. S. *et al.* Risk factors and treatment for recurrent vulvar squamous cell carcinoma. *Critical Reviews in Oncology/Hematology* (2016) doi:10.1016/j.critrevonc.2016.07.007.
- 29 Ignatov, T., Eggemann, H., Burger, E., Costa, S. D. & Ignatov, A. Adjuvant radiotherapy for vulvar cancer with close or positive surgical margins. *J. Cancer Res. Clin. Oncol.* 142, 489–495 (2016).
- 30 Modesitt, S. C., Waters, A. B., Walton, L., Fowler, W. C. & Van Le, L. Vulvar intraepithelial neoplasia 111: occult cancer and the impact of margin status on recurrence. *Obstet. Gynecol.* 92, 962–966 (1998).
- 31 Cohen, P. A., Anderson, L., Eva, L. & Scurry, J. Clinical and molecular classification of vulvar squamous precancers. *Int. J. Gynecol. Cancer* 29, 821–828 (2019).
- 32 Green, N., Adedipe, T., Dmytryshyn, J., Preti, M. & Selk, A. Management of Vulvar Cancer Precursors: A Survey of the International Society for the Study of Vulvovaginal Disease. *J. Low. Genit. Tract Dis.* 24, 387–391 (2020).
- 33 Committee Opinion No.675: Management of Vulvar Intraepithelial Neoplasia. *Obstet. Gynecol.* 128, e178–e182 (2016).
- 34 Jin, C. & Liang, S. Differentiated Vulvar Intraepithelial Neoplasia: A Brief Review of Clinicopathologic Features. *Arch. Pathol. Lab. Med.* 143, 768–771 (2019).
- 35 Reyes, M. C. & Cooper, K. An update on vulvar intraepithelial neoplasia: terminology and a practical approach to diagnosis. *J. Clin. Pathol.* 67, 290–294 (2014).
- 36 Sherman, V. *et al.* The high rate of familial lichen sclerosus suggests a genetic contribution: An observational cohort study. *J. Eur. Acad. Dermatology Venereol.* 24, 1031–1034 (2010).
- 37 Neill, S. M., Lewis, F. M., Tatnall, F. M. & Cox, N. H. British Association of Dermatologists' guidelines for the management of lichen sclerosus 2010. *Br. J. Dermatol.* 163, 672–682 (2010).
- 38 Lee, A., Bradford, J. & Fischer, G. Long-term Management of Adult Vulvar Lichen Sclerosus: A Prospective Cohort Study of 507 Women. *JAMA dermatology* 151, 1061–1067 (2015).
- 39 Vandborg, M. P. *et al.* Reasons for diagnostic delay in gynecological malignancies. *Int. J. Gynecol. Cancer* 21, 967–974 (2011).
- 40 Cohen, A. F., Burggraaf, J., Van Gerven, J. M. A., Moerland, M. & Groeneveld, G. J. The use of biomarkers in human pharmacology (Phase I) studies. *Annu. Rev. Pharmacol. Toxicol.* 55, 55–74 (2015).
- 41 Atkinson, A. J. *et al.* Biomarkers and surrogate endpoints: preferred definitions and conceptual framework. *Clin. Pharmacol. Ther.* 69, 89–95 (2001).
- 42 Kruijzinga, M. D. *et al.* Development of Novel, Value-Based, Digital Endpoints for Clinical Trials: A Structured Approach Toward Fit-for-Purpose Validation. *Pharmacol. Rev.* 72, 899–909 (2020).
- 43 Rissmann, R., Moerland, M. & van Doorn, M. B. A. Blueprint for mechanistic, data-rich early phase clinical pharmacology studies in dermatology. *Br. J. Clin. Pharmacol.* 86, 1011–1014 (2020).
- 44 van der Kolk, T. *et al.* Comprehensive, Multimodal Characterization of an Imiquimod-Induced Human Skin Inflammation Model for Drug Development. *Clin. Transl. Sci.* 11, 607–615 (2018).
- 45 Rijsbergen, M. *et al.* Mobile e-diary application facilitates the monitoring of patient-reported outcomes and a high treatment adherence for clinical trials in dermatology. *J. Eur. Acad. Dermatology Venereol.* 34, 633–639 (2020).
- 46 Ring, C., Cox, N. & Lee, J. B. Dermatoscopy. *Clin. Dermatol.* 39, 635–642 (2021).
- 47 Cengiz, F. P., Emiroglu, N. & Hofmann Wellenhof, R. Dermoscopic and clinical features of pigmented skin lesions of the genital area. *An. Bras. Dermatol.* 90, 178–183 (2015).
- 48 Katkar, R. A., Tadinada, S. A., Amaechi, B. T. & Fried, D. Optical Coherence Tomography. *Dent. Clin. North Am.* 62, 421–434 (2018).
- 49 Wan, B. *et al.* Applications and future directions for optical coherence tomography in dermatology. *Br. J. Dermatol.* 184, 1014–1022 (2021).
- 50 Wessels, R. *et al.* Optical coherence tomography in vulvar intraepithelial neoplasia. <https://doi.org/10.1117/1.JBO.17.11.116022.17>, 116022 (2012).
- 51 Kirillin, M., Motovilova, T. & Shakhova, N. Optical coherence tomography in gynecology: a narrative review. *J. Biomed. Opt.* 22, 1 (2017).
- 52 Hofmann-Wellenhof, R., Pellacani, G., Malvehy, J. & Soyer, H. P. *Reflectance confocal microscopy for skin diseases. Reflectance Confocal Microscopy for Skin Diseases* (Springer Berlin Heidelberg, 2012). doi:10.1007/978-3-642-21997-9.
- 53 Kadouch, D. J. *et al.* Diagnostic accuracy of confocal microscopy imaging vs. punch biopsy for diagnosing and subtyping basal cell carcinoma. *J. Eur. Acad. Dermatology Venereol.* 31, 1641–1648 (2017).
- 54 Braga, J. C. T. *et al.* Learning reflectance confocal microscopy of melanocytic skin lesions through histopathologic transversal sections. *PLoS One* 8, (2013).
- 55 Fouques, C. *et al.* Reflectance confocal microscopy of vulvar epithelial neoplasia: a pilot study. *British Journal of Dermatology* vol. 177 e196–e199 (2017).
- 56 Cinotti, E. *et al.* Dermoscopic and reflectance confocal microscopy features of two cases of vulvar basal cell carcinoma. *Dermatol. Pract. Concept.* 8, 68–71 (2018).
- 57 Feng, L. *et al.* Imaging of Vulva Syringoma With Reflectance Confocal Microscopy. *Front. Med.* 8, (2021).
- 58 Löhmussaar, K., Boretto, M. & Clevers, H. Human-Derived Model Systems in Gynecological Cancer Research. *Trends in Cancer* 6, 1031–1043 (2020).
- 59 NE, S. & RA, D. The mighty mouse: genetically engineered mouse models in cancer drug development. *Nat. Rev. Drug Discov.* 5, 741–754 (2006).
- 60 J, C., F, M., SC, R. & DR, F. Vaginal tamoxifen for treatment of vulvar and vaginal atrophy: Pharmacokinetics and local tolerance in a rabbit model over 28 days. *Int. J. Pharm.* 570, (2019).
- 61 Danso, M. O. *et al.* Exploring the potentials of nurture: 2(nd) and 3(rd) generation explant human skin equivalents. *J. Dermatol. Sci.* 77, 102–109 (2015).
- 62 Carlson, M. W., Alt-Holland, A., Egles, C. & Garlick, J. A. Three-dimensional tissue models of normal and diseased skin. *Curr. Protoc. cell Biol.* Chapter 19, (2008).
- 63 Bouwstra, J. A., Helder, R. W. J. & El Ghalbzouri, A. Human skin equivalents: Impaired barrier function in relation to the lipid and protein properties of the stratum corneum. *Adv. Drug Deliv. Rev.* 175, 113802 (2021).
- 64 Garlick, J. A. Engineering skin to study human disease – tissue models for cancer biology and wound repair. *Adv. Biochem. Eng. Biotechnol.* 103, 207–239 (2007).
- 65 Hanahan, D. & Weinberg, R. A. Hallmarks of cancer: the next generation. *Cell* 144, 646–674 (2011).
- 66 De Wever, O. & Mareel, M. Role of tissue stroma in cancer cell invasion. *J. Pathol.* 200, 429–447 (2003).
- 67 Janson, D., Saintigny, G., Mahé, C. & Ghalbzouri, A. El. Papillary fibroblasts differentiate into reticular fibroblasts after prolonged in vitro culture. *Exp. Dermatol.* 22, 48–53 (2013).
- 68 Janson, D., Rietveld, M., Mahé, C., Saintigny, G. & El Ghalbzouri, A. Differential effect of extracellular matrix derived from papillary and reticular fibroblasts on epidermal development in vitro. *Eur. J. Dermatol.* 27, 237–246 (2017).
- 69 Commandeur, S. *et al.* Functional characterization of cancer-associated fibroblasts of human cutaneous squamous cell carcinoma. *Exp. Dermatol.* 20, 737–742 (2011).
- 70 Dongre, H. *et al.* Establishment of a novel cancer cell line derived from vulvar carcinoma associated with lichen sclerosus exhibiting a fibroblast-dependent tumorigenic potential. *Exp. Cell Res.* 386, 11684 (2020).
- 71 Hernot, S., van Manen, L., Debie, P., Mieog, J. S.

-
- D. & Vahrmeijer, A. L. Latest developments in molecular tracers for fluorescence image-guided cancer surgery. *The Lancet Oncology* (2019) doi:10.1016/S1470-2045(19)30317-1.
- 72 Vahrmeijer, A. L., Hutteman, M., Van Der Vorst, J. R., Van De Velde, C. J. H. & Frangioni, J. V. Image-guided cancer surgery using near-infrared fluorescence. *Nature Reviews Clinical Oncology* vol. 10 507–518 (2013).
- 73 James, M. L. & Gambhir, S. S. A molecular imaging primer: modalities, imaging agents, and applications. *Physiol. Rev.* 92, 897–965 (2012).
- 74 Boonstra, M. C. *et al.* Selecting Targets for Tumor Imaging: An Overview of Cancer-Associated Membrane Proteins. *Biomark. Cancer* (2016) doi:10.4137/bic.s38542.
- 75 van Oosten, M., Crane, L. M. A., Bart, J., van Leeuwen, F. W. & van Dam, G. M. Selecting potential targetable biomarkers for imaging purposes in colorectal cancer using target selection criteria (TASC): A novel target identification tool. *Translational Oncology* vol. 4 71–82 (2011).

SECTION I

NON-INVASIVE CLINICAL TOOLS TO DISCOVER VULVAR SKIN BIOMARKERS

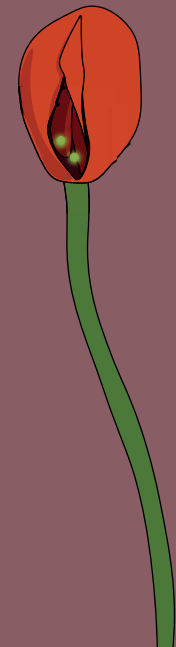
CHAPTER 2

Dermatoscopy and dynamic optical coherence tomography in vulvar HSIL and lichen sclerosus: a prospective feasibility study

B.W. Huisman^{1,2*}, L. Pagan^{1,2*}, R.G.C. Naafs¹, W. ten Voorde¹,
R. Rissmann^{1,2,4}, J.M.J. Piek⁵, J. Damman⁶, M.J. Juachon¹, M. Osse¹,
T. Niemeyer-van der Kolk¹, C.L.M. van Hees³, M.I.E. van Poelgeest^{1,2}

** Both authors contributed equally*

- 1 Centre for Human Drug Research, Leiden, NL
- 2 Department of Obstetrics and Gynaecology, Leiden University Medical Center, Leiden, NL
- 3 Department of Dermatology, Erasmus Medical Centre, Rotterdam, NL
- 4 Leiden Academic Centre for Drug Research, Leiden University, Leiden, NL
- 5 Department of Obstetrics and Gynaecology and Catharina Cancer Institute, Eindhoven, NL
- 6 Department of Pathology, Erasmus MC, University Medical Center, Rotterdam, NL



Abstract

OBJECTIVE To examine potential discriminatory characteristics of dermatoscopy and dynamic optical coherence tomography (D-OCT) on vulvar high-grade squamous intraepithelial lesions (vHSIL) and lichen sclerosus (LS) compared to healthy vulvar skin.

METHODS Non-invasive imaging measurements using dermatoscopy and D-OCT were obtained at several time-points, including lesional and non-lesional vulvar skin. Morphologic features of vHSIL and LS were compared to healthy controls. Epidermal thickness and blood flow were determined using D-OCT. Patients reported tolerability of each study procedure, including reference vulvar biopsies.

MAIN OUTCOME MEASURES Feasibility and tolerability of imaging modalities, dermatoscopy and OCT characteristics, OCT epidermal thickness and D-OCT dermal blood flow.

RESULTS The application of dermatoscopy and D-OCT is feasible and tolerable. In vHSIL, dermatoscopic warty structures were present. In LS, sclerotic areas and arborizing vessels were observed. Structural OCT in the vulvar area aligned with histology for hyperkeratosis and dermal-epidermal junction visualisation. Currently, the OCT algorithm is unable to calculate the epidermal thickness of the uneven vulvar area. D-OCT showed statistically significant increased blood flow in LS patients (mean \pm SD 0.053 \pm 0.029) to healthy controls (0.040 \pm 0.012, $p=0.0024$).

CONCLUSIONS The application of dermatoscopy and D-OCT is feasible and tolerable in vHSIL and LS patients. Using dermatoscopy and D-OCT, we describe potential characteristics to aid differentiation of diseased from healthy vulvar skin, which could complement clinical assessments.

Introduction

Vulvar high-grade intraepithelial lesions (vHSIL) and lichen sclerosus (LS) can develop in the vulvar region.¹ Both diseases can predispose to vulvar squamous cell carcinoma (vSCC).^{2,3} vHSIL is caused by high-risk human papillomavirus (HPV), such as type 16 and 18. The cause of LS is unknown, but a genetic and (auto)immune etiologic role has been suggested.^{4,5} Both vulvar diseases may cause itch, pain or a burning sensation. LS may result in vulvar disfigurement. Inadequate clinical recognition and delayed or inadequate treatment may have detrimental consequences. These issues are partly caused by low incidence of the diseases, the difficulty to recognize lesions among patients and healthcare professionals, in addition to social stigma and taboo.^{6,7} As a consequence, vHSIL and LS have a considerable physical, sexual and psychological impact on affected patients.^{6,8} Preferably, the diagnostic process of these vulvar diseases should be improved by objective and non-invasive, disease-specific biomarkers. A prerequisite in biomarker validation is its ability to discriminate healthy from diseased tissue.⁹ Examples of potential novel techniques are dermatoscopy and dynamic optical coherence tomography (D-OCT). Dermatoscopy is routinely applied by dermatologists as an adjunctive tool to ameliorate subsurface structure visualization and pattern identification to aid diagnosis of melanoma, basal cell carcinoma and other cutaneous disorders.¹⁰ Its application on the vulvar area is currently limited to research purposes of vulvar pigmented lesions.¹¹⁻¹³ D-OCT is a non-invasive imaging technique that provides real-time cross-sectional images of biological structures based on differences in tissue optical properties. It has been incorporated in the daily ophthalmology practice for diagnosis of retinal diseases.¹⁴ In addition, D-OCT has been applied as a research tool in dermatology for characterisation of non-melanoma skin cancer.¹⁵⁻¹⁸ In gynaecology, only a few studies in cervical, vulvar and ovarian tissue suggest potential for D-OCT to differentiate between healthy and (pre)malignant tissue of epithelial origin.¹⁹⁻²² The study objective was to examine potential discriminatory characteristics of dermatoscopy and D-OCT on premalignant vulvar skin compared to healthy vulvar skin. Therefore, we examined dermatoscopy and D-OCT in a standardized clinical trial on both vHSIL and LS patients and healthy controls.

Methods

A prospective, healthy volunteer-matched, single-centre trial conducted at the Centre for Human Drug Research in Leiden was performed from February 2021 to October 2021. The Declaration of Helsinki was the guiding principle for trial execution. The study was approved by an independent medical ethics committee 'Medisch-Ethische Toetsingscommissie Leiden Den Haag Delft'. All subjects provided written informed consent before participation. The trial was registered with the 'Nederlands Trial Register' (NL73964.058.20) and EudraCT (2020-002201-2). These imaging results are part of a multi-modal clinical study investigating research methods across various domains to identify biomarkers that could improve vulvar disease identification and therapeutic response monitoring (Figure S1).^{9,23}

STUDY DESIGN AND SUBJECTS

In total, 25 women (Fitzpatrick skin type I-III), aged 25-73 with a body mass index (BMI) <30 kg/m² were included, categorized as: five vHSIL patients (≥1 sharply margined histologically confirmed vHSIL lesion ≥15mm), ten LS patients (clinical and/or histological diagnosis confirmation) and ten healthy controls. Main exclusion criteria were having a significant other disease as judged by the investigator, pregnancy, other vulvar dermatological conditions, immunocompromised state, sexually transmitted disease, acquired immunodeficiency syndrome or hepatitis. For standardization purposes, the wash-out for topically applied products on the vulvar area was ≥14 days.²⁴ All subjects visited the clinical research department on Day 0 (0h=baseline, 3h and 6h), Day 1 and Day 7 (Figure S2). LS patients also visited the clinic on Day 21 and 35, as follow-up for a 4-week standard of care treatment with corticosteroid ointment clobetasol 0.05% (Dermovate, GlaxoSmithKline, Brentford, UK) starting at Day 8. At each visit, clinical assessments and non-invasive imaging measurements were performed. Biopsies were obtained at Day 0 for all subjects and on Day 35 for LS patients.

ANOGENITAL EXAMINATION AND VULVAR LESION MAPPING

Examination of the anogenital region and study procedures were performed in a gynaecological chair. All patients were assessed by trained physicians (BH and LP) and discussed with an oncological gynaecologist specialized in vulvar disease (MVP) at baseline. All procedures were performed on selected target areas, including a lesional and non-lesional site for all patients.

IMAGING

Dermatoscopy

MACROSCOPIC IMAGING Macroscopic dermatoscopic images of the vulvar surface were obtained using a FotoFinder Medicam 1000 with the Bodystudio – Automated Total Body Mapping (FotoFinder Systems GmbH, Bad Birnbach, Germany) for photo analysis and documentation (Figure S3). Microscopic images were obtained with a D-Scope IV dermatoscopy lens with polarized light and analyzed using FotoFinder universe. Dermatoscopy includes a follow-up photo documentation function. An open cap was used to compensate for the uneven character of vulvar skin, especially if irregular due to disease. The cap was removed and cleaned using liquid alcohol on a tissue after image acquisition. The whole procedure took approximately 1-2 minute per patient.

MICROSCOPIC IMAGING As an exploratory measure, individual dermatoscopic characteristic or a set of characteristics were assessed for discriminatory potential for vulvar diseases. Scoring of the presence or absence of these characteristics in decoded microscopic images was performed by an expert dermatologist who was fully blinded for patient type (CH). The following characteristics were appraised per image: colour of the skin (red, pink, yellow, grey, brown, white or other); vessel concentration (increased, normal, decreased or invisible) and vessel concentration (dotted, hairpin, linear, linear serpentine, thin/thick arborizing, thick root-like, other or not visible). The presence or absence of scales, ecchymoses, purpura, yellow-white structureless areas, white circles, peppering, comedo-like openings, ulceration and warty structures were reported, as previously described in literature of dermatoscopy characteristics of genital lesions.^{25,26} In total, 85 photos were scored (15 vHSIL, 40 LS and 30 HV) obtained at Day 0, 7 and 35.

D-OCT

Skin morphology analysis up to a depth of 1 mm was performed by D-OCT using the Vivosight Dx (Michelson Diagnostics Ltd., United Kingdom). The VivoSight Dx handheld probe captures a 6 mm x 6 mm scan in approximately 60 seconds. Generally, the operator used two hands, one to stabilise the vulvar area of interest and one to place the handheld device on the skin. The images were displayed on a monitor for review (Figure S4). Scans with artefacts due to movement were excluded from analysis and directly

retaken. Structural OCT employs light reflectance to generate a black and white image perpendicular to the scanned skin. In addition, D-OCT allows the *in vivo* evaluation of blood vessels and their distribution within specific lesions based on speckle variance. The incorporated VivoSight software was employed to automatically determine epidermal thickness and blood flow. The data was stored and analysed using VivoSight version 4.15 and VivoTools software version 4.15. Qualitative assessments were performed by three trained OCT operators (BH, LP and WV).

EPIDERMAL THICKNESS Epidermal thickness was determined using the algorithms incorporated in the software. Additional manual epidermal thickness analyses were performed with ImageJ (version Java 1.8.0_172, Bethesda, Maryland, USA). Using a self-generated macro, three consecutive vertical lines were drawn per scan, indicating the thickness of the epidermal layer. The mean, SD, minimum and maximum epidermal thickness was determined per set of 120 consecutive scans per patient. Due to the exploratory nature of this measurement and time-consuming manual calculations, only baseline and post-treatment (LS) scans were analysed manually for epidermal thickness.

BLOOD FLOW D-OCT blood flow was determined using the algorithms incorporated in the software. The quantification of the blood flow was based on the average speckle signal returning at the detector at dermal depth from 0.10 to 0.35mm to reduce distortions from artefacts.²⁷

HISTOLOGICAL ANALYSIS

Vulvar tissue samples were obtained using a 4mm punch biopsy acquired by trained physicians (BH, LP and MVP) at the end of Day 0. The skin was anaesthetised using subcutaneous lidocaine prior to the procedure. The obtained biopsies were formalin fixed paraffin embedded (FFPE) and stained for hematoxylin and eosin (HE) by the pathology department of the Erasmus Medical Centre (EMC, Rotterdam, The Netherlands) following clinical protocols. Slides were scored by a dermatopathologist (JD). Dysplasia was assessed by the epidermal levels of atypia and scored as warty and/or basaloid types. Lichen sclerosus was diagnosed by the histological characteristics of LS.^{28,29} INNO-LIPA HPV Genotyping Extra (Eurofins NMDL-LCPL, Rijswijk, The Netherlands) was used for HPV typing.³⁰

PATIENT REPORTED OUTCOMES

The ‘burdensome questionnaire’ comprised of 100 mm lines on which the patient indicated how burdensome they found each study procedure, with 0 mm representing no burden at all and 100 mm representing the most burdensome procedure possible (Figure S5). The e-diary (Promasys® EPRO platform) with a reminder and photograph function (with corresponding time stamps) was used to monitor at-home drug compliance.³¹

STATISTICAL ANALYSIS

Dermatoscopic observations were summarized and shown descriptively. To determine the differences between patient groups, a two-sided unpaired t-test on averages of two groups (vHSIL, LS or healthy) at baseline were performed. This was performed for epidermal thickness and blood flow measurements of the D-OCT. A paired, two-tailed t-test was performed comparing mean D-OCT values pre- to post treatment. The differences for the burdensome questionnaire were analysed using a paired student’s t-test comparing dermatoscopy and D-OCT to the biopsy procedure. The analyses were computed in SAS 9.4 and GraphPad version 9.3.1.

Results

In total, 25 women, of which 5 patients with vHSIL and 10 patients with LS and 10 healthy controls were enrolled and all patients finished the study (Table S1). Menopausal status was equally distributed among groups.

DERMATOSCOPY

Vulvar skin of a representative subject of each cohort (vHSIL, LS and healthy controls) captured by dermatoscopy is presented in a macroscopic overview and a microscopic image (Figure S6).

MICROSCOPIC CHARACTERISTICS Examples of dermatoscopic characteristics are shown in Figure 1 and the frequency of observations per group are summarized in Figure 2. The most prominent characteristic of vHSIL were warty structures (4/5), which could be accompanied by some scales and peppering. The colour of vHSIL skin was highly variable, but never yellow. Women with Fitzpatrick skin type >3 were not included in this study, so colour findings could vary based on the analyzed population. Vessels

were present with dotted or linear vessel. LS vulvar skin colour was usually scored as pink or white and typically showed white structureless areas (8/10) and/or increased vessel concentration (8/10), with arborizing and/or thick root-like vessel morphology. The vulvar skin of healthy controls was mostly scored as yellow (8/10), with normal vessel pattern of dotted or linear vessels, sometimes accompanied by white circles (4/10). Occasionally white structureless areas or peppering was observed (3/10). No changes were observed in dermatoscopic characteristics of LS skin before and after 4-week clobetasol treatment (data not shown).

D-OCT

MORPHOLOGICAL CHARACTERISTICS Vulvar HSIL is histologically characterized by hyperkeratosis and parakeratosis, acanthosis with club-shaped rete ridges, cytonuclear atypia, disorientation of individual epithelial cells and an intact basement membrane.³

Figure 3 shows a side-to-side comparison of OCT images to corresponding histology of all three disease entities (Figure A: vHSIL, Figure B: LS and Figure C: HV). Hyperkeratosis could be identified in the structural OCT image of a vHSIL lesion in the hyperreflective stratum corneum. In addition, the OCT image shows the broadening of the epidermis in the club-shaped pattern associated with acanthotic vHSIL with an intact dermal-epidermal junction as observed in histology. Lichen sclerosus is histologically characterized by hyperkeratosis, thinning of the epidermis with loss of the rete ridge pattern and dermal changes, including sclerosis.²⁹

In the OCT image, these changes can also be identified, especially the disorganized extracellular matrix reflecting the dermal changes. Nuclear and cellular changes cannot be visualized using OCT. In addition, we observed that resolution was occasionally lost deeper into the skin under a hyperkeratotic and hyperreflective stratum corneum or sclerotic area. These OCT findings are pronounced in vHSIL and LS compared to healthy vulvar skin. Histologically healthy vulvar skin has a normal epidermal thickness in the absence of characteristics observed in diseased vulvar skin. These features could also be visualized in OCT recordings.

EPIDERMAL THICKNESS In total 77.5% (vHSIL), 56.9% (LS) and 91.2% (healthy control) of the measurements using the incorporated algorithm failed as an impossible epidermal thickness of 0 μm was reported (Figure S7). Therefore,

manual epidermal thickness measurements were performed (Figure 4A+B). No significant differences in epidermal thickness were identified comparing lesional or non-lesional vHSIL to healthy controls. The epidermis (mean \pm SD) of pre-clobetasol lesional LS (0.13 \pm 0.10 μm) was statistically significant thinner compared to healthy controls (0.19 \pm 0.06 μm), $p=0.0312$. No differences were observed between pre- and post-clobetasol-treated LS (0.127 \pm 0.10 μm vs 0.118 \pm 0.034, $p=0.643$).

BLOOD FLOW At baseline, higher blood flow (mean \pm SD) measured by D-OCT was observed in non-lesional vHSIL (0.063 \pm 0.040) compared to lesional vHSIL (0.044 \pm 0.025), $p=0.0255$ (Figure 4C). No differences were detected between lesional vHSIL and healthy controls (0.040 \pm 0.017, $p=0.347$). In addition, blood flow in non-lesional vHSIL skin differed significantly from healthy controls (0.063 \pm 0.040, $p=0.0001$). Blood flow was significantly higher in pre-treatment lesional LS (0.053 \pm 0.029) compared to non-lesional LS (0.034 \pm 0.019, $p<0.0001$) and healthy controls (0.040 \pm 0.012, $p=0.0024$) (Figure 4D). Blood flow in non-lesional LS did not differ significantly compared to healthy controls ($p=0.077$). When baseline was compared to post-treatment measurements, no differences were observed between pre- and post-clobetasol-treated LS (0.057 \pm 0.042) ($p=0.532$). Blood flow measurements could fluctuate over time (Day 0, 2, 8, 22 and 36), depending on sample location (lesional vs non-lesional) (Figure S8).

HISTOLOGICAL ANALYSIS

All clinical diagnoses of non-lesional and lesional skin of vHSIL, non-lesional LS and healthy controls were confirmed in biopsy (Table S2). The biopsies of lesional LS were classified as LS in 3/10 cases. The remaining 7 were classified as normal skin with inflammatory reactive changes (e.g. acanthosis, lymphohistiocytic inflammation), although clinical diagnosis had been confirmed by a specialized gynaecologist (MVP) prior to enrollment. Positivity for HPV 16 was identified in 4/5 lesional vHSIL biopsies. One lesional LS biopsy tested positive for HPV type 53, while no HPV was found in non-lesional or healthy control biopsies.

PATIENT-FRIENDLINESS AND TREATMENT COMPLIANCE

All imaging methods applied in this study were considered mildly burdensome and therefore patient-friendly across cohorts. The vulvar biopsy

procedure was considered substantially more burdensome than all non-invasive imaging procedures, with mean reported scores over 20 mm (Figure S9). For LS patients, treatment compliance measured with the electronic diary was 99%.

Discussion

MAIN FINDINGS

This exploratory study shows that the application of dermatoscopy and D-OCT is feasible and tolerable in vHSIL and LS patients. The most prominent finding with dermatoscopy was the presence of sclerotic areas and arborizing vessels in LS and warty structures for vHSIL. Structural OCT images could be aligned for both diseases with histology for characteristics such as hyperkeratosis and dermal-epidermal junction visualisation. A novel finding in this study was the increased blood flow measured by the algorithm of the D-OCT in vulvar LS compared to healthy tissue. Epidermal thickness determination by OCT should be considered for research purposes only at this stage.

STRENGTHS AND LIMITATIONS

The main strength of this study is the prospective trial design in vulvar patients and healthy controls including within-subject lesional and non-lesional control. Image acquisition and analyses were performed in a structured manner, allowing for side-to-side comparisons of techniques. The study was carried out in a clinical research facility that allowed for standardized image and measurement acquisition (i.e. light conditions, temperature and operators). The dermatoscopic follow-up functionality allowed for exact traceability of image location throughout the study (Figure S3). In addition, the biopsy location aligned with the obtained non-invasive measurements. Performing a data-rich pilot trial in vulvar disease has inherently resulted in a modest sample sizes.³²

Unfortunately, vSCC patients could not be recruited, mainly due to the short and emotionally intense period between the diagnosis and timely scheduled surgical excision. The initial intention of this pilot trial had been to include vSCC patients to portray the complete pathway from healthy vulvar skin to vSCC. This statement could be expanded to all patients visiting the vulvar consultation office with a variety of vulvar diseases, as the

possible discriminative nature of promising characteristics should be validated in a practical sample. In addition, to contribute a diverse and representative study population in a follow-up study, women with all Fitzpatrick skin types should be included. Finally, seven out of ten histological assessments of LS patients were incongruent with the clinical diagnosis. This discrepancy is not considered a limitation in itself, but highlights the heterogeneous nature of the vulvar skin, as well as vHSIL and LS. This clinical, morphological, and histological variability could influence the findings of our study and should be considered in further interpretation.

INTERPRETATION

Dermatoscopy is an integrative part of the dermatologists' evaluation of potentially malignant cutaneous lesions.¹⁰ However, the evaluation of vulvar disease using sophisticated imaging devices is uncommon in daily vulvar clinic or gynecological practice.³³ An expanding catalogue of reports describe dermatoscopy for vulvar lesions, but a well-established and structured approach of image acquisition and reporting remains lacking.^{11,12,34-36} Observations in intraepithelial neoplasia have been summarized in a recent review, although the overview does not include stratification for sex or disease subtypes (i.e. vHSIL or the HPV-independent differentiated vulvar intraepithelial neoplasia).³⁷ The currently recognized characteristics include red to white structureless areas in addition to presence of dotted, glomerular and linear vessels. Grey-brownish dots have been described in pigmented intraepithelial neoplasia lesions. Our dermatoscopy results in vHSIL concur with literature, although the modest patient population restricts further comparisons. In addition, features identified in vHSIL could also be found in LS or healthy controls, rendering none of the identified characteristics disease specific. The only distinctive feature in our study were the warty structures in vHSIL. However, this observation adds little clinical value as this feature is clear upon visual inspection by the examining clinician. Plus, many vulvar diagnoses may present as warty structures, such as condylomata acuminata or papillomatosis.³⁸ On D-OCT, we found an increased blood flow in non-lesional vHSIL compared to healthy vulvar skin. This observation may be due to a more extensively inflamed vulvar area, besides the clinically observable vHSIL lesion(s). This implies that non-lesional, apparently healthy, vulvar skin of vHSIL patients should not be considered a valid healthy control, i.e. within-patient controls can cause potential

confounding. The same notion applies for non-lesional LS skin, which can appear without clinical signs of LS but in fact may comprise of pre-clinical diseased vulvar skin. Our conclusions may have been influenced by the small cohort and potential artefacts from warty lesional structures on the blood flow measurements. Histologically, acanthosis is a well-known feature vHSIL.³ Structural OCT analysis non-invasively found a thicker epidermis for lesional vHSIL than healthy vulvar skin, as reported once previously.²¹ However, the OCT software algorithm is inadequate for epidermal thickness measurements, most likely due to anatomically irregular vulvar structures. Unfortunately, manual epidermal thickness determination is too time-consuming for clinical application at this stage. Improvement of the software algorithm for vulvar skin would be required to make this OCT parameter applicable for practical implementation. Several reports have described dermatoscopic features of LS, both in men and women.³⁹⁻⁴⁴ A recent review summarized dermatoscopic features of LS, which reportedly appears with structureless areas, red globules in a white background with a decrease, or *desertification*, of vessels.³⁷ Our observations are in line with these results, with the notable exception with regard to vascular changes in a number of cases. We found more pronounced vasculature primarily consisting of thick and thin arborizing vessels in approximately 40% of LS cases. Generally, these patients presented clinically with a loss of vulvar architecture. Literature is yet undecided whether dermatoscopic vascular patterns could correlate to disease duration.^{25,43}

These newly described dermatoscopic thick and thin arborizing vessels concur with established histological features of hyalinized, stiff vessels in the dermis of LS.^{28,29} These stiff vessels translated into the observed increase in blood flow in lesional LS vulvar skin, as measured by D-OCT. We hypothesize that this could be the result of sclerosis and damage to the connective tissue in LS, affecting the microvasculature of the dermis.⁴⁵ The observed increase in dermal blood flow in LS has not previously been objectified by D-OCT, but has previously been described using Doppler.⁴⁶

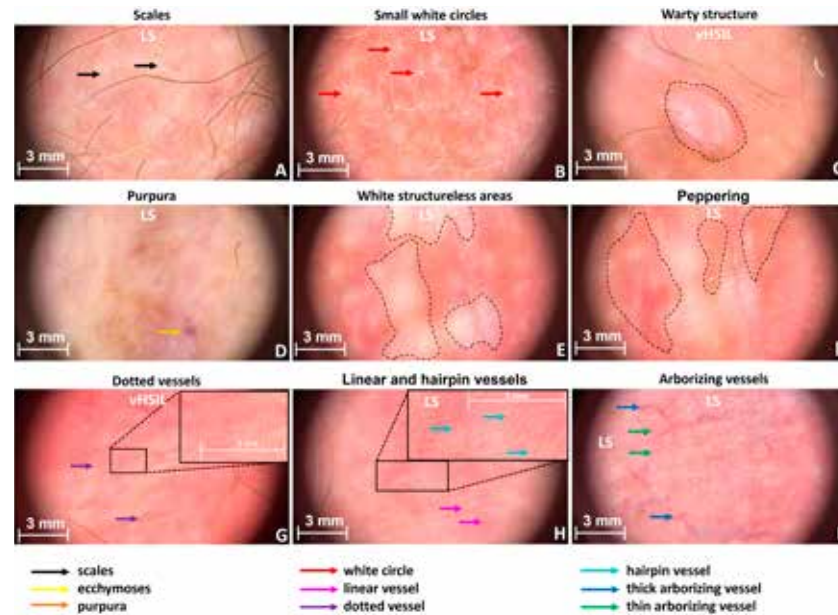
Histologically, the vulvar epidermis in LS is thinner compared to healthy vulvar skin.^{29-47,48} We confirm epidermal thinning in LS numerically and morphologically using non-invasive structural OCT measurements.

Conclusions

This study describes a structured, prospective approach to identify sophisticated imaging methods to identify disease characteristics for vHSIL and LS. Using dermatoscopy and D-OCT, we described potential characteristics to aid differentiation of diseased from healthy vulvar skin, which can complement clinical assessments. Dermatoscopy is a promising tool that may facilitate clinical recognition and follow-up of vHSIL and LS after expansion of patient groups and clinical validation. Vulvar biopsies can be obtained on a limited basis, whilst non-invasive techniques can be used repeatedly, minimizing patient burden as demonstrated in this study. The step to clinical integration of D-OCT is considered inappropriate at this stage due to the suboptimal algorithms and remaining questions on the applicability of the biomarker for the clinical practice. Imaging techniques should always be preceded by visual examination for the establishment of a clinical differential diagnosis. Our findings need to be confirmed in larger, more diverse cohorts including suspicious lesions of the vulva over time before implementation in the vulvar clinic.

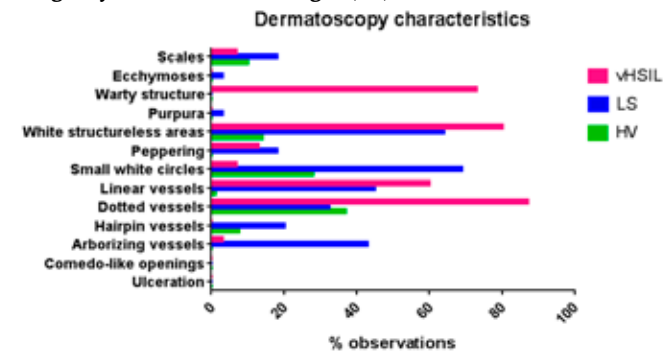
Figure 1 Representative images showing examples of scored characteristics.

A) Scales (LS) B) Small white circles (LS) C) Warty structure (vHSIL) D) Purpura (LS) E) White structureless areas (LS) F) Peppering (LS) G) Dotted vessels (vHSIL) H) Linear and hairpin vessels (LS) I) Thick and thin arborizing vessels (LS).



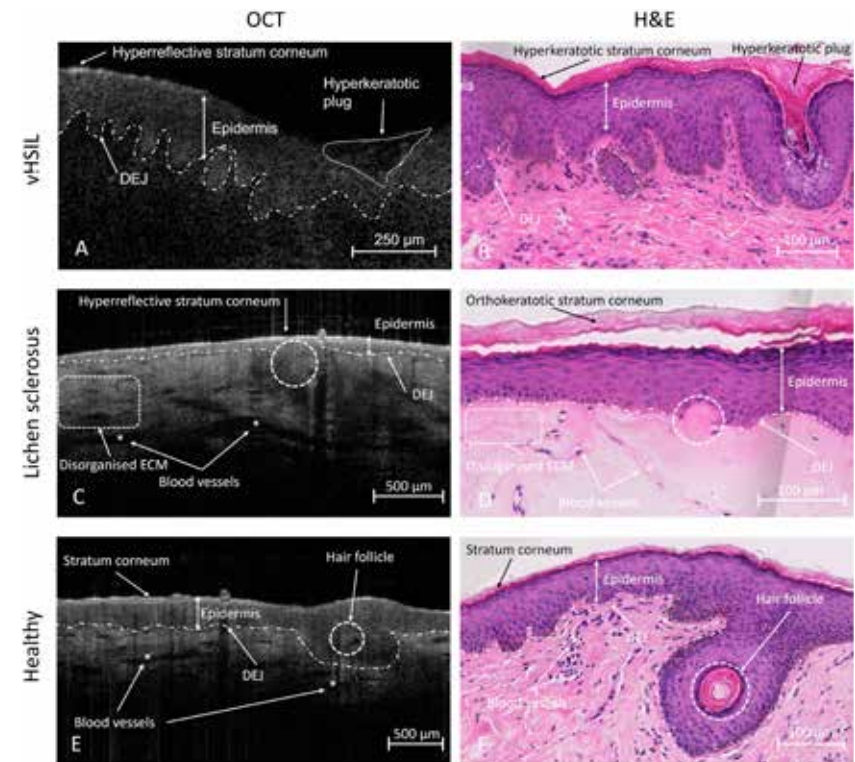
vHSIL=vulvar high-grade squamous intraepithelial lesion, LS=lichen sclerosis

Figure 2 Percentage of observed characteristics per patient group (85 photos were scored: 15 vHSIL, 40 LS and 30 HV) from the scoring of microscopic dermatoscopy images by a blinded dermatologist (CH).



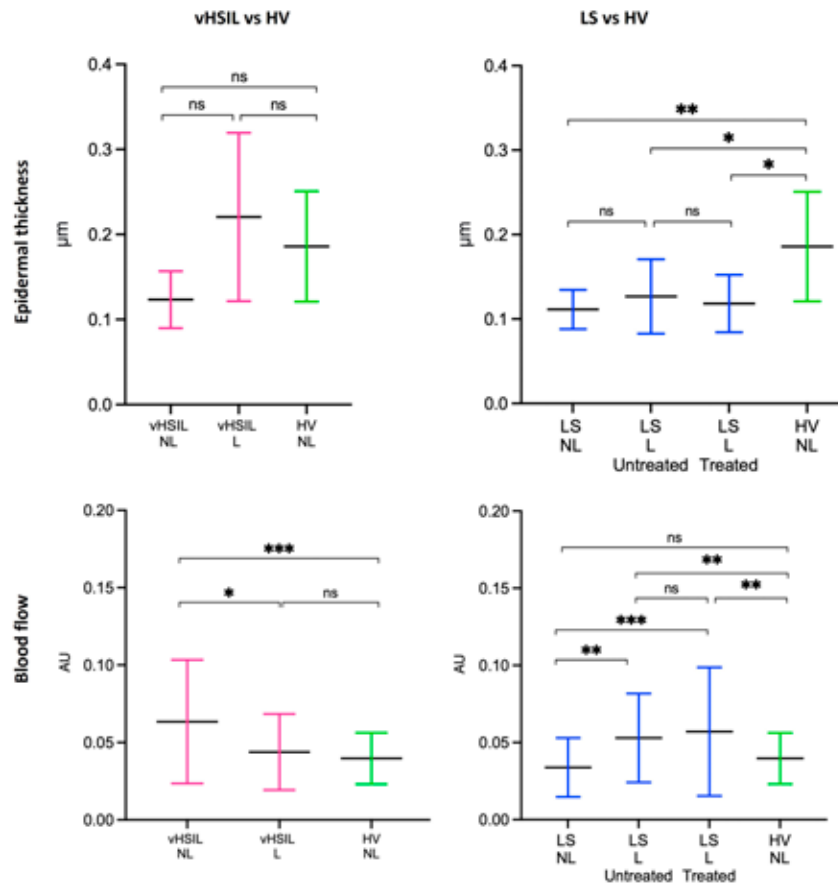
vHSIL=vulvar high-grade squamous intraepithelial lesion, LS=lichen sclerosis, HV=healthy vulva.

Figure 3 Structural OCT recordings compared to aligned histological assessments of A+B) vHSIL, C+D) lichen sclerosis and E+F) healthy volunteers. Asterisks (*) indicate blood vessels.



OCT=optical coherence tomography, H&E=hematoxylin and eosin, vHSIL=vulvar high-grade squamous intraepithelial lesion; DEJ=dermal-epidermal junction; ECM=extracellular matrix

Figure 4 D-OCT epidermal thickness measurements (manually determined using ImageJ) and blood flow measurements (determined by incorporated algorithm). Measurements were assessed at baseline (D1H0) and, for LS only, post-treatment (D35). The mean and standard deviations are displayed for each group. A) Epidermal thickness in μm (y-axis) is plotted against measurements clustered per patient group (x-axis). B) The average blood flow measured between a skin depth of 0.10-0.35 μm at non-biopsy sites of vHSIL and LS subjects compared to healthy controls. The mean and standard deviations are displayed for each group, as well as individual data points. Blood flow in AU (y-axis) plotted against measurements clustered per patient group (x-axis).



ns= $p > 0.05$, *= $p < 0.05$, **= $p < 0.01$, ***= $p < 0.001$, ****= $p < 0.0001$. vHSIL=vulvar high-grade squamous intraepithelial lesion, LS=lichen sclerosus, HV=healthy vulva. L=lesional and NL=non-lesional skin.

REFERENCES

- Voss FO, Thuijs NB, Vermeulen RFM, Wilthagen EA, van Beurden M, Bleeker MCG. The vulvar cancer risk in differentiated vulvar intraepithelial neoplasia: A systematic review. *Cancers (Basel)*. 2021;13(24). doi:10.3390/cancers13246170/S1
- Hacker NF, Eifel PJ, van der Velden J. Cancer of the vulva. *Int J Gynecol Obstet*. 2012;119:S90-S96. doi:https://doi.org/10.1016/S0020-7292(12)60021-6
- Hoang LN, Park KJ, Soslow RA, Murali R. Squamous precursor lesions of the vulva: current classification and diagnostic challenges. *Pathology*. 2016;48(4):291-302. doi:10.1016/j.pathol.2016.02.015
- Sherman V, McPherson T, Baldo M, Salim A, Gao X, Wojnarowska F. The high rate of familial lichen sclerosus suggests a genetic contribution: An observational cohort study. *J Eur Acad Dermatol Venereol*. 2010;24(9):1031-1034. doi:10.1111/j.1468-3083.2010.03572.x
- Cooper SM, Ali I, Baldo M, Wojnarowska F. The association of lichen sclerosus and erosive lichen planus of the vulva with autoimmune disease: a case-control study. *Arch Dermatol*. 2008;144(11):1432-1435. doi:10.1001/ARCHDERM.144.11.1432
- Lockhart J, Gray NM, Cruickshank ME. The development and evaluation of a questionnaire to assess the impact of vulval intraepithelial neoplasia: a questionnaire study. *BJOG*. 2013;120(9):1133-1142. doi:10.1111/1471-0528.12229
- Lockhart J, Gray N, Cruickshank M. The development and evaluation of a questionnaire to assess the impact of vulval intraepithelial neoplasia: a questionnaire study. *BJOG-An Int J Obstet Gynaecol*. 2013;120(9):1133-1143. doi:10.1111/1471-0528.12229
- Grimm D, Eulenburger C, Brummer O, et al. Sexual activity and function after surgical treatment in patients with (pre)invasive vulvar lesions. *Support Care Cancer*. 2016;24(1):419-428. doi:10.1007/s00520-015-2812-8
- Kruizinga MD, Stuurman FE, Exadaktylos V, et al. Development of Novel, Value-Based, Digital Endpoints for Clinical Trials: A Structured Approach Toward Fit-for-Purpose Validation. *Pharmacol Rev*. 2020;72(4):899-909. doi:10.1124/PR.120.000028
- Ring C, Cox N, Lee JB. Dermatoscopy. *Clin Dermatol*. 2021;39(4):635-642. doi:10.1016/J.CLINDERMATOL.2021.03.009
- Rongier-Savle S, Julien V, Duru G, Raudrant D, Dalle S, Thomas L. Features of pigmented vulval lesions on dermoscopy. *Br J Dermatol*. 2011;164(1):54-61. doi:10.1111/j.1365-2133.2010.10043.x
- Ferrari A, Zalaudek I, Argenziano G, et al. Dermoscopy of pigmented lesions of the vulva: a retrospective morphological study. *Dermatology*. 2011;222(2):157-166. doi:10.1159/000323409
- Cengiz FP, Emiroglu N, Hofmann Wellenhof R. Dermoscopic and clinical features of pigmented skin lesions of the genital area. *An Bras Dermatol*. 2015;90(2):178-183. doi:10.1590/ABD1806-4841.20153294
- Fujimoto J, Swanson E. The Development, Commercialization, and Impact of Optical Coherence Tomography. *Invest Ophthalmol Vis Sci*. 2016;57(9):OCT1-OCT13. doi:10.1167/iov.16-19963
- Marschall S, Sander B, Mogensen M, Jørgensen TM, Andersen PE. Optical coherence tomography-current technology and applications in clinical and biomedical research. *Anal Bioanal Chem*. 2011;400(9):2699-2720. doi:10.1007/S00216-011-5008-1
- Wan B, Ganier C, Du-Harpur X, et al. Applications and future directions for optical coherence tomography in dermatology. *Br J Dermatol*. 2021;184(6):1014-1022. doi:10.1111/BJD.19553
- Katkar RA, Tadinada SA, Amaechi BT, Fried D. Optical Coherence Tomography. *Dent Clin North Am*. 2018;62(3):421-434. doi:10.1016/j.cden.2018.03.004
- Markowitz O, Schwartz M, Feldman E, et al. Evaluation of Optical Coherence Tomography as a Means of Identifying Earlier Stage Basal Cell Carcinomas while Reducing the Use of Diagnostic Biopsy. *J Clin Aesthet Dermatol*. 2015;8(10):14. Accessed June 10, 2022. /pmc/articles/PMC4633207/
- Kirillina M, Motovilova T, Shakhova N. Optical coherence tomography in gynecology: a narrative review. *J Biomed Opt*. 2017;22(12):1. doi:10.1117/1.JBO.22.12.121709
- Escobar PF, Belinson JL, White A, et al. Diagnostic efficacy of optical coherence tomography in the management of preinvasive and invasive cancer of uterine cervix and vulva. *Int J Gynecol Cancer*. 2004;14(3):470-474. doi:10.1136/ijgc-00009577-200405000-00008
- Wessels R, Bruin DM de, Faber DJ, et al. Optical coherence tomography in vulvar intraepithelial neoplasia. <https://doi.org/10.1117/1.JBO.17.11.116022>. doi:10.1117/1.JBO.17.11.116022
- Xu L, Ma Q, Lin S, et al. Study on the application and imaging characteristics of optical coherence tomography in vulva lesions. *Sci Rep*. 2022;12(1):3659. doi:10.1038/S41598-022-07634-1
- Rissmann R, Moerland M, van Doorn MBA. Blueprint for mechanistic, data-rich early phase clinical pharmacology studies in dermatology. *Br J Clin Pharmacol*. Published online 2020. doi:10.1111/bcp.14293
- Hehir M, Vivier A Du, Eilon L, Danie Mj, Shenoy Evb. Investigation of the pharmacokinetics of clobetasol propionate and clobetasone butyrate after a single application of ointment. *Clin Exp Dermatol*. 1983;8(2):143-151. doi:10.1111/j.1365-2230.1983.tb01758.x
- Borghi A, Virgili A, Corazza M. Dermoscopy of Inflammatory Genital Diseases: Practical Insights. *Dermatol Clin*. 2018;36(4):451-461. doi:10.1016/j.det.2018.05.013
- Borghi A, Corazza M, Minghetti S, Toni G, Virgili A. Clinical and dermoscopic changes of vulvar lichen sclerosus after topical corticosteroid treatment. *J Dermatol*. 2016;43(9):1078-1082. doi:10.1111/1346-8138.13374
- Themstrup L, Welzel J, Ciardo S, et al. Validation of Dynamic optical coherence tomography for non-invasive, *in vivo* microcirculation imaging of the skin. *Microvasc Res*. 2016;107:97-105. doi:10.1016/j.mvr.2016.05.004

- Available from: <https://pubmed.ncbi.nlm.nih.gov/36232952/>
- 23 Han SN, Vergote I, Amant F. Weekly paclitaxel-carboplatin in the treatment of locally advanced, recurrent, or metastatic vulvar cancer. *Int J Gynecol Cancer* [Internet]. 2012 Jun [cited 2022 Sep 28];22(5):865–8. Available from: <https://pubmed.ncbi.nlm.nih.gov/22552830/>
 - 24 Witteveen PO, van der Velden J, Vergote I, Guerra C, Scarabeli C, Coens C, et al. Phase II study on paclitaxel in patients with recurrent, metastatic or locally advanced vulvar cancer not amenable to surgery or radiotherapy: a study of the EORTC-GCG (European Organisation for Research and Treatment of Cancer – Gynaecological Cancer Group). *Ann Oncol Off J Eur Soc Med Oncol* [Internet]. 2009 [cited 2022 Sep 28];20(9):1511–6. Available from: <https://pubmed.ncbi.nlm.nih.gov/19487487/>
 - 25 Karanam V, Marslin G, Krishnamoorthy B, Chellan V, Siram K, Natarajan T, et al. Poly (□-caprolactone) nanoparticles of carboplatin: Preparation, characterization and in vitro cytotoxicity evaluation in U-87 MG cell lines. *Colloids SuRF B Biointerfaces* [Internet]. 2015 Jun 1 [cited 2022 Sep 29];130:48–52. Available from: <https://pubmed.ncbi.nlm.nih.gov/25899843/>
 - 26 Khan MA, Zafaryab M, Mehdi SH, Quadri J, Rizvi MMA. Characterization and carboplatin loaded chitosan nanoparticles for the chemotherapy against breast cancer in vitro studies. *Int J Biol Macromol* [Internet]. 2017 Apr 1 [cited 2022 Sep 29];97:115–22. Available from: <https://pubmed.ncbi.nlm.nih.gov/28082219/>
 - 27 Carboplatin-paclitaxel- and carboplatin-docetaxel-induced cytotoxic effect in epithelial ovarian carcinoma in vitro- PubMed [Internet]. [cited 2022 Sep 28]. Available from: <https://pubmed.ncbi.nlm.nih.gov/10570433/>
 - 28 Raitanen M, Rantanen V, Kulmala J, Helenius H, Grénman R, Grénman S. Supra-additive effect with concurrent paclitaxel and cisplatin in vulvar squamous cell carcinoma in vitro. *Int J cancer* [Internet]. 2002 Jul 10 [cited 2022 Sep 29];100(2):238–43. Available from: <https://pubmed.ncbi.nlm.nih.gov/12115575/>
 - 29 Sawatani Y, Komiyama Y, Nakashiro KI, Uchida D, Fukumoto C, Shimura M, et al. Paclitaxel Potentiates the Anticancer Effect of Cetuximab by Enhancing Antibody-Dependent Cellular Cytotoxicity on Oral Squamous Cell Carcinoma Cells In Vitro. *Int J Mol Sci* [Internet]. 2020 Sep 1 [cited 2022 Sep 29];21(17):1–11. Available from: <https://pubmed.ncbi.nlm.nih.gov/11309356/>
 - 30 Calcitriol (1,25-dihydroxycholecalciferol) enhances paclitaxel antitumor activity in vitro and *in vivo* and accelerates paclitaxel-induced apoptosis- PubMed [Internet]. [cited 2022 Sep 29]. Available from: <https://pubmed.ncbi.nlm.nih.gov/11309356/>
 - 31 Human Tissue and Medical Research: Code of Conduct for responsible use (2011). [cited 2022 Sep 29]; Available from: www.federa.org
 - 32 Thakoersing VS, Gooris GS, Mulder A, Rietveld M, El Ghalbzouri A, Bouwstra JA. Unraveling barrier properties of three different in-house human skin equivalents. *Tissue Eng- Part C Methods*. 2012 Jan 1;18(1):1–11.
 - 33 Freedberg IM, Tomic-Canic M, Komine M, Blumenberg M. Keratins and the keratinocyte activation cycle. *J Invest Dermatol* [Internet]. 2001 [cited 2022 Aug 16];116(5):633–40. Available from: <https://pubmed.ncbi.nlm.nih.gov/11348449/>
 - 34 Moll R, Franke WW, Schiller DL, Geiger B, Krepler R. The catalog of human cytokeratins: patterns of expression in normal epithelia, tumors and cultured cells. *Cell* [Internet]. 1982 [cited 2022 Aug 16];31(1):11–24. Available from: <https://pubmed.ncbi.nlm.nih.gov/6186379/>
 - 35 Roig-Rosello E, Rousselle P. The Human Epidermal Basement Membrane: A Shaped and Cell Instructive Platform That Aging Slowly Alters. *Biomolecules* [Internet]. 2020 Dec 1 [cited 2022 Aug 16];10(12):1–32. Available from: <https://pubmed.ncbi.nlm.nih.gov/33260936/>
 - 36 Kortekaas KE, Bastiaannet E, van Doorn HC, de Vos van Steenwijk PJ, Ewing-Graham PC, Creutzberg CL, et al. Vulvar cancer subclassification by HPV and P53 status results in three clinically distinct subtypes. *Gynecol Oncol* [Internet]. 2020 Dec 1 [cited 2021 May 17];159(3):649–56. Available from: <https://pubmed.ncbi.nlm.nih.gov/32972785/>
 - 37 Tessier-Cloutier B, Kortekaas KE, Thompson E, Pors J, Chen J, Ho J, et al. Major P53 immunohistochemical patterns in in situ and invasive squamous cell carcinomas of the vulva and correlation with TP53 mutation status. *Mod Pathol* 2020 338 [Internet]. 2020 Mar 20 [cited 2022 Aug 16];33(8):1595–605. Available from: <https://www.nature.com/articles/s41379-020-0524-1>
 - 38 Quail DF, Joyce JA. Microenvironmental regulation of tumor progression and metastasis. *Nat Med* [Internet]. 2013 Nov [cited 2022 Aug 16];19(11):1423–37. Available from: <https://pubmed.ncbi.nlm.nih.gov/24202395/>
 - 39 Hogervorst M, Rietveld M, de Grijl F, El Ghalbzouri A. A shift from papillary to reticular fibroblasts enables tumour-stroma interaction and invasion. *Br J Cancer* [Internet]. 2018 Apr 1 [cited 2021 Oct 28];118(8):1089–97. Available from: <https://pubmed.ncbi.nlm.nih.gov/29551776/>
 - 40 Kalluri R, Zeisberg M. Fibroblasts in cancer. *Nat Rev Cancer* [Internet]. 2006 May [cited 2021 Dec 28];6(5):392–401. Available from: <https://pubmed.ncbi.nlm.nih.gov/16572188/>
 - 41 Their JP. Epithelial-mesenchymal transitions in tumour progression. *Nat Rev Cancer* [Internet]. 2002 [cited 2021 Dec 28];2(6):442–54. Available from: <https://pubmed.ncbi.nlm.nih.gov/12189386/>
 - 42 Abdulrahman Z, Kortekaas KE, De Vos Van Steenwijk PJ, Van Der Burg SH, Van Poelgeest MIE. The immune microenvironment in vulvar (pre)cancer: review of literature and implications for immunotherapy. *Expert Opin Biol Ther* [Internet]. 2018 Dec 2 [cited 2022 Aug 16];18(12):1223–33. Available from: <https://pubmed.ncbi.nlm.nih.gov/30373410/>
 - 43 Räsänen K, Vaheri A. Activation of fibroblasts in cancer stroma. *Exp Cell Res* [Internet]. 2010 [cited 2022 Sep 29];316(17):2713–22. Available from: <https://pubmed.ncbi.nlm.nih.gov/20451516/>

SECTION III

MOLECULAR TARGET IDENTIFICATION OF VULVAR CARCINOMAS

CHAPTER 5

Potential targets for tumor-specific imaging of vulvar squamous cell carcinoma: a systematic review of candidate biomarkers.

B.W. Huisman^{a,b}, J. Burggraaf^{a,c,d}, A.L. Vahrmeijer^d, J.W. Schoones^e,
R.A. Rissmann^{a,c}, C.F.M. Sier^d, M.I.E. van Poelgeest^{a,b}



a Centre for Human Drug Research, Leiden, NL

b Department of Gynecology, Leiden University Medical Center, Leiden, NL

c Leiden Academic Center for Drug Research, Leiden University, Leiden, NL.

d Department of Surgery, Leiden University Medical Center, Leiden, NL

e Walaeus Library, Leiden University Medical Center, Leiden, NL

Abstract

INTRODUCTION Vulvar squamous cell carcinoma (vSCC) is a rare malignancy with an increasing incidence, especially in young women. Surgical treatment of vSCC is associated with significant morbidity and high recurrence rates, which is related to the limited ability to distinguish (pre)malignant from healthy tissue. There is a need for new tools for specific real-time detection of occult tumor lesions and localization of cancer margins in patients with vSCC. Several tumor-specific imaging techniques are developed to recognize malignant tissue by targeting tumor markers. We present a systematic review to identify, evaluate, and summarize potential markers for tumor-specific imaging of vSCC.

METHODS Relevant papers were identified by a systematic cross-database literature search developed with assistance of an experienced librarian. Data were extracted from eligible papers and reported based on the Preferred Reporting Items for Systematic reviews and Meta-Analyses (PRISMA) guidelines. vSCC-specific tumor markers were valued based on a weighted scoring system, in which each biomarker was granted points based on ranked eligibility criteria: I) percentage expression, II) sample size, and III) *in vivo* application.

RESULTS In total 627 papers were included of which 22 articles met the eligibility criteria. Twelve vSCC-specific tumor markers were identified and of these 7 biomarkers were considered most promising: EGFR, CD44V6, GLUT1, MRP1, MUC1, CXCR-4 and VEGF-A.

DISCUSSION This overview identified 7 potential biomarkers that can be used in the development of vSCC-specific tracers for real-time and precise localization of tumor tissue before, during, and after treatment. These biomarkers were identified in a small number of samples, without discriminating for vSCC-specific hallmarks such as HPV-status. Before clinical development, experimental studies should first aim at validation of these biomarkers using immunohistochemistry and cell line-based examination, discriminating for HPV-status and the expression rate in lymph nodes and precursor lesions.

Introduction

Vulvar carcinomas represent around 2-5% of all gynecological cancers and the incidence is rising, especially in young women.¹ Vulvar squamous cell carcinoma (vSCC) is the most common histopathological type and constitutes 80-90% of all vulvar cancers. There are two different pathophysiological pathways for vSCC: (I) a high-risk human papillomavirus (HPV) dependent type, accounting for 20% of all vSCC's, which is often associated with high grade squamous intraepithelial lesion (HSIL) and occurs mostly in younger women, and (II) an HPV-independent type associated with lichen sclerosis which is mostly observed in older women.²

Surgery with or without adjuvant (chemo)radiotherapy is the cornerstone of treatment of vSCC. Surgical treatment is frequently associated with significant morbidity, which is partly related to the limited ability to distinguish between healthy and malignant tissue, both before and during surgery. Positive surgical margins are associated with high local recurrence rates up to 40% and corresponding poor survival (5-year survival for recurrent vSCC is reported to be 25-50%).^{3,4} In addition, precursor lesions are often found adjacent to the tumor, which are sometimes difficult to identify clinically with current available imaging modalities. Consequently, incorrect identification results in re-excisions, local recurrences, regional metastases and associated worse prognosis. Moreover, when (pre)malignant lesions are located near the urethra, clitoris, or anus, surgery may be technically challenging with suboptimal results, ensuing in a decreased quality of life. This underlines the high unmet medical need for clinicians to more optimally discriminate tissue abnormalities of the vulva.

Currently there are no real-time techniques to distinguish (pre)malignant from healthy tissue during surgery, equivalent to the pathological assessment of hematoxylin/eosin stained vulvar tissue sections suspected of tumor invasion. Gynecologists rely on visual and tactile information, and experience for the identification of tumor tissue or distinction of tissue margins, before, during and after treatment. Treatment of patients can be improved upon the availability of safe and specific real-time detection of occult tumor lesions and localization of cancer margins. Such techniques will enhance personalized treatment decisions and minimize the risk of residual disease.

Molecular imaging integrates advanced imaging modalities with probes targeting molecular biomarkers of interest. This technique plays a signifi-

cant role in accurate diagnosis of several cancer types and is generally safe to apply. An imaging probe consists of a contrast label, such as radionuclides for nuclear based imaging, paramagnetic or electron opaque substances for radiological techniques, or bioluminescent or fluorescent molecules for optical imaging,⁵ which is conjugated to a molecular imaging agent with high affinity for a biomarker selectively expressed at the surface of tumor(-associated) cells (Figure 1). Small molecules, peptides, aptamers, antibodies, protein fragments and nanoparticles have been used as molecular imaging agents. After administration of an imaging probe, real-time images of the tissue of interest can be obtained by a suitable camera system that generates optical contrast between tumor and surrounding healthy tissue.⁶ This review will mainly focus on imaging agents applicable for optical imaging, as this modality benefits of its high-spatial resolution and real-time localization. An example of optical imaging coupled with image-guided surgery is Fluorescent Guided Surgery (FGS), which has been widely explored in the last decade.⁶ Particularly, the use of near-infrared (NIR) fluorescence dyes can most likely provide sufficient tissue penetration for vulvar carcinoma, though thus far, targeted imaging has not been used to detect VSCC.

The following characteristics define a potential protein marker for targeted imaging: extracellular biomarker localization, expression pattern, tumor-to-healthy tissue ratio, percentage and distribution of positive cells, and previous use of the biomarker for *in vivo* targeted imaging.^{7,8} Based on these criteria we rank the feasibility of different vulva-specific biomarkers, found through systematic analysis of the scientific literature using the PRISMA guidelines. The purpose of this review is to provide an overview of potential tumor specific targets for VSCC. These vulva-specific biomarkers could serve as targets for molecular imaging and help develop a structured approach of tumor-visualization.

Methods

This study was performed according to the PRISMA guidelines.⁹

SEARCH STRATEGY

Relevant scientific papers were identified by a systematic online cross-database search performed in July 2019, using PubMed, Embase, Web of Science, Cochrane Library and Academic Search Premier. Search strategies for all

databases were adapted from the PubMed strategy and developed with assistance of an experienced librarian of the Walaeus Library of the Leiden University Medical Center (JS). The search strategy consisted of the medical subject headings and text words related to the keywords 'vulvar carcinoma', 'target proteins' and abbreviations thereof. See Appendix I for the complete search strategies for each database.

ELIGIBILITY

Clinical trials (phase I, II, and III), and prospective or retrospective cohort studies were included. The following eligibility criteria were set: (1) Report of cell surface protein expression in more than 40% of the human VSCC tumor or tumor-associated cells, such as stromal cells, and (2) Evaluation of cell surface protein expression by immunohistochemistry. Results from flow cytometry analysis of cell lines were considered as advantageous but non-decisive. Animal studies, (systematic) reviews, not-English published abstracts and case reports were excluded.

TARGET SELECTION

Tumor-specific imaging is based on the distinction between malignant and healthy tissue. However, information about the expression of the target in non-malignant vulvar tissue and the pattern of expression is mostly lacking in the included studies. It was therefore chosen to leave these characteristics out of the target selection and refer to these if known in the descriptive text of the potential marker headings in the result section. To select potential tumor specific targets for optical imaging in VSCC, a weighted scoring system was used, adapted from the target selection criteria (tasc) scoring system.^{8,10} Biomarkers were granted points (0-2), based on three criteria (table 1). The criteria were prioritized to value certain criteria more important than others. The percentage expression score (criterion I) was chosen the most determinative factor and granted most weight, followed by the criteria *in vivo* application score (criterion II, based on the review of herot et al.⁶), indicating previously use of the target for imaging of other cancer types. The least weight was assigned to the sample size score (criterion III). If more than one publication described the same target, the scoring system was applied to all articles. An average expression rate and a total sample size (n) was calculated for the particular target. Some publications described multiple potential targets.

Table 1 Target scoring system. Eligible biomarkers are granted points (0–2) based on three criteria: I) Percentage expression: percentage of vSCC samples expressing the target of interest; II) In vivo application: previously *in vivo* application of an imaging agent against the target of interest; III) Sample size: total number of vSCC samples tested within a study.

Target scoring system	0	1	2
I Percentage expression	50 – 65%	66 – 80%	>81%
II <i>In vivo</i> application	No		Yes
III Sample size	0 – 9	10 – 50	>50

Results

STUDY SELECTION

The literature searches yielded 1207 records: PubMed n=440; Embase n=439; Web of Science n=237; Cochrane Library n=9; Academic Search Premier n=82. After removal of duplicates, 627 records were available for screening. One investigator (BH) reviewed all titles and abstracts for eligibility based on the above-mentioned criteria, from which 151 full-text articles were obtained. Of the full-text articles, 129 did not meet the eligibility criteria: 76 articles described targets not expressed at the cell surface membrane, 29 articles reported a high expression of the target in healthy vulvar tissue and/or lower expression rates (<40%) of the target in vSCC, 8 articles were not about the expression in vSCC and for 8 articles no full-text was available. In case the investigator (BH) doubted the eligibility of an article, a second investigator (MVP) reviewed the paper and eligibility for inclusion in the review was based on consensus. In total, 22 scientific papers were included, describing 12 potential tumor targets for vSCC. See Figure 2 for the PRISMA flow diagram of the study selection.

CANDIDATE TARGETS

The 12 targets for tumor-specific imaging of vSCC evaluated in the selected 22 scientific papers were scored according to the target scoring system indicated in Table 1. Scores were summarized in Table 2. With an expression average of 65% or higher (score >0): EGFR,¹⁻²¹ CD44V6,²²⁻²⁵ GLUT,²⁶⁻²⁸ MRP1,^{12,13} MUC1²⁹ and CXCR-4³⁰ were considered potential candidates for tumor-specific imaging of vSCC. Although VEGF-A^{22,27,31} showed an average expression of 45% (score 0), it fulfilled both other criteria and therefore

this marker was included as well. The other evaluated targets were considered less potential, based on the granted scores (CD34,³² CA IX,²⁷ SPARC M,¹³ CCND1,¹⁵ BCRP¹²). The seven potential biomarkers for tumor-specific imaging in vSCC are described below. Description of the biomarkers is based on their physiological role, expression in tumor and healthy tissue and the availability of clinical tracers targeted against these biomarkers.

EGFR

Physiological role – Epidermal growth factor receptor (EGFR) is a transmembrane glycoprotein and one of the four members of the Human Epidermal growth factor Receptor (HER) family of tyrosine kinase receptors, consisting of EGFR/HER1, HER2/ERB2, HER3/ERBB3 and HER4/ERB4.³³ Epidermal growth factor binding to EGFR leads to cell proliferation. EGFR in normal epithelium of the skin is mainly expressed in proliferating keratinocytes.³⁴

Tumor upregulation/expression – Squamous carcinomas frequently over-express EGFR, which is thought to be characteristic for the loss of differentiation among keratinocytes and associated with a poor prognosis.^{12,18} Based on this literature search, 11 scientific papers described EGFR expression in vSCC with a total of 747 vSCC immunohistochemically stained samples. Of these samples an average of 67% stained positive (range 36-96%), with a median of 73%. One study observed positive staining for EGFR to be associated with good to moderate grade of differentiation (p=0.01).¹⁶ Another study found a progressive increase in EGFR expression from healthy vulvar tissue to primary malignant tissue to metastatic lesions within the same patient.¹⁸ EGFR expression was reported to be similar among vSCC samples with various FIGO stages.^{19,20} Two articles reported no difference in EGFR expression for HPV-dependent or HPV-independent samples.^{14,19} However, another article described stronger EGFR positivity for IHC mainly in HPV-independent vSCC samples and concluded that EGFR expression trends toward a negative correlation with P16 expression.¹⁵ EGFR expression in relation to lymph node metastases showed that increased expression in the primary vulvar malignancy was significantly associated with presence of lymph node metastases. Tissue of these lymph node metastases showed 88% EGFR expression.¹⁸

Expression in non-malignant vulvar tissue – One study reported EGFR expression in some basal cells in 40% of healthy vulvar tissue, in highly dysplastic cells in 40% of the VIN III and in many neoplastic cells in 80% of

vulvar condylomata acuminata.²¹ These data are consistent with another study wherein 26 out of 61 (43%) healthy vulvar tissue samples stained positive for EGFR.¹⁸ Identical to expression patterns in normal skin, receptor expression was confined to the basal and parabasal keratinocytes and was lost as the cells migrated upward toward the surface of the epithelium. No tumor to healthy ratios for EGFR have been described.

Clinical tracers – A variety of anti-EGFR drugs are currently FDA approved or tested in clinical trials. Moreover, humanized anti-EGFR monoclonal antibodies as panitumumab and cetuximab conjugated to a fluorophore (IRDye800CW) are being tested in several clinical studies for FGS purposes in e.g. head and neck squamous cell carcinomas (HNSCC) and oropharyngeal squamous cell carcinomas (OSCC). In a dose-escalation study with cetuximab labeled to near-infrared fluorophore (IRDye800CW) no adverse events higher than grade 2 were reported.³⁵

CD44V6

Physiological role – CD44 (HCAM, Pgp-1, Hermes antigen) is a cell-surface glycoprotein involved in cell-cell and cell-matrix adhesion and is widely expressed in a variety of human tissues. It interacts as a receptor with hyaluronic acid (HA) but can also bind with other ligands as collagens or matrix metalloproteinases (MMP's). These interactions trigger cell activation, motility and adhesion to other cells. Different isoforms of CD44 exist due to complex alternative splicing of transcripts of the CD44 gene. Various CD44 isoforms were broadly investigated in multiple tissue types and revealed CD44V6 expression to be mainly observed in normal human thyroid, breast, cervix, placenta and skin tissue.³⁶

Tumor expression – Aberrant expression of CD44 isoforms like CD44V6 in human tumors indicates a loss of splice control in malignant cells and has been associated with poor prognosis in human malignancies as breast and oropharyngeal cancer.^{23,37} The major role of isoform v6 involves cell migration and invasion and is thereby a metastatic determinant in aggressive stages of several human cancers, mainly in squamous cell carcinomas.³⁸ Patients expressing CD44V6 in vulvar cancer showed significantly poorer overall and relapse free survival compared with patients whose tumors lacked CD44V6 expression.^{24,25} In the 4 included scientific papers from this literature search, the average expression of CD44V6 on VSCC tissue was 59% (range 33-99%). Different staining patterns were used to score

CD44V6; even the same author used different cut-offs for the conducted studies.^{23,25} Two studies concluded CD44V6 expression not to be correlated to FIGO stage, tumor grade, PTNM classification, histologic grade or type of treatment.^{23,24} One study described CD44V6 staining patterns in primary tumors compared to lymph node metastases and found no obvious differences.²⁴ CD44V6 expression in relation to HPV status was not described in the included scientific papers.

Table 2 Potential targets for tumor-specific imaging of vscC. Tumor markers are shown, followed by the number of included papers relating to this target based on the literature search. Each extracted biomarker is granted points based on ranked criteria; I) percentage expression, II) sample size, and III) *in vivo* application. Solitary patient trials are scored in the *in vivo* application category. EGFR-Epidermal Growth Factor Receptor, CD44V6-CD44 variant 6, GLUT1-Glucose transporter 1, MRP1 -Multidrug resistance-associated protein, MUC1-Mucine 1, CXCR-4-C-X-C chemokine receptor type 4, VEGF-A-Vascular endothelial growth factor A, CA IX-Carbonic anhydrase IX, SPARC M-Secreted protein acidic and cysteine-rich M, CCND1-Cyclin D1, BCRP-Breast cancer resistance protein.

Tumor marker	Expression		In vivo application		Sample size		Included papers	
	average %	score	yes/no	score	(n)	score	(n)	Author, year
EGFR	70	1	yes	2	747	2	11	Fons 2009, Palisoul 2017, Koncar 2017, Lee 2007, Woelber 2012, Oonk 2007, Dong 2015, Johnson 1997, de Melo 2014, Brustmann 2007, Wu 2001
CD44V6	59*	1*	no	0	249	2	4	Fons 2007, Tempfer 1996, Hefler 2002, Tempfer 1998
GLUT1	68	1	no	0	166	2	3	Van de Nieuwenhof 2010, Li 2012, Mayer 2014
MRP1	78	1	no	0	79	2	2	Palisoul 2017, Koncar 2017
MUC1	81	1	no	0	30	1	1	Wu 2000
CXCR-4	68	1	no	0	22	1	1	Shiozaki 2013
VEGF-A	45	0	yes	2	100	1	3	Fons 2007, Li 2012, Obermair 1996
CD34	58	0	no	0	158	2	1	Dhokal 2013
CA IX	52	0	no	0	25	1	1	Li 2012
SPARC M	49	0	no	0	35	1	1	Koncar 2017
CCND1	47	0	no	0	131	1	1	Woelber 2012
BCRP	44	0	no	0	25	1	1	Palisoul 2017

* Borderline value, investigators decided to include this target based on the number of included papers and the total sample size

Expression in non-malignant vulvar tissue – None of the included articles has examined the expression of CD44V6 in healthy vulvar or dysplastic tissue.

Clinical tracers – Several peptides³⁹ and antibodies⁴⁰ have shown potency in CD44V6-targeting. For example, the humanized monoclonal anti-CD44V6 antibody bivatuzumab was shown to be safe in clinical trials and reliably visualized HNSCC lesions by nuclear imaging in humans.⁴¹ Thereafter, bivatuzumab was conjugated with both a near-infrared fluorescent dye (IRDye800CW) and a radioactive label (Indium-111) to perform dual-modality imaging in a HNSCC xenograft mice-model. Bivatuzumab accurately detected human HNSCC xenografts in mice and showed CD44V6 to be a suitable target *in vivo*.⁴²

GLUT1

Physiological role – Glucose transporter 1 (GLUT1, solute carrier family 2, facilitated glucose transporter member 1/SLC2A1) is encoded by the SLC2A1 gene. This uniporter protein is located in the cell membrane and facilitates the transport of glucose into the cell. It is widely expressed on placental tissue, red blood cells and normal capillaries of the brain, consistently with the high uptake of glucose in these cells.⁴³

Tumor expression – Increased glucose intake is also seen after malignant transformation of tissue triggered by hypoxia-induced gene expression.⁴⁴ VSCC is a solid tumor with such a glycolytic phenotype. GLUT1 expression was analyzed in 3 studies with a total sample size of 166 and was on average expressed in 68% (range 50-100%) of the VSCC samples. In general a diffuse staining of a large tumor area was observed, with a focally increased staining intensity, both cytoplasmic and membranous. Less differentiated tumors demonstrated lower GLUT1 expression levels. In several cases, GLUT1 expression was observed directly adjacent to a blood vessel/vascularized tumor stroma. However, the pattern of GLUT1 clearly indicated that a large part of its expression is presumably unrelated to hypoxia. One study investigating increased GLUT1 expression in relation to primary tumor characteristics as differentiation grade, FIGO stage or recurrences found no significant associations.²⁶ In the included scientific papers, GLUT1 expression in relation to HPV status and staining patterns in metastases was not described.

Expression in non-malignant vulvar tissue – Healthy vulvar tissue showed weak staining expressed in basal cells and prickle cells.^{27,28} One study described GLUT1 expression in dysplastic tissue to be comparable to the

observed low expression in healthy vulvar tissue,²⁸ while another study reported expression levels of dysplastic tissue to be more comparable to up-regulated expression as seen in VSCC tissue.²⁷

Clinical tracers – Up to now, no clinical studies have been performed with GLUT1 binding tracers. One pre-clinical study showed that a monoclonal GLUT1 antibody conjugated to iron oxide nanoparticles could effectively target GLUT1 positive tumor cells in infantile hemangioma using MRI.⁴⁵ But, being a glucose channel, GLUT1 targeting is more easily established by determining the accumulation of labelled glucose into tumor cells. Metabolic PET scanning with 18F-fluoro-deoxy-glucose (FDG) makes use of this principle and is widely used in the clinic for tumor imaging, including nodal staging in vulvar cancer.⁴⁶ A near-infrared version, IRDye800CW 2-DG, has been developed and showed specificity in several tumor models in mice, but these data are not yet confirmed in a clinical study.⁴⁷

MRP1

Physiological role – Multidrug resistance-associated protein 1, MRP1 (GS-X), is a protein that in humans is encoded by the ABCB1 gene. MRP1 is a member of the ATP-binding cassette transporters. This type of protein transports molecules across extra- and intracellular membranes. It has been speculated that MRP1 protects against carcinogens by preventing them from entering epithelial cells and is therefore ubiquitously expressed in almost all human tissues.⁴⁸ This transporter may therefore play a role in disrupting optimal cytotoxic agent efficacy by its capacity to mediate efflux of drugs.⁴⁹

Tumor expression – Overexpression of MRP1 is known to occur in cancers as neuroblastoma, breast, and prostate,⁵⁰ but little is known about the involvement in VSCC. MRP1 expression has been tested in two studies with a total of 79 VSCC samples included, showing 80% expression on average (range 77-82%). One study described expression of MRP1 in primary (26/34 samples, 77%) compared to metastatic alteration (22/28 samples, 79%), including metastatic lymph nodes and other distant metastases.¹² MRP1 expression in relation to other tumor characteristics such as FIGO stage or HPV-status have not been described.

Expression in non-malignant vulvar tissue – None of the included articles has examined the expression of MRP1 in healthy vulvar or dysplastic tissue.

Clinical tracers – To our knowledge, no clinical studies have been performed with MRP1 binding tracers. Pre-clinical research on inhibition of

MRP1-mediated transport to avoid multidrug resistance showed that mifepristone, doramapimod and celecoxib are potential inhibitors of MRP1 efflux.⁵⁰ Knowing that these small molecules show high specificity for MRP1, indicates their potential for tumor-specific tracer. Furthermore, a small recombinant scFv antibody directed to an extracellular epitope of the MRP1 in viable malignant cells was isolated. These small Fv-based recombinant antibodies possess superior tumor penetration capabilities and may possibly be used to selectively target drugs or tumor cells expressing MRP1.⁵¹ As for GLUT1, MRP1 targeting is more easily established by determining the cellular uptake of a non-binding tracer selectively passing MRP1 transporters into tumor cells. These tracers could be potential for imaging of MRP1 over-expressing tissues. MRP1 tracers are tested *in vitro* for different application, as for instance to study multidrug resistance.⁵²

MUC1

Physiological role – Mucine 1 (MUC1) is a membrane-bound protein belonging to the mucin family. This protein is O-glycosylated, plays a role in intracellular signaling and is critically important for the formation of a protective mucous barrier on epithelial surfaces. This protein is normally expressed on the apical surface of epithelial cells of mucosal surfaces as stomach and pancreas.⁵³

Tumor expression – Overexpression and changes in glycosylation are associated with carcinogenic development. The one study reporting on MUC1 expression in VSCC tested three monoclonal antibodies (MA695, CA15-3 and DF3) on vulvar tissues. These showed on average positive MUC1 expression of 81% (100%, 84% and 60% for Ma695, CA15-3 and DF3, respectively) in 30 VSCC samples tested. Increased MUC1 expression was related to the degree of differentiation of VSCC, prevalence of expression increased gradually from well through moderately to poorly differentiated VSCC. The prevalence and intensity of MUC1 expression was tested in 15 of the 30 VSCC samples by Ma695, and found to be higher in HPV-negative (48%, 13/15 samples) compared to HPV-positive tissues (8%, 2/15 samples). There were no significant associations between MUC1 expression and clinical stage or lymph node metastases in VSCC.²⁹

Expression in non-malignant vulvar tissue – MUC1 expression by Ma695 in VSCC was higher than the expression in VIN III, HPV-independent VIN III (4/5) and HPV-dependent VIN III (0/1). Both HPV-independent VIN I-II (n=4),

HPV-dependent VIN I-II (n=6), HPV-dependent vulvar condylomata acuminata (n=10) and healthy vulvar tissue (n=5) did not stain positive for MUC1 according to one study.²⁹

Clinical tracers – Due to its overexpression in several other cancers, MUC1 has emerged as a potential target for cancer therapy.⁵⁴ Monoclonal antibody development has historically been hampered by the abundant presence of aberrant glycosylation of MUC1 on tumor cells. The humanized IgG1 antibody (PankoMab-GEX) is directed against a glycol-epitope and has been shown to be safe, well tolerated, and promising for anti-tumor activity, suggesting a possible use as imaging tracer.⁵⁵ Mouse studies with another MUC1 antibody showed selectivity for ovarian cancer MR imaging.⁵⁶ Other, non-antibody based tracers like peptides and aptamers specifically binding MUC1 for imaging applications are under development. These ligands are relatively easy and cheaper to produce than antibodies, with low toxicity and immunoreactivity. A disadvantage for fluorescent based imaging might be the rapid systemic clearance resulting in a too short circulation half-life. It was shown that aptamers directed against the mucin 1 (MUC1) antigen, demonstrated high specificity and uniform penetration in tumor xenografts.⁵⁷

CXCR-4

Physiological role – C-X-C chemokine receptor type 4 (CXCR-4, fusin, CD184) is a specific receptor for stromal cell-derived factor-1. This factor is endowed with potent chemotactic activity for lymphocytes. CXCR-4 is located on the surface of the (tumor)cell membrane and acts with the CD4 protein to support HIV entering into cells.

Tumor expression – CXCR-4 is known to be overexpressed in at least 23 types of cancer, including breast cancer and prostate cancer.⁵⁸ The only study including CXCR-4 in VSCC showed 68% expression in 22 tested samples.³⁰ Expression was mainly seen at the invasive front, at the invading tumor clusters in deep stroma and in lymph node metastases. The expression rates of CXCR-4 in primary tumors were shown to be similar in node-negative and node-positive disease. But at metastatic sites, the expression rate of CXCR-4 in node positive diseases was very high. CXCR-4 expression tended to be increased for higher FIGO stages (III-IV) compared to lower stages (I-II) although this was not statistically significant (P=0.08). Furthermore, expression was associated with poor disease prognosis but

was not an independent prognostic factor. HPV-status in relation to CXCR-4 expression was not described.³⁰

Expression in non-malignant vulvar tissue – No information is available on expression in healthy tissue. None of the intraepithelial lesions (n=7) stained positive for CXCR-4.³⁰

Clinical tracers – Antibodies, aptamers and peptides against CXCR-4 are extensively evaluated for molecular imaging purposes, with promising results.⁵⁹ An anti-CXCR-4 peptide conjugated to a NIR-dye was tested *in vivo* at mice bearing human osteosarcoma xenografts. This showed high NIR signal intensity within the CXCR-4-positive tumor and within CXCR-4 receptor-positive organs.⁶⁰ The T140 peptide antagonist for CXCR-4 was synthesized, containing fluorescent rhenium and technetium for fluorescence or SPECT dual modality imaging.⁶¹ The diagnostic performance of ⁶⁸Ga-Pentixafor, a recently introduced CXCR-4-directed PET tracer in a small cohort of breast cancer patients, showed that tumor detection was feasible but performed less than a glucose based ¹⁸F-FDG tracer.⁶² As CXCR-4 is also natively expressed in immune-related cells, background staining in these tissues must be taken into consideration when evaluating *in vivo* imaging results.⁵⁹

VEGF-A

Physiological role – Vascular endothelial growth factor A (VEGF-A) is a heparin binding glycoprotein that mainly interacts with the VEGF-R1 and-R2 receptors present on endothelial cell membranes and some cancer cells. VEGF-A is important for angiogenesis by induction of proliferation and migration of vascular endothelial cells.

Tumor expression – The protein is encoded by the VEGF-A gene and known to be upregulated in many, especially hypoxic, tumors.⁶³ Abnormal blood vessel formation can form if VEGF-A expression is upregulated or disrupted, leading to pathological angiogenesis. The three included scientific papers show an average VEGF-A expression of 45% in VSCC samples (range 25-70%). It is important to notice that one author observed membranous expression of VEGF-A in tumor cells,²² whereas others described the expression to be dominantly in the cytoplasm of epidermal prickles and tumor cells associated with micro vessels.^{27,31} One author reported no clinically significant correlation between VEGF-A expression in relation to the distribution of FIGO stage (p=0.58), histopathological stage (p=0.69), and histological

grade (p=0.09).³¹ HPV-status in relation to VEGF-A expression was not mentioned in any of the included articles.^{22,27,31}

Expression in non-malignant vulvar tissue – One author observed strong VEGF-A staining in 17% (2/12 samples) of healthy tissue and 70% (7/10 samples) of VIN tissue.²⁷ Other included authors did not describe VEGF-A expression in non-malignant tissue.

Clinical tracers – VEGF-A is relatively well investigated in clinical trials for tumor imaging purposes in various cancer types. For instance, the therapeutic antibody bevacizumab (anti-VEGF) is being tested in various clinical feasibility trials (phase 1 and 2) for detection of tumors over-expressing VEGF-A.⁶ Fluorescence imaging with bevacizumab labelled to IRDye800CW enabled in-situ detection of additional malignant lesions in peritoneal carcinomatosis of colorectal origin.⁶⁴ Additional studies with fluorescently labeled bevacizumab are planned in for instance endometriosis (NCT02975219). In addition, ranibizumab is an FDA approved humanized monoclonal antibody with potential for targeting of VEGF-A as well, however more expensive compared to bevacizumab.

Discussion

In this systematic review, we provide an overview of tumor-specific biomarkers as potential candidates for tumor-specific imaging in VSCC patients. Seven potential targets were identified from the literature, including EGFR, CD44V6, GLUT1, MRP1, MUC1, CXCR-4 and VEGF-A.

EGFR was the most frequently evaluated biomarker in VSCC, and showed an expression in 70% of the 747 tested samples. Based on the availability of FDA approved anti-EGFR antibodies and the knowledge obtained from previously executed clinical trials, targeted imaging of VSCC with use of EGFR has high potential, although the relatively high expression found in healthy vulvar tissue is a major concern.²¹ The expression of VEGF-A was lower with 45% of the 100 samples tested, however, this target could also be easily used in a clinical setting because of the availability of FDA approved antibodies. Research in the field of CD44V6 is mainly performed in HNSCC, which has two different pathophysiological pathways, similar to VSCC (via a non-viral or an HPV-driven oncogenic pathway). Therefore, the concept tested on this target could easily be translated to application in VSCC. GLUT1 shows a relatively high expression in VSCC compared to healthy tissue. MRP1 seems to

have less potency as a tracer, since this protein is ubiquitously expressed in almost all healthy tissues. MUC1 and CXCR-4 expression were both evaluated in only one small study with 30 and 22 samples, respectively.

This review is based on the available literature with respect to the expression of tumor-specific targets in vSCC. Although the analysis pinpoints several potential imaging targets, it should be emphasized that the studies from which the data are generated were not specifically designed to prospectively evaluate imaging targets. For such a purpose, these studies should be supplemented with more details on marker expression in relation to HPV-status, expression in precursor lesions and metastatic lymph node tissue, and most ideally in comparison with other vSCC-specific targets. The importance of the understanding and incorporation of these vSCC-specific details on marker expression in further research, will be explained in the following sections.

HPV-independent and HPV-dependent vulvar cancers represent two distinct types of vSCC and have different precursor lesions and clinical outcomes.² HPV status has not been examined in relation to target expression in most studies, except for EGFR and MUC1. These targets showed a higher expression in HPV-independent tissue samples compared to HPV-dependent samples. HPV infected cells are known to express the oncoproteins E6 and E7, however these are expressed in the cell nucleus and therefore seem not targetable for optical imaging. An HPV status dependent proteomics study of vulvar samples could elicit potential proteins expressed exclusively at either type. Considering HPV status during target selection could result in a more accurate and precise identification in both HPV-dependent and HPV-independent (pre)malignant vulvar lesions.

This knowledge about HPV-related expression could also be valuable for detection of precursor lesions vulvar HSIL and dVIN, as these lesions may sometimes be difficult to identify clinically and can progress to invasive vulvar cancer if left untreated. Unfortunately, information on expression in precursor lesions is mostly lacking for the listed biomarkers.

Tumor-specific imaging of lymph node metastases could also be used in the treatment for patients with vSCC. Lymph node metastases are considered one of the most important prognostic factor affecting disease-free and overall survival for vSCC patients.⁶⁵ Patients with early stage vSCC have a 25% risk of lymph node metastases at the time of diagnosis. Sentinel lymph node mapping, a non-tumor specific imaging technique, is used for

the detection of lymph node metastases in these patients.⁶⁶ The detection of lymph node metastases by targeted optical imaging could result in a further reduction of surgery-related morbidity. Most of the included studies reported on differences in expression in the primary tumor based on presence or absence of lymph node metastases. However, some studies reported on target expression in lymph node tissue: in 14 patients with lymph node metastases mean EGFR expression was 88% versus 65% in the primary tumor,¹⁸ CXCR-4 expression was seen in 100% of the lymph node metastases (n=4)³⁰ and in all cases in which the primary tumor stained positive for CD44V6 (3/10) a positive CD44V6 staining in the respective lymph node metastases was ascertained. This data could be useful in targeted detection of these nodes.²⁴

Other candidates for tumor-specific imaging in vSCC could be tumor-specific targets that are identified in OSCC or HNSCC, such as UPAR. Boonstra et al described the applicability of an UPAR specific multimodal tracer in an oral cancer model, combining SPECT with intraoperative guidance.⁶⁷ In addition, the use of photodynamic therapy, with for instance 5-ALA, that showed great potential for both diagnosis and treatment of premalignant vulvar lesions.^{68,69} Proteomics or surfaceome studies could identify new and specific vSCC and precursor targets. Until now, these type of studies are lacking in vulvar (pre)cancers.

This review has several limitations. First, the set of potential biomarkers is based on general tumor marker expression, without discriminating for vSCC-specific hallmarks as HPV-status. Second, only 22 studies could be included verifying expression of a small number of vulvar samples. Furthermore, the evaluation of targets was performed using different scoring systems, yielding results that are difficult to compare with wide ranges of expression. In addition, no tumor-to-healthy cell ratio could be estimated for the selected biomarkers.

Future studies should include the immunohistochemical analysis of potential targets in vSCC and its precursors. Cohorts should at least include HPV-independent and HPV-dependent vSCC samples and precursor lesions, healthy vulvar tissue samples and preferably tissue of respective lymph node metastases. It is desirable that two antibodies targeting the same biomarker will be used to test differences in sensitivity. Afterwards, cell line-based research should be executed to validate a biomarkers potency as tumor-specific target for vSCC, whereafter an antibody or peptide

conjugated to a fluorophore could be tested in vitro and in a tumor mouse model. Eventually, these findings might have clinical implications in terms of the development of a vSCC-specific probe for the safe and specific real-time detection of occult tumor lesions.

Conclusions

Based on the current literature, we identified seven biomarkers as potential targets for vSCC-specific molecular imaging. This overview can be used as a first step towards the development of a structured approach of tumor-visualization in patients with vSCC, which could be used for pre-surgical diagnosis and real-time and precise localization of vulvar cancer.

Figure 1 Optical imaging using Fluorescent Guided Surgery (FGS). A) An example of an imaging probe used for optical imaging, which consists of a fluorophore (contrast label) conjugated to an antibody (imaging probe). B) Schematic illustration of a tumor cell and a healthy cell expressing different biomarkers (pink, orange or blue receptors/proteins). The imaging probe is able to bind to the overexpressed biomarker of interest on the tumor cell (pink receptor). The healthy cell does not express this particular biomarker and stays unstained. Using a proper imaging modality, the tumor cell expressing green fluorescence light can be distinguished from the healthy cell.

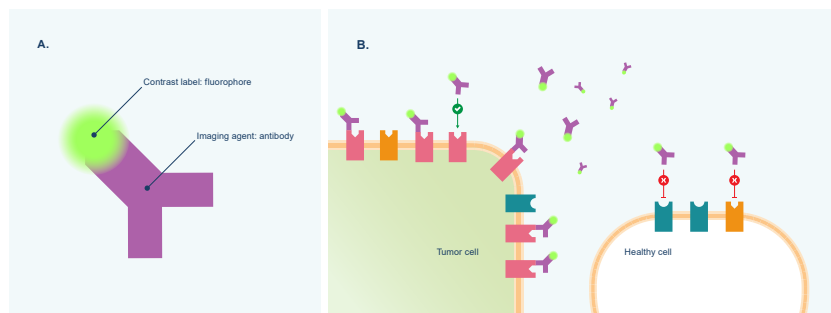
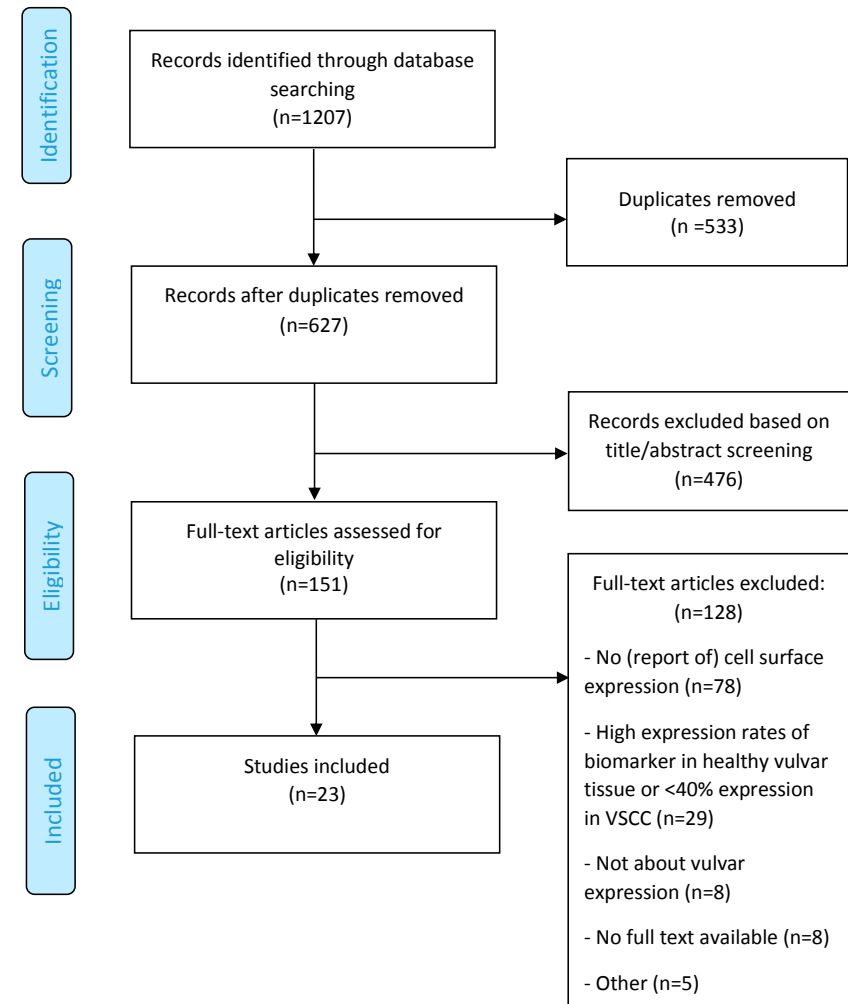


Figure 2 PRISMA flow diagram of literature search and selection process.



REFERENCES

- 1 Cancer Stat Facts: Vulvar Cancer, <https://seer.cancer.gov/statfacts/html/vulva.html>. 2019, assessed June 2019).
- 2 S. de Sanjose, L. Alemany, J. Ordi, S. Tous, M. Alejo, S.M. Bigby, E.A. Joura, P. Maldonado, J. Laco, et al., Worldwide human papillomavirus genotype attribution in over 2000 cases of intraepithelial and invasive lesions of the vulva, *Eur J Cancer* 49(16) (2013) 3450-61.
- 3 N.C. Te Grootenhuys, A.W. Pouwer, G.H. de Bock, H. Hollema, J. Bulten, A.G.J. van der Zee, J.A. de Hullu, M.H.M. Oonk, Prognostic factors for local recurrence of squamous cell carcinoma of the vulva: A systematic review, *Gynecol Oncol* 148(3) (2018) 622-31.
- 4 L.S. Nooij, F.A. Brand, K.N. Gaarenstroom, C.L. Creutzberg, J.A. de Hullu, M.I. van Poelgeest, Risk factors and treatment for recurrent vulvar squamous cell carcinoma, *Crit Rev Oncol Hematol* 106 (2016) 1-13.
- 5 C. Martelli, A. Lo Dico, C. Diceglie, G. Lucignani, L. Ottobirini, Optical imaging probes in oncology, *Oncotarget* 7(30) (2016) 48753-87.
- 6 S. Hernot, L. van Manen, P. Debie, J.S.D. Mieog, A.L. Vahrmeijer, Latest developments in molecular tracers for fluorescence image-guided cancer surgery, *The Lancet Oncology* 20(7) (2019) e354-e367.
- 7 M.C. Boonstra, S.W. de Geus, H.A. Prevoo, L.J. Hawinkels, C.J. van de Velde, P.J. Kuppen, A.L. Vahrmeijer, C.F. Sier, Selecting Targets for Tumor Imaging: An Overview of Cancer-Associated Membrane Proteins, *Biomarkers in cancer* 8 (2016) 119-33.
- 8 M. van Oosten, L.M. Crane, J. Bart, F.W. van Leeuwen, G.M. van Dam, Selecting Potential Targetable Biomarkers for Imaging Purposes in Colorectal Cancer Using TArget Selection Criteria (TASC): A Novel Target Identification Tool, *Transl Oncol* 4(2) (2011) 71-82.
- 9 D. Moher, L. Shamseer, M. Clarke, D. Ghersi, A. Liberati, M. Petticrew, P. Shekelle, L.A. Stewart, Preferred reporting items for systematic review and meta-analysis protocols (PRISMA-P) 2015 statement, *Systematic reviews* 4 (2015) 1.
- 10 S.E. Bosma, P.B. van Driel, P.C. Hogendoorn, P.S. Dijkstra, C.F. Sier, Introducing fluorescence guided surgery into orthopedic oncology: A systematic review of candidate protein targets for Ewing sarcoma, *J Surg Oncol* 118(6) (2018) 906-14.
- 11 G. Fons, d. van, V. M. Burger, K.F. ten, Validation of tissue microarray technology in vulvar cancer, *Int J Gynecol Pathol* 28(1) (2009) 76-82.
- 12 M.L. Palisoul, M.M. Mullen, R. Feldman, P.H. Thaker, Identification of molecular targets in vulvar cancers, *Gynecol Oncol* 146(2) (2017) 305-13.
- 13 R.F. Koncar, R. Feldman, E.M. Bahassi, S.N. Hashemi, Comparative molecular profiling of HPV-induced squamous cell carcinomas, *Cancer Med* 6(7) (2017) 1673-85.
- 14 T.S. Lee, Y.T. Jeon, J.W. Kim, J.K. Won, N.H. Park, I.A. Park, Y.S. Juhn, S.B. Kang, H.P. Lee, Y.S. Song, Increased cyclooxygenase-2 expression associated with inflammatory cellular infiltration in elderly patients with vulvar cancer, *Ann N Y Acad Sci* 1095 (2007) 143-53.
- 15 L. Woelber, S. Hess, H. Bohlken, P. Tennstedt, C. Eulenburger, R. Simon, F. Giesecking, F. Jaenicke, S. Mahner, M. Choschzick EGFR gene copy number increase in vulvar carcinomas is linked with poor clinical outcome, *J Clin Pathol* 65(2) (2012) 133-9.
- 16 M.H. Oonk, G.H. de Bock, D.J. van der Veen, K.A. Ten Hoor, J.A. de Hullu, H. Hollema, A.G. van der Zee, EGFR expression is associated with groin node metastases in vulvar cancer, but does not improve their prediction, *Gynecol Oncol* 104(1) (2007) 109-13.
- 17 F. Dong, S. Kojiro, D.R. Borger, W.B. Growdon, E. Oliva, Squamous Cell Carcinoma of the Vulva: A Subclassification of 97 Cases by Clinicopathologic, Immunohistochemical, and Molecular Features (P16, P53 and EGFR), *Am J Surg Pathol* 39(8) (2015) 1045-53.
- 18 G.A. Johnson, R. Mannel, M. Khalifa, J.L. Walker, M. Wren, K.W. Min, D.M. Benbrook, Epidermal growth factor receptor in vulvar malignancies and its relationship to metastasis and patient survival, *Gynecol Oncol* 65(3) (1997) 425-9.
- 19 M.B. de Melo, A.M. Fontes, A.M. Lavorato-Rocha, I.S. Rodrigues, B.L. de, G. Baiocchi, M.M. Stiepcich, F.A. Soares, R.M. Rocha, EGFR expression in vulvar cancer: clinical implications and tumor heterogeneity, *Hum Pathol* 45(5) (2014) 917-25.
- 20 H. Brustmann, Epidermal growth factor receptor is involved in the development of an invasive phenotype in vulvar squamous lesions, but is not related to MIB-1 immunoreactivity, *Int J Gynecol Pathol* 26(4) (2007) 481-9.
- 21 X. Wu, Y. Xin, J. Yao, K. Hasui, S. Tsuyama, S. Yonezawa, F. Murata, Expression of epithelial growth factor receptor and its two ligands, transforming growth factor-alpha and epithelial growth factor, in normal and neoplastic squamous cells in the vulva: an immunohistochemical study, *Med Electron Microsc* 34(3) (2001) 179-84.
- 22 G. Fons, M.P. Burger, F.J. ten Kate, d. van, V, Identification of potential prognostic markers for vulvar cancer using immunohistochemical staining of tissue microarrays, *Int J Gynecol Pathol* 26(2) (2007) 188-93.
- 23 C. Tempfer, G. Gitsch, G. Haeusler, A. Reinthaller, H. Koelbl, C. Kainz, Prognostic value of immunohistochemically detected CD44 expression in patients with carcinoma of the vulva, *Cancer* 78(2) (1996) 273-7.
- 24 L.A. Hefler, N. Concin, D. Mincham, J. Thompson, N.B. Swarte, M.A. van Eijkeren, D.M. Sie-Go, I. Hammond, A.J. McCartney, C.B. Tempfer, P. Speiser, The prognostic value of immunohistochemically detected CD44v3 and CD44V6 expression in patients with surgically staged vulvar carcinoma: a multicenter study, *Cancer* 94(1) (2002) 125-30.
- 25 C. Tempfer, G. Sliutz, G. Haeusler, P. Speiser, A. Reinthaller, G. Breitenecker, N. Vavra, C. Kainz, CD44v3 and v6 variant isoform expression correlates with poor prognosis in early-stage vulvar cancer, *Br J Cancer* 78(8) (1998) 1091-4.
- 26 H.P. van de Nieuwenhof, J.A. de Hullu, J.H. Kaanders, J. Bulten, L.F. Massuger, L.C. van Kempen, Hemoglobin level predicts outcome for vulvar cancer patients independent of GLUT-1 and CA-1x expression in tumor tissue, *Virchows Arch* 457(6) (2010) 693-703.
- 27 Y.Z. Li, S.L. Li, X. Li, L.J. Wang, J.L. Wang, J.W. Xu, Z.H. Wu, L. Gong, X.D. Zhang, Expression of endogenous hypoxia markers in vulvar squamous cell carcinoma, *Asian Pac J Cancer Prev* 13(8) (2012) 3675-80.
- 28 A. Mayer, M. Schmidt, A. Seeger, A.F. Serras, P. Vaupel, H. Schmidberger, GLUT-1 expression is largely unrelated to both hypoxia and the Warburg phenotype in squamous cell carcinomas of the vulva, *BMC Cancer* 14 (2014) 760.
- 29 X. Wu, J.F. Yao, Y. Xin, S. Tsuyama, S. Yonezawa, F. Murata, Expression of mucin 1 (MUC1) in benign, premalignant and malignant vulvar tumors, *Acta Histochem Cytoc* 33(4) (2000) 267-73.
- 30 T. Shiozaki, T. Tabata, N. Ma, T. Yamawaki, T. Motohashi, E. Kondo, K. Tanida, T. Okugawa, T. Ikeda, Association of CXCL12 chemokine receptor type 4 expression and clinicopathologic features in human vulvar cancer, *Int J Gynecol Cancer* 23(6) (2013) 1111-7.
- 31 A. Obermair, P. Kohlberger, D. Bancher-Todesca, C. Tempfer, G. Sliutz, S. Leodolter, A. Reinthaller, C. Kainz, G. Breitenecker, G. Gitsch, Influence of microvessel density and vascular permeability factor/vascular endothelial growth factor expression on prognosis in vulvar cancer, *Gynecol Oncol* 63(2) (1996) 204-9.
- 32 H.P. Dhakal, J.M. Nesland, M. Forsund, C.G. Trope, R. Holm, Primary tumor vascularity, HIF-1alpha and VEGF expression in vulvar squamous cell carcinomas: their relationships with clinicopathological characteristics and prognostic impact, *BMC Cancer* 13 (2013) 506.
- 33 X. Liu, P. Wang, C. Zhang, Z. Ma, Epidermal growth factor receptor (EGFR): A rising star in the era of precision medicine of lung cancer, *Oncotarget* 8(30) (2017) 50209-20.
- 34 S. Pastore, F. Mascia, V. Mariani, G. Girolomoni, The epidermal growth factor receptor system in skin repair and inflammation, *J Invest Dermatol* 128(6) (2008) 1365-74.
- 35 W.J. Rosenthal EL, de Boer E, et al., Safety and Tumor Specificity of Cetuximab-IRDye800 for Surgical Navigation in Head and Neck Cancer., *Clin Cancer Res.* (21(16):3658-66. doi:10.1158/1078-0432.CCR-14-3284) (2015).
- 36 S.B. Fox, J. Fawcett, D.G. Jackson, I. Collins, K.C. Gatter, A.L. Harris, A. Gearing, D.L. Simmons, Normal human tissues, in addition to some tumors, express multiple different CD44 isoforms, *Cancer Res* 54(16) (1994) 4539-46.
- 37 L. Chai, H. Liu, Z. Zhang, F. Wang, Q. Wang, S. Zhou, S. Wang, CD44 expression is predictive of poor prognosis in pharyngolaryngeal cancer: systematic review and meta-analysis, *Tohoku J Exp Med* 232(1) (2014) 9-19.
- 38 M. Todaro, M. Gaggianesi, V. Catalano, A. Benfante, F. Iovino, M. Biffoni, T. Apuzzo, I. Sperduti, S. Volpe, G. Cocorullo, G. Gulotta, F. Dieli, R. De Maria, G. Stassi, CD44V6 is a marker of constitutive and reprogrammed cancer stem cells driving colon cancer metastasis, *Cell stem cell* 14(3) (2014) 342-56.
- 39 S.M.P. Vadevoo, S. Gurung, F. Khan, M.E. Haque, G.R. Gunassekaran, L. Chi, U. Permpoon, B. Lee, Peptide-based targeted therapeutics and apoptosis imaging probes for cancer therapy, *Arch Pharmacol Res* 42(2) (2019) 150-8.
- 40 D. Spiegelberg, J. Nilvebrant, CD44V6-Targeted Imaging of Head and Neck Squamous Cell Carcinoma: Antibody-Based Approaches, *Contrast media & molecular imaging* 2017 (2017) 2709547.
- 41 J.W. Stroemer, J.C. Roos, M. Sproll, J.J. Quak, K.H. Heider, B.J. Wilhelm, J.A. Castelijns, R. Meyer, M.O. Kwakkelstein, G.B. Snow, G.R. Adolf, G.A. van Dongen, Safety and biodistribution of 99mTechnetium-labeled anti-CD44V6 monoclonal antibody B1WA 1 in head and neck cancer patients, *Clin Cancer Res* 6(8) (2000) 3046-55.
- 42 J. Odenthal, M. Rijpkema, D. Bos, E. Wagena, H. Croes, R. Grenman, O. Boerman, R. Takes, P. Friedl, Targeting CD44V6 for fluorescence-guided surgery in head and neck squamous cell carcinoma, *Scientific reports* 8(1) (2018) 10467.
- 43 A. Carruthers, J. DeZutter, A. Ganguly, S.U. Devaskar, Will the original glucose transporter isoform please stand up! *Am J Physiol Endocrinol Metab* 297(4) (2009) E836-48.
- 44 J. Wang, C. Ye, C. Chen, H. Xiong, B. Xie, J. Zhou, Y. Chen, S. Zheng, L. Wang, Glucose transporter GLUT1 expression and clinical outcome in solid tumors: a systematic review and meta-analysis, *Oncotarget* 8(10) (2017) 16875-86.
- 45 C.H. Sohn, S.P. Park, S.H. Choi, S.H. Park, S. Kim, L. Xu, S.H. Kim, J.A. Hur, J. Choi, T.H. Choi. MR1 molecular imaging using GLUT1 antibody-Fe3O4 nanoparticles in the hemangioma animal model for differentiating infantile hemangioma from vascular malformation, *Nanomed-Nanotechnol* 11(1) (2015) 127-35.
- 46 C. Crivellaro, P. Guglielmo, E. De Ponti, F. Elisei, L. Guerra, S. Magni, M. La Manna, G. Di Martino, C. Landoni, A. Buda, 18F-FDG PET/CT in preoperative staging of vulvar cancer patients: is it really effective? *Medicine* 96(38) (2017) e7943.
- 47 J.L. Kovar, W. Volcheck, E. Sevcik-Muraca, M.A. Simpson, D.M. Olive, Characterization and performance of a near-infrared 2-deoxyglucose optical imaging agent for mouse cancer models, *Anal Biochem* 384(2) (2009) 254-62.
- 48 J. Yin, J. Zhang, Multidrug resistance-associated protein 1 (MRP1/ABCC1) polymorphism: from discovery to clinical application, *Zhong Nan Da Xue Xue Bao Yi Xue Ban* 36(10) (2011) 927-38.
- 49 M. Munoz, M. Henderson, M. Haber, M. Norris, Role of the MRP1/ABCC1 multidrug transporter protein in cancer, *IUBMB Life* 59(12) (2007) 752-7.
- 50 A. Sampson, B.G. Peterson, K.W. Tan, S.H. Iram, Doxorubicin as a fluorescent reporter identifies novel

- MRP1 (ABCC1) inhibitors missed by calcein-based high content screening of anticancer agents, *Biomed Pharmacother* 118 (2019) 109289.
- 51 L. Binyamin, Y.G. Assaraf, M. Haus-Cohen, M. Stark, Y. Reiter, Targeting an extracellular epitope of the human multidrug resistance protein 1 (MRP1) in malignant cells with a novel recombinant single chain Fv antibody, *Int J Cancer* 110(6) (2004) 882-90.
- 52 C. Vanpouille, N. Le Jeune, D. Kryza, A. Clotagatide, M. Janier, F. Dubois, N. Perek, Influence of multidrug resistance on (18)F-FCH cellular uptake in a glioblastoma model, *Eur J Nucl Med Mol Imaging* 36(8) (2009) 1256-64.
- 53 P.E. Constantinou, B.P. Danysh, N. Dharmaraj, D.D. Carson, Transmembrane mucins as novel therapeutic targets, Expert review of endocrinology & metabolism 6(6) (2011) 835-848.
- 54 S. Nath, P. Mukherjee, MUC1: a multifaceted oncoprotein with a key role in cancer progression, *Trends Mol Med* 20(6) (2014) 332-42.
- 55 W. Fiedler, S. DeDosso, S. Cresta, J. Weidmann, A. Tessari, M. Salzberg, B. Dietrich, H. Baumeister, S. Goletz, L. Gianni, C. Sessa, A phase I study of PankoMab-GEX, a humanised glyco-optimised monoclonal antibody to a novel tumour-specific MUC1 glycopeptide epitope in patients with advanced carcinomas, *Eur J Cancer* 63 (2016) 55-63.
- 56 D. Shahbazi-Gahrouei, M. Abdolahi, Detection of MUC1-expressing ovarian cancer by C595 monoclonal antibody-conjugated SPIOs using MR imaging, *Sci World J* (2013) 609151.
- 57 A.C. Perkins, S. Missailidis, Radiolabelled aptamers for tumour imaging and therapy, *The quarterly journal of nuclear medicine and molecular imaging: official publication of the Italian Association of Nuclear Medicine (AIMN) [and] the International Association of Radiopharmacology (IAR), [and] Section of the Society of Nuclear Medicine (SNM)* 51(4) (2007) 292-6.
- 58 A. Muller, B. Homey, H. Soto, N. Ge, D. Catron, M.E. Buchanan, T. McClanahan, E. Murphy, W. Yuan, S.N. Wagner, J.L. Barrera, A. Mohar, E. Verastegui, A. Zlotnik, Involvement of chemokine receptors in breast cancer metastasis, *Nature* 410(6824) (2001) 50-6.
- 59 J. Kuil, T. Buckle, F.W. van Leeuwen, Imaging agents for the chemokine receptor 4 (CXCR4), *Chem Soc Rev* 41(15) (2012) 5239-61.
- 60 Y. Lin, Y. Lin, X. Lin, X. Sun, K. Luo, Combination of PET and CXCR4-Targeted Peptide Molecule Agents for Noninvasive Tumor Monitoring, *JouRNAL of Cancer* 10(15) (2019) 3420-6.
- 61 W.L. Turnbull, L. Yu, E. Murrell, M. Milne, C.L. Charron, L.G. Luyt, A dual modality (99m)Tc/Re(i)-labelled T140 analogue for imaging of CXCR4 expression, *Organic & biomolecular chemistry* 17(3) (2019) 598-608.
- 62 T. Vag, K. Steiger, A. Rossmann, U. Keller, A. Noske, P. Herhaus, J. Ettl, M. Niemeyer, H.J. Wester, M. Schwaiger, PET imaging of chemokine receptor CXCR4 in patients with primary and recurrent breast carcinoma, *EJNMMI research* 8(1) (2018) 90.
- 63 H.L. Goel, A.M. Mercurio, VEGF targets the tumour cell, *Nature reviews. Cancer* 13(12) (2013) 871-82.
- 64 N.J. Harlaar, M. Koller, S.J. de Jongh, B.L. van Leeuwen, P.H. Hemmer, S. Kruijff, R.J. van Ginkel, L.B. Been, J.S. de Jong, G. Kats-Ugurlu, M.D. Linssen, A. Jorritsma-Smit, M. van Oosten, W.B. Nagengast, V. Ntziachristos, G.M. van Dam, Molecular fluorescence-guided surgery of peritoneal carcinomatosis of colorectal origin: a single-centre feasibility study, *The lancet. Gastroenterology & hepatology* 1(4) (2016) 283-90.
- 65 G. Bogani, A. Cromi, M. Serati, S. Uccella, V.D. Donato, J. Casarin, E.D. Naro, F. Ghezzi, Predictors and Patterns of Local, Regional, and Distant Failure in Squamous Cell Carcinoma of the Vulva, *Am J Clin Oncol* 40(3) (2017) 235-40.
- 66 M.H. Oonk, H. Hollema, A.G. van der Zee, Sentinel node biopsy in vulvar cancer: Implications for staging, *Best Pract Res Clin Obstet Gynaecol* 29(6) (2015) 812-21.
- 67 M.C. Boonstra, P. Van Driel, S. Keereweer, H. Prevoo, M.A. Stammes, V.M. Baart, C. Lowik, A.P. Mazar, C.J.H. van de Velde, A.L. Vahrmeijer, C.F.M. Sier, Preclinical uPAR-targeted multimodal imaging of locoregional oral cancer, *Oral Oncol* 66 (2017) 1-8.
- 68 S. Booth, D. Poole, K. Moghissi, Initial experience of the use of photodynamic therapy (PDT) in recurrent malignant and pre-malignant lesions of the vulva, *Photodiagn Photodyn* 3(3) (2006) 156-61.
- 69 L. Leufflen, A. Francois, J. Salleron, C. Barlier, G. Dolivet, F. Marchal, L. Bezdetnaya, Photodynamic diagnosis with methyl-5-aminolevulinat in squamous intraepithelial lesions of the vulva: Experimental research, *Photodiagn Photodyn* 13(5) (2018) e0196753.

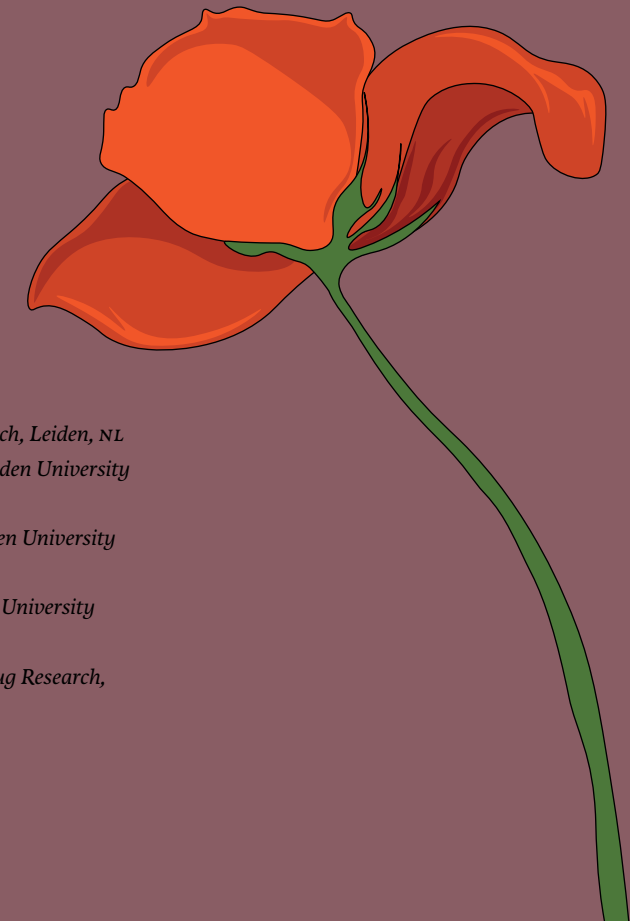
CHAPTER 6

Integrin $\alpha\beta 6$ as a target for tumor-specific imaging of vulvar squamous cell carcinoma and adjacent premalignant lesions

Bertine W. Huisman^{1,2}, Merve Cankat^{1,2}, Tjalling Bosse³, Alexander L. Vahrmeijer⁴, Robert Rissmann^{1,5}, Jacobus Burggraaf^{1,4,5}, Cornelis F. M. Sier^{4,6*} and Mariette I. E. van Poelgeest^{1,2*}

* These authors share co-senior authorship

- 1 Center for Human Drug Research, Leiden, NL
- 2 Department of Gynecology, Leiden University Medical Center, Leiden, NL
- 3 Department of Pathology, Leiden University Medical Center, Leiden, NL
- 4 Department of Surgery, Leiden University Medical Center, Leiden, NL
- 5 Leiden Academic Center for Drug Research, Leiden University, Leiden, NL
- 6 Percuro BV, Leiden, NL



Abstract

Surgical removal of vulvar squamous cell carcinoma (vSCC) is associated with significant morbidity and high recurrence rates. This is at least partially related to the limited visual ability to distinguish (pre)malignant from normal vulvar tissue. Illumination of neoplastic tissue based on fluorescent tracers, known as fluorescence-guided surgery (FGS), could help resect involved tissue and decrease ancillary mutilation. To evaluate potential targets for FGS in vSCC, immunohistochemistry was performed on paraffin-embedded premalignant (high grade squamous intraepithelial lesion and differentiated vulvar intraepithelial neoplasia) and vSCC (human papillomavirus (HPV)-dependent and-independent) tissue sections with healthy vulvar skin as controls. Sections were stained for integrin $\alpha\text{v}\beta\text{6}$, CAIX, CD44V6, EGFR, EPCAM, FR α , MRP1, MUC1 and UPAR. The expression of each marker was quantified using digital image analysis. H-scores were calculated and percentages positive cells, expression pattern, and biomarker localization were assessed. In addition, tumor-to-background ratios were established, which were highest for (pre)malignant vulvar tissues stained for integrin $\alpha\text{v}\beta\text{6}$. In conclusion, integrin $\alpha\text{v}\beta\text{6}$ allowed for the most robust discrimination of vSCC's and adjacent premalignant lesions compared to surrounding healthy tissue in immunohistochemically stained tissue sections. The use of an $\alpha\text{v}\beta\text{6}$ targeted near-infrared fluorescent probe for FGS of vulvar (pre)malignancies should be evaluated in future studies.

Introduction

Vulvar squamous cell carcinoma (vSCC) is a rare type of cancer with an incidence of 1.5–2.7 per 100,000 women, necessitating specialized centralized care.¹ Overall incidence worldwide is increasing. For the Dutch population, this increase is mainly observed in younger women.^{2,3} There are two major pathways for the development of vSCC. Human papilloma virus (HPV)-dependent vSCC (20%) are caused by high-risk HPV types, predominantly HPV 16. HPV-dependent vSCC arises in the background of precursor lesions named high grade squamous intraepithelial neoplasia (HSIL). Another precursor of vSCC is differentiated vulvar intraepithelial neoplasia (dVIN), which often arises in elderly women with lichen sclerosus (LS), a chronic inflammatory skin disease. For dVIN, the cumulative risk of malignant progression to vSCC is estimated to be as high as 50% after 10 years and

this type of vSCC has a poor survival compared to HPV-dependent vSCC.^{1,4–6} The cornerstone of treatment for vSCC consists of surgery with or without radiochemotherapy.^{7,8} Even in early-stage disease, the recurrence rate is up to 40% after 10 years, requiring repeated local surgery or (re)irradiation.⁹

In more than half of the vSCC patients, surgery in the vulvar area, in particular when the tumor is located near the urethra, clitoris, or anus, is associated with significant morbidity, including disfigurement, sexual dysfunction, and psychological problems.¹⁰ These morbidities are partly caused by the limited ability to distinguish between healthy and (pre)malignant tissue during surgery. The recognition and excision of vulvar lesions relies on the gynecologist's visual and tactile skills, experience, and information obtained from histological biopsies. Recognition by the gynecologist is even harder when the vulvar architecture is complicated by deformation associated with inflammation, atrophy, or previous treatments.^{2,11} Positive surgical margins are associated with higher risk for local recurrence and poor survival.^{12,13} In addition, precursor lesions are often found adjacent to the tumor, which are sometimes difficult to identify clinically and therefore not treated adequately. Consequently, better identification and timely recognition of vulvar (pre)malignant lesions may result in prevention of re-excisions, local recurrences, metastases, and associated prognosis. Real time visualization during fluorescence-guided surgery (FGS) could aid in resolving this problem.

FGS is a promising technique for real-time detection of occult tumor lesions and localization of cancer margins. The procedure makes use of a cell-specific targeting agent, linked to a near-infrared fluorescent (NIRF) dye or radiolabel, which can be visualized in real time by an advanced imaging system. Clinical studies on various cancer types have shown that FGS improves the recognition of tumor tissue significantly, primarily in cases with incomplete visual and tactile information.^{14,15} Proper identification of tumor-specific targets for molecular imaging is key to the success of FGS.¹⁶ In the last decade, FGS targets have been explored for cancer types including ovarian, colorectal, and head-and-neck cancer.^{17–21} Until now, potential targets for FGS in vSCC have not been studied.

The aim of this study was to examine the expression of previously identified vSCC-specific membrane-associated targets based on the available literature and candidate targets for other squamous cancers in dVIN, HSIL, and vSCC tissues. To determine their suitability as a target for tumor-specific imaging in vulvar (pre)malignancies. The markers assessed are integrin

alphavbeta6 ($\alpha v \beta 6$), carbonic anhydrase IX (CAIX), CD44 variant 6 (CD44v6), epidermal growth factor receptor (EGFR), epithelial cell adhesion molecule (EPCAM), folate receptor α (FR α), multidrug resistance-associated protein (MRP1), mucin 1 (MUC1), and urokinase plasminogen activator receptor (UPAR).^{17,18,20,22-24}

Materials and Methods

TISSUE SAMPLES

Pretreatment vSCC samples and precursor lesions, i.e., dVIN and HSIL (without information on treatment status) were collected from the pathology department of Leiden University Medical Center. Sample selection was based on original diagnosis described in the pathology report and the size of the available tissues. Non-squamous vulvar cancers were excluded. Formalin fixed paraffin embedded (FFPE) HPV-negative vulvar tissue from healthy anonymized women who underwent labia reduction surgery was included as control. Sample collection was approved by the local ethics review board (Medische Ethische Toetsingscommissie Leiden Den Haag Delft-reference number B19.025). All routinely made hematoxylin-eosin- (H&E), P16- (over-expressed in dysplastic tissue related to HPV infection; HSIL and HPV-dependent vSCC tissues) and P53-stained slides were reviewed by an expert gynecologic pathologist (TB) blinded to immunohistochemical results and lesions diagnosed and delineated.²⁵⁻²⁸ Intentionally, fifteen samples were collected of each vulvar tissue type/group, i.e., healthy, dVIN, HPV-independent vSCC, HSIL and HPV-dependent vSCC. Some samples were excluded because the original diagnosis of a tissue could not be confirmed or (pre)malignant cells were no longer present in the tissue sample.

IMMUNOHISTOCHEMISTRY

FFPE tissue blocks were sectioned into tissue sections of 4 μ m. Sections were deparaffinized in xylene and rehydrated via serially diluted ethanol solutions. Endogenous peroxide was blocked for 20 min with 0.3% hydrogen peroxide diluted in demineralized water. Appropriate antigen retrieval was performed depending on the antibody (Table S1). Subsequently, sections were incubated overnight at room temperature (RT) with the primary antibodies. The optimal dilution for each of the antibodies was determined

beforehand on vulvar normal and/or squamous cell carcinoma test tissue. Slides were washed three times with phosphate-buffered saline (PBS, PH 7.5) before 30 min incubation at RT with the appropriate secondary antibody, followed by another washing step. Staining was visualized with 3,3-diaminobenzidine tetrahydrochloride solution (DAB, K3468, Agilent Technologies, Inc., Santa Clara, CA, USA) for approximately 5 min at RT and counterstained for 20 s with hematoxylin (4085.9002, VWR International, Amsterdam, The Netherlands). After dehydration, the slides were mounted with Pertex (0081EX, Histolab, Askim, Sweden). Control staining's were performed (Table 1 and Figure S1).

DIGITAL PATHOLOGY IMAGE ANALYSIS

Stained sections were digitalized with a Panoramic Digital Slide Scanner (3D Histech, Budapest, Hungary), stored as tiled tiff format, and imported into QuPath (version 2.0.0). QuPath is an open-source software tool for digital pathology image analysis.²⁹⁻³¹ Based on delineation of tissues by pathologist TB, tumor and premalignant borders were manually annotated in QuPath by BH and MC and copied to sequential sections. Within all these tissue annotations, cell detection, cell classification and staining quantification was conducted by a script (Script S1). After running the script, an export file of the results was automatically generated in MS excel. This export file included intensity thresholds for positive stained cells, divided in three categories: low (1+), medium (2+) or high (3+) intensity staining (examples of by QuPath processed image are shown in Figure S2, Figure S3).

MARKER STAINING

Based on the number of positive cells and their intensity, QuPath automatically generated H-scores by the formula:

$1 \times (\% \text{ cells threshold } 1+) + 2 \times (\% \text{ cells threshold } 2+) + 3 \times (\% \text{ cells threshold } 3+)$ for all annotations. H-scores range from 0 to 300, giving more relative weight to higher-intensity staining in a tissue section. The following H-score categories were defined: 0-50 low, 50-250 medium and 250-300 high marker staining.³² Median, minimum and maximum H-scores per vulvar tissue type were calculated. In addition, tumor-to-background ratios (TBR's) were calculated by dividing the median H-score of vulvar (pre)malignant tissue by the median H-score for healthy vulvar tissue.

Table 1 Antibodies used for immunohistochemical analysis, including source, clone, stock, dilutions, antigen retrieval applied and positive control tissue per biomarker tested.

Bio-marker	Source	Clone number	Catalogue number	Stock	Dilution	Antigen retrieval	Positive control
$\alpha\text{v}\beta\text{6}$	Biogen, Inc., Cambridge, MA, USA	6.2A1	62A1CE02	50 $\mu\text{g}/\text{ml}$	1/100	0.4% pepsin (S3002 Agilent) 37 °C for 15 min.	Normal colon
CA IX	Santa Cruz Biotechnology, Inc., Danvers, MA, USA	H-11	Sc-365900	200 $\mu\text{g}/\text{ml}$	1/2500	Target retrieval solution, PH 6.1 (K8005 Agilent)	Normal stomach
CD44V6	Abcam, Cambridge, UK	VFF7	ab30436	1 mg/ml	1/3200	Target retrieval solution, PH 6.1 (K8005 Agilent) ^{6.1}	Normal skin
EGFR	Dako, Glostrup, Denmark	E30	M7239	286 $\mu\text{g}/\text{ml}$	1/600	0.4% pepsin (S3002 Agilent) 37 °C for 10 min.	Normal placenta
EPCAM	LUMC, department of pathology ¹	323/A3	-	0.4 mg/ml	1/1600	0.1% trypsin (T7409 Sigma Aldrich) 37° C for 30 min.	Colon tumor
FR α	BioCare Medical, Pacheco, CA, USA	26B3.F2	BRI 4006K AA (KIT)	Assay kit	N.A.	Ready-to-use	Long tumor
MRP1	Santa Cruz Biotechnology, Inc., Danvers, MA, USA	QCRL-1	SC-18835	200 $\mu\text{g}/\text{ml}$	1/400	Target retrieval solution, PH 6.1 (K8005 Agilent)	Normal placenta
MUC1	Invitrogen, Waltham, MA, USA	E29	MA5-14077	0.2 mg/ml	1/4800	Target retrieval solution, PH 9.0 (K8004 Agilent)	Normal colon
UPAR	Monopar ²	ATN617	-	0.48 mg/ml	1/200	Target retrieval solution, PH 6.1 (K8005 Agilent)	Colon tumor
P16	Roche, Almere, Netherlands	E6H4	06695248001	Ready-to-use	1/25	TRIS/EDTA	Normal cervix
P53	DAKO, Satna Clara, CA, USA	DO-7	GA61661-2	237 mg/l	1/2000	TRIS/EDTA	Normal cervix

¹ Kindly provided by Jaap van Eendenburg, department of pathology LUMC, Netherlands.

² Kindly provided by Andrew Mazar, Monopar Therapeutics Inc., United States of America.

FGS CRITERIA

A potential protein marker for FGS based on IHC-staining was defined by fulfillment of all the following criteria.^{16,22,33}

- a median H-score in (pre)malignant tissue being at least twice as high as the median H-score in healthy control and stromal tissue;³⁴
- a minimum median H-score in (pre)malignant tissue of at least 25;
- homogeneous expression throughout the tumor;
- cell surface protein expression.

STATISTICS

Median, minimum, and maximum H-scores were extracted from Qupath and TBR's calculated (Table 2). To test for favorable TBR's, a statistical analysis was performed on the comparison of median H-scores per vulvar tissue types (healthy vulva (HV)/dVIN, HV/HPV-independent vSCC, HV/HSIL, HV/HPV-dependent vSCC, dVIN/HPV-independent vSCC, HSIL/HPV-dependent vSCC) using a Mann-Whitney U test. Statistical analyses were performed using Graphpad Prism version 9.1.0 for MacOS (Graphpad Prism Software, San Diego, CA, USA). These results were presented in boxplots with 1st and 3rd quartiles. Several tissue sections contained different tissue type annotations located at one section. Only H-scores of annotations of the predefined tissue type of a patient were included in this analysis. Annotations located near the predefined tissue type annotation (e.g., vSCC patient with adjacent healthy tissue) were not included. As the data were not expected to be normally distributed, a Mann-Whitney U test was used to test for statistical significance of difference in group medians. No adjustment was considered for multiple testing issues due to the exploratory nature of this study. Thus, hypothesis testing results with $p < 0.05$ were considered statistically significant. For marker(s) that showed potential as FGS target based on the selection criteria (Section 2.5), a spaghetti plot was generated for data visualization. The lines in this plot represent patients, the dots are average H-scores per vulvar tissue type within a vSCC patients tissue section. This plot was completed for both HPV-dependent and-independent vSCC patients. No statistical analysis was performed; these data were used for visualization of H-scores and corresponding TBR's per patient.

Results

TISSUE CHARACTERISTICS

In total, 10 dVIN, 16 HPV-independent vSCC, 15 HSIL, 13 HPV-dependent vSCC tissues and 15 healthy vulvar controls were included for biomarker expression evaluation. Due to incidental poor slide quality, not all selected tissue samples could be scored for each marker.

IMMUNOHISTOCHEMICAL MARKER STAINING

Hereafter, a narrative description of the staining of each marker will be given categorized by the previously mentioned four FGS criteria (Section 2.5). Markers are listed in alphabetic order.

αvβ6—Integrin Alpha6

- I Stromal tissue lacked *αvβ6* expression. Healthy vulvar epithelium showed no or low expression of *αvβ6*. If *αvβ6* was present in healthy vulvar tissue, it was mainly located in the spinosal and basal layer of the epithelium (Figure 1A). In addition, *αvβ6* expression was higher in normal vulvar tissues wherein sebaceous glands were present (11/15 healthy vulvar tissues) compared with vulvar tissue sections that lacked those glands. *αvβ6* staining within sebaceous glands was low to moderate (Figure 1A). The median H-score of healthy vulvar tissue was significantly lower compared with median H-scores of all vulvar (pre) malignant tissue types (Figure 2), resulting in TBR's >2 (Table 2).
- II Moderate *αvβ6* expression was observed in 4/8 dVIN, 14/16 HPV-independent vSCC, 4/13 HSIL and 10/13 HPV-dependent vSCC tissues (Figure 1B-E respectively). *αvβ6* expression lacked in 2/16 HPV-independent vSCC and 3/13 HPV-dependent vSCC tissues. The other premalignant tissues showed low expression. More intense *αvβ6* staining was found in HSIL adjacent to HPV-dependent vSCC (average H-score 42) compared with isolated HSIL (average H-score 114). This difference was not observed for dVIN. Median H-scores per vulvar (pre)malignant tissues type were all above 25 (Table 2).
- III *αvβ6* was homogeneously expressed in all HPV-independent vSCC tissues. 2/10 HPV-dependent vSCC tissues showed a patchy staining pattern throughout the tumor, for 2/10 expression was restricted to the spinosal and/or basal layers, the remainder showed homogeneous

Table 2 Median, minimum (min), maximum (max) H-scores and tumor-to-background ratios (TBRs) for each marker per vulvar tissue group are presented. TBRs > 2 are displayed in green (IGS criterion 1, Section 2.5) and a minimum median H-scores of at least 25 in orange (IGS criterion 2, Section 2.5). HPV- vSCC=HPV-independent vSCC and HPV + vSCC=HPV-dependent vSCC.

	<i>αvβ6</i>			CAIX			CD44v6					
	Median	Min	Max	TBR	Median	Min	Max	TBR	Median	Min	Max	TBR
Healthy (n=15)	9	2	31	-	2	0	19	-	240	173	283	-
dVIN (n=10)	59 ^b	20	216	6,6	7b	1	65	3,5	248	123	275	1,0
HPV- vSCC (n=16)	118	0	231	13,1	9 ^a	1	77	4,5	196	96	271	0,8
HSIL (n=15)	42 ^b	3	145	4,7	5	1	92	2,5	223	119	279	0,9
HPV+ vSCC (n=13)	93	7	213	10,3	6	1	102	3,0	118a	51	267	0,5
	EGFR			EpcAM			FRα					
	Median	Min	Max	TBR	Median	Min	Max	TBR	Median	Min	Max	TBR
Healthy (n=15)	61	2	200	-	2	0	12	-	3	1	43	-
dVIN (n=10)	40	2	138	0,7	5	0	11	2,5	1	1	3	0,3
HPV- vSCC (n=16)	129	4	253	2,2	3	0	17	1,5	4a	2	7	1,3
HSIL (n=15)	10	0	213	0,2	2	0	17	1,0	2	0	28	0,7
HPV+ vSCC (n=13)	25	5	106	0,4	7 ^a	0	91	3,5	4	2	60	0,3
	MRPI			MUC1			UPAR					
	Median	Min	Max	TBR	Median	Min	Max	TBR	Median	Min	Max	TBR
Healthy (n=15)	4	0	29	-	11	1	81	-	6	1	22	-
dVIN (n=10)	8	0	24	2,0	63	20	206	5,7	12 ^b	2	35	2,0
HPV- vSCC (n=16)	13 ^c	0	42	0,3	34 ^a	3	184	3,1	37 ^c	5	91	6,2
HSIL (n=15)	2	0	22	0,5	40	3	201	3,6	6 ^c	0	73	1,0
HPV+ vSCC (n=13)	2	0	17	0,5	62	14	176	5,6	19 ^a	1	125	3,1

a = 1 tissue section missing, b = 2 tissue sections missing, c = 3 tissue sections missing

expression. To a greater or lesser extent in all dVIN and HSIL tissues, as for healthy vulvar tissue, $\alpha\text{v}\beta\text{6}$ expression was restricted to the spinosal and/or basal layers (Figure 1A,D).

IV $\alpha\text{v}\beta\text{6}$ showed cell membrane staining.

CAIX—Carbonic Anhydrase IX

- I Stromal and healthy vulvar epithelium lacked CAIX staining (Figure 1F). The median H-score of healthy vulvar tissues was significantly lower compared with median H-scores of dVIN, HSIL and HPV-dependent VSCC tissue groups (Figure 2), resulting in TBR's > 2 (Table 2). The median H-score of HPV-independent VSCC tissue group was not tested significantly higher compared with the median H-score of healthy vulvar tissue (TBR 4.5, Table 2).
- II Most vulvar (pre)malignant tissues showed low CAIX expression (Figure 1H-J), 1-2 samples per tissue group showed moderate CAIX expression (Figure 1G). Median H-scores per vulvar (pre)malignant tissues type were all below 25 (Table 2).
- III If CAIX staining was observed, it was positioned in the spinosal and/or basal layers of the vulvar epidermis in a heterogeneous and patchy pattern (Figure 1G-J).
- IV CAIX showed cell membrane staining.

CD44V6—CD44 Variant 6

- I Stromal tissue lacked CD44V6 staining. Healthy vulvar epithelium showed in 7/15 tissues high CD44V6 expression, the remaining tissues showed moderate expression (Figure 1K). TBR's were inverse for all (pre)malignant vulvar tissue types, indicating downregulation of CD44V6 in (pre)malignant compared with healthy tissue (Figure 2). Consequently, TBR's were not in favor for FGS application at the surface of the vulva (Table 2).
- II Predominantly moderate CD44V6 staining was observed in vulvar (pre)malignant tissues (Figure 1L-O), in 5/10 dVIN, 3/16 HPV-independent VSCC, 5/15 HSIL and 1/12 HPV-dependent VSCC tissues high CD44V6 expression was observed. Median CD44V6 H-scores per vulvar (pre)malignant tissues type were all above 25 (Table 2).
- III CD44V6 showed homogenous expression.
- IV CD44V6 showed cell membrane staining.

EGFR—Epithelial Cell Adhesion Molecule

- I EGFR staining was observed in glands, blood vessels and adnexa. Healthy vulvar epithelium showed moderate EGFR expression in 10/15 tissues (Figure 1P) and low expression in 5/15 tissues. TBR's were inverse for all (pre)malignant vulvar tissue types, indicating downregulation of EGFR in (pre)malignant tissue compared with healthy (Figure 2) Consequently, TBR's were not in favor for FGS application at the surface of the vulva (Table 2).
- II EGFR was moderately expressed in 5/10 dVIN, 11/16 HPV-independent VSCC, 5/15 HSIL and 2/13 HPV-dependent VSCC tissues (Figure 1Q,R), the expression in the remaining samples was low (Figure 1S,T, except 1 HPV-independent VSCC with high expression). HSIL showed a median H-score below 25, the H-scores for other vulvar (pre)malignant tissue types were at least 25 (Table 2).
- III EGFR was gradually expressed in healthy vulvar epithelium, being more strongly expressed in the stratum basal compared with the stratum corneum. For (pre)malignant tissues the expression patterns were diverse. Homogenous (Figure 1R), patchy (Figure 1Q,S) and on/off expression patterns (Figure 1T) were observed in these tissues.
- IV EGFR showed cell membrane staining.

EpCAM—Epithelial Cell Adhesion Molecule

- I EPCAM staining was not observed in stromal tissue, except for the endothelial lining of blood vessels. Healthy vulvar epithelium lacked EPCAM expression (Figure 1U). The median H-score of healthy vulvar tissue was not significantly different compared with any vulvar (pre)malignant tissue group (Figure 2), resulting in TBR's < 2 , except for dVIN with an TBR of 2.5 (Table 2).
- II EPCAM expression was absent or low for all vulvar (pre)malignant tissue types (Figure 1V-Y), with median H-scores below 25 (Table 2).
- III No pattern could be recognized due to the low expression of EPCAM in vulvar tissues.
- IV EPCAM showed cell membrane staining on the endothelial lining of blood vessels.

FR α —Folate Receptor α

- I FR α staining was absent in both stromal and healthy vulvar epithelium (Figure 1Z). The median H-score of healthy vulvar tissue was significantly lower compared with the median H-score of dVIN tissue (Figure 2), resulting in a TBR >2 . TBR's for other (pre)malignant tissue groups were <2 (Table 2).
- II FR α expression was absent or low for all vulvar (pre)malignant tissue types (Figure 1AA-DD), with median H-scores below 25 (Table 2).
- III No pattern could be recognized due to the low expression of FR α in all vulvar tissues.
- IV Cell membrane staining for FR α was observed in lung tumor tissue (control).

MRP1—Multidrug Resistance-Associated Protein

- I Low to moderate MRP1 staining was observed in stromal cells and several sebaceous glands of a few healthy and (pre) malignant tissues. No MRP1 expression was observed in healthy vulvar epithelium (Figure 1EE). The median H-score of healthy vulvar tissue was not significantly lower compared with any median H-score of (pre)malignant tissues (Figure 2), resulting in TBR's <2 (Table 2).
- II MRP1 expression was absent or low for all vulvar (pre)malignant tissue types (Figure 1FF-II), with median H-scores below 25 (Table 2).
- III No expression pattern could be recognized due to the overall low expression of MRP1.
- IV In both stromal vulvar tissue as in placental tissue (control), cytoplasmic and membranous presence of MRP1 was observed on cells.

MUC1—Mucin 1

- I Stromal tissue lacked MUC1 staining, except for sebaceous glands positioned in the dermis, which showed moderate or high MUC1 expression (Figure 1JJ). Half of the healthy vulvar epithelial tissues lacked MUC1 expression (Figure 1JJ), others showed low expression restricted to the stratum spinosum. The median H-score of healthy vulvar tissue was significantly lower compared with median H-scores of all vulvar (pre)malignant tissue types (Figure 2), resulting in TBR's >2 (Table 2).

- II Moderate MUC1 expression was observed in 5/10 dVIN (Figure 1KK), 6/16 HPV-dependent vSCC, 6/14 HSIL and 7/13 HPV-dependent vSCC tissues, the remaining tissues showed low expression (Figure 1LL-NN). Median H-scores for MUC1 expression per vulvar (pre)malignant tissues type were all above 25 (Table 2).
- III The expression pattern was heterogenous and patchy throughout all tissue samples.
- IV MUC1 showed cell membrane staining.

uPAR—Urokinase Plasminogen Activator Receptor

- I Low stromal expression of uPAR was observed in healthy and (pre)malignant tissues. Healthy vulvar epithelium lacked uPAR staining (Figure 1OO). The median H-score of healthy vulvar tissues was significantly lower compared with median H-scores of dVIN, HPV-dependent and independent vSCC tissue groups (Figure 2), resulting in TBR's >2 (Table 2). For the HSIL group, the TBR <2 .
- II Moderate uPAR expression was observed in 4/12 HPV-independent vSCC (Figure 1QQ), 1/12 HSIL and 2/12 HPV-dependent vSCC tissues (Figure 1SS), the remaining vulvar (pre)malignant tissues showed low or absent expression (Figure 1PP,RR). Only the median H-score for uPAR expression in the HPV-independent vSCC tissue group was above 25 (Table 2).
- III uPAR was heterogeneously expressed throughout (pre)malignant vulvar tissue.
- IV uPAR showed cell membrane staining and sometimes cytoplasmic staining in cells.

EVALUATION OF FGS CRITERIA

Based on biomarker expression in the vulvar tissue cohort (Section 3.2), only $\alpha v\beta 6$ meets all four criteria required to serve as a potential target for tumor-specific imaging in vulvar (pre)malignancies. Therefore, further evaluation of biomarker expression in individual vSCC sections was performed for $\alpha v\beta 6$. Representative examples of $\alpha v\beta 6$ -stained HPV-dependent and HPV-independent vSCC sections, processed by Qupath, are shown in Figures S2 and S3 respectively. The other biomarkers were excluded for further analysis because CAIX, EPCAM, MRP1 showed H-scores for (pre)malignant tissue below 25, TBR's for CD44v6 and EGFR appeared to be inverse and heterogeneous expression was observed for MUC1 and uPAR.

αvβ6 Expression in Individual vSCC Tissue Sections

Evaluation of $\alpha v\beta 6$ expression on an individual level was not performed for all patients, as 7/16 HPV-independent and 3/13 HPV-dependent vSCC tissue sections did not contain adjacent healthy and/or precursor tissue. In 7/9 HPV-independent and 4/10 HPV-dependent vSCC patients TBR's > 2, based on H-scores of both malignant and premalignant compared with healthy, were observed (represented by a green line, Figure 3). In 3/10 HPV-dependent vSCC sections only favorable TBR's for premalignant compared to healthy were observed (represented by an orange line, Figure 3). In 2/9 HPV-independent and 3/10 HPV-dependent vSCC's TBR's were not in favor of FGS at all (indicated by a red line, Figure 3). Based on this pilot, $\alpha v\beta 6$ could serve as a suitable target for tumor-specific imaging in vulvar (pre)malignancies for 78% of HPV-dependent vSCC patients (with adjacent dVIN tissue) and 40% of HPV-dependent vSCC patients. As not all cases showed $\alpha v\beta 6$ positivity, CAIX, MUC1 and UPAR TBRs were plotted against $\alpha v\beta 6$ TBR's for all 19 above-mentioned vSCC patients, to check case-by-case for an alternative target in case of $\alpha v\beta 6$ negativity (Figure S4). Those alternative targets were chosen as they showed TBR's > 2 for a part of the vSCC patients. In a few cases MUC1 or UPAR might serve as an alternative target (left upper quadrant, Figure S4.).

Discussion

Demarcation of vulvar (pre)malignancies during diagnosis, staging and surgery is often difficult for clinicians. This phenomenon contributes to significant morbidity and high recurrence rates of up to 40% for vSCC patients after treatment. FGS could improve resection precision of involved tissue and decrease mutilating surgeries. To our knowledge, no data have been published on the use of FGS for vSCC or precursor lesions. Therefore, we used IHC to evaluate target expressions on vulvar tissues to assess their potential for FGS. Our selection of targets was based on (I) enhanced expression in vulvar tumors as described in the available literature and (II) effectiveness of tracers against these targets obtained from studies with other tumor types.^{17,18,20,22-24}

Out of 9 candidates we assessed, integrin $\alpha v\beta 6$ emerged as the most promising target for FGS of vSCC based on immunohistochemistry. This conclusion is based on the upregulated homogeneous expression of $\alpha v\beta 6$

in vSCC's compared with surrounding stromal tissue and normal squamous epithelium of the healthy control group. Resulting in TBR's well above the set limit of 2. These suitable TBR's were confirmed within vSCC patient's using IHC. $\alpha v\beta 6$ showed suitable TBR's in 78% of HPV-independent and 40% of HPV-dependent vSCC patients (Figure 3). TBR's for $\alpha v\beta 6$ in premalignancies dVIN and HSIL were lower compared with vSCC, but still above the indicated threshold. Higher $\alpha v\beta 6$ expression was found in HSIL adjacent to HPV-dependent vSCC's compared with isolated HSIL, encouraging more effective removal of adjacent HSIL during vSCC surgery.

CAIX, EPCAM, MRP1 and FR α showed no or low expression in vulvar malignant tissues and were therefore excluded from further evaluation. CD44V6 and EGFR showed an overall high expression in all tissues, including normal squamous epithelium, resulting in reversed TBR's. If desired, these last two markers could help discriminate infiltrating tumor tissue with FGS, due to the absence of both markers in surrounding stromal tissue. Alternatively, these markers may be used for reversed fluorescence imaging, with distinctive higher expression of the target in healthy compared with malignant tissue.³⁵ MUC1 and UPAR were excluded from further evaluation due to their heterogenous or patchy expression pattern in vulvar malignant tissue.

Although several markers (EGFR, CD44V6, MRP1, MUC1 and CAIX) were identified as potential targets for FGS of vSCC's based on our systematic review, their candidacies were not always confirmed in this study.²² This discordance might be explained by the absence of normal tissue as well as the choice of antibodies and different methods applied in the various IHC studies. Effects of expression patterns per antibody are for example explained in an IHC study on cervical cancer tissues.³⁶ Finding the antibody with the highest expression pattern in tumor tissue was not the goal of this study. Instead, we chose to apply antibodies most similar to 'corresponding' clinically available FGS in order to (I) translate the IHC results in to an imaging setting and (II) accelerate a future clinical translation if a target/tracer combination showed potential.

Several observations should be considered when proceeding with $\alpha v\beta 6$ as a target for FGS in vSCC. First, with the used integrin $\alpha v\beta 6$ antibody we observed positively stained sebaceous glands just below the vulvar epithelium in the healthy control tissue. The sac-like alveoli of sebaceous glands are composed of stratified cuboidal or polyhedral epithelial cells. We noticed

more sebaceous glands positioned in epithelium of the control vulvar tissues compared with adjacent normal tissue in vSCC samples. The healthy control tissue was obtained from younger women. Sebaceous gland activity is known to decrease in women after menopause, which might be advantageous for TBR-ratios in elderly vulvar cancer patients.^{37,38} Whether the remaining positively stained $\alpha v\beta 6$ glands lead to difficulties during FGS in younger patients is hard to predict. We assume that the fluorescent signal of these glands will be inferior to the superficial and more enhanced expression in tumors. Another observation that should be considered when proceeding with $\alpha v\beta 6$ as target, is the fact that not all vSCC samples showed enhanced $\alpha v\beta 6$ expression. Minimal or absent $\alpha v\beta 6$ expression was noted in two HPV-independent and two HPV-dependent vSCC samples, resulting in 14% of vSCC cases. In comparison with other squamous tumor, this 'on/off' phenomenon was seen in 13% cutaneous squamous cell carcinoma patients.²⁰ For the $\alpha v\beta 6$ -negative cases, we assessed if other examined targets could be used instead. Not one of the other examined markers met all four FGS criteria (Section 2.5) and could generally be used for $\alpha v\beta 6$ -negative cases. However, a case-by-case evaluation should be performed for personalized alternatives in case of $\alpha v\beta 6$ -negativity. In some cases, MUC1 or UPAR might serve as an alternative vSCC-target for FGS in case of $\alpha v\beta 6$ negativity (Figure S4, left upper quadrant).

An explanation for the different expression patterns of integrin $\alpha v\beta 6$ in vSCC remains elusive. A hallmark function of $\alpha v\beta 6$ is the activation of transforming growth factor- $\beta 1$ (TGF-1) to modulate innate immune surveillance in e.g., skin. Therefore, it is possible that different expression patterns of $\alpha v\beta 6$ are explained by the difference in tumor-immune infiltration.³⁸ In addition, different FIGO stages of included tumors may explain variation in expression patterns. High-grade progressive tumors show different levels of cell-adhesion compared with low-grade tumors and integrins are cell surface receptors responsible for cell-to-matrix and cell-to-cell adhesion.³⁸⁻⁴⁰ Structural differences in expression patterns, especially those observed between the virally and non-virally induced tumors, should be confirmed in larger cohort studies. The availability of patients' medical history including FIGO stage, detailed demographics, surgical margins, and other characteristics could improve the value of the data set substantially. Especially the assessment of whether $\alpha v\beta 6$ is overexpressed in associated locoregional lymph node metastases compared with background tissue

and negative lymph nodes. IF TBR's for involved lymph nodes are applicable, FGS positive nodes could improve overall survival.⁴¹ In addition, future research should investigate whether adjuvant radiotherapy, as part of treatment for locally advanced and metastatic disease, is of influence on $\alpha v\beta 6$ expression patterns.

As indicated above, evaluation of $\alpha v\beta 6$ as a target for FGS of vulvar (pre)malignancies was chosen based on promising (pre)clinical results in other cancer types.²⁰ The benefit of this is the availability of imaging agents targeting $\alpha v\beta 6$, like the recently developed linear peptide A20FMDV2 or knottin-peptide R01-MG.^{42,43} For FGS application the latter peptide was conjugated to fluorescent tracer IRDye800CW to improve complete resection of patients with pancreatic ductal adenocarcinoma. In subcutaneous and orthotopic mouse pancreatic tumor models R01-MG-IRDye800 showed specific targeting to $\alpha v\beta 6$ and holds promise as a tool to recognize pancreatic cancer with FGS.⁴² Another example of a fluorescent imaging agent is cRGD-ZW800-1, that binds primarily to $\alpha v\beta 3$ but has also affinity for $\alpha v\beta 6$. This agent is already assessed for clinical use in colorectal cancer imaging.⁴⁴ No data can be found on $\alpha v\beta 3$ expression in vulvar tissue. Therefore, the potential of this imaging agent for FGS in vSCC should be further investigated.

Although this paper focused on immunohistochemical evaluation of molecular imaging targets meant for FGS, $\alpha v\beta 6$ could also be used as target for imaging with PET or SPECT/CT.^{45,46} In addition, $\alpha v\beta 6$ could be used as target for different treatment modalities. It's suitability for this purposes indicated by several anticancer strategies based on $\alpha v\beta 6$ targeting, including immunoliposomes used as vectors in tumor targeted therapy.⁴⁷ Future research should focus on evaluation of $\alpha v\beta 6$ -targeting probes in *ex vivo* models, for instance in 3D vulvar skin-tumor models, as a step towards clinical translatability.^{48,49} Presuming that targets expressed on vSCC-cells are mostly unoccupied in-situ, so that an $\alpha v\beta 6$ -targeted FGS probe will be able to access the ligand binding site. Besides multiple deployment of this $\alpha v\beta 6$ target, it would also be nice to verify in future studies IF the modality FGS on itself might be useful for other vulvar diseases, as e.g., Paget disease of the vulva, which often extends beyond the visible lesion.

Next to the limited size of the cohort a limitation of this study is the pre-selection of biomarkers. The selection was based on enhanced expression of targets as described in the available literature and effectiveness of tracers against these targets obtained from studies with other tumor

types.^{17,18,20,22-24} Alternatively, an ‘omics’ search could be performed in combination with artificial intelligence to detect all currently (un)known targets and check their expression on vulvar healthy compared to (pre)malignant tissues. Nevertheless, promising target/tracer combinations based on ‘omics’ findings should still be evaluated in the clinic. Another limitation is the slight overestimation of Qupath for epithelial cells in stromal areas, which was observed in most tissue sections. As this phenomenon was equally observed in all differently selected tissue types, we assessed that it does not affect the tumor-to-background ratio substantially. It might even underestimate this ratio as almost all stromal cells stained negative. In addition, the semi-automated analysis using Qupath on small cohorts is labor intensive, even compared to visual scoring of IHC-stained sections. It is therefore desirable to further optimize this method, before testing the potential of targets for IGS application on a larger cohort of tissues. A self-learning algorithm can be drawn based on this training set for future reference. Furthermore, since this study was limited by scarcity of vulvar (pre) malignant tissues, it was not possible to define the sensitivity and specificity for IGS suitability per marker. However, this set could be used as a ‘training set’ for a future multicenter study wherein sufficient vulvar tissue samples can be included.

Conclusions

$\alpha v \beta 6$ is a promising target for tumor-specific (pre- and intra-operative) molecular imaging of vSCC lesions, which can be hard to distinguish from healthy tissue. For HPV-unrelated vSCC’s with adjacent dVIN, that comprise the vast majority of all vSCC’s, $\alpha v \beta 6$ has shown great potential for precise discrimination at the superficial tissue margins. Further research is needed to validate the use of an $\alpha v \beta 6$ -targeted probe for FGS of vulvar (pre) malignancies. Finally, it should be verified whether addition of this technique leads to fewer recurrences and surgery-related morbidities for vSCC patients.

SUPPLEMENTARY MATERIALS The following are available online at www.mdpi.com/xxx/s1, Table S1: Antigen retrieval methods applied: pepsin, trypsin and DAKO citrate buffers; Script S1: Script used for digital pathology image analysis using Qupath; Figure S1: Zoomed images of immunohistochemical

control staining’s of nine examined markers, Figure S2: By Qupath processed tissue sections of a patient with HPV-dependent vSCC, Figure S3: By Qupath processed tissue sections of a patient with HPV-independent vSCC with tissue transition zones, Figure S4: Comparison of MUC1, CAIX and UPAR TBR’s against $\alpha v \beta 6$ TBR’s for vSCC patients.

Figure 1 Representative images of $\alpha v\beta 6$ (A-E), CAIX (F-J), CD44V6 (K-O), EGFR (P-T), EPCAM (U-Y), FR α (Z-DD), MRP1 (EE-II), MUC1 (JJ-NN) and UPAR (OO-SS) expression in healthy vulvar tissue with (sebaceous) glands, differentiated vulvar intraepithelial neoplasia (dVIN), human papilloma virus-independent vulvar squamous cell carcinoma (HPV-independent VSCC), high grade squamous intraepithelial lesion (HSIL) and human papilloma virus-dependent vulvar squamous cell carcinoma (HPV-dependent VSCC). All images show only the predefined tissue type of that section (no adjacent tissue). Scale bars represent 500 μ m.

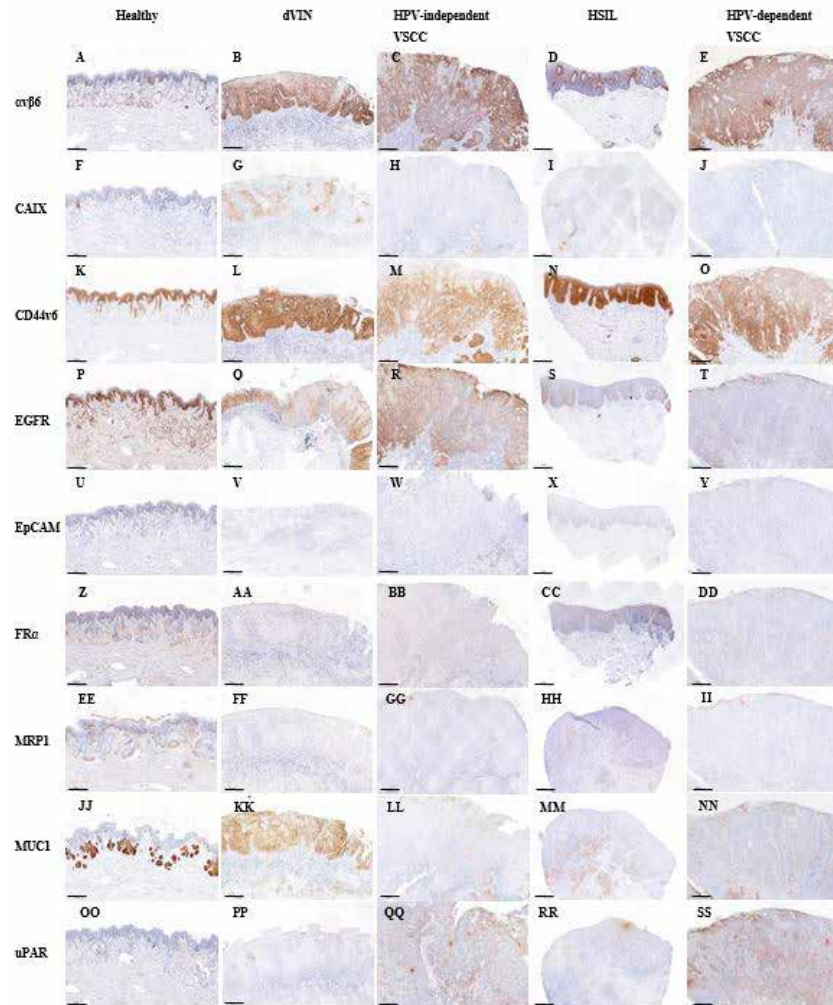
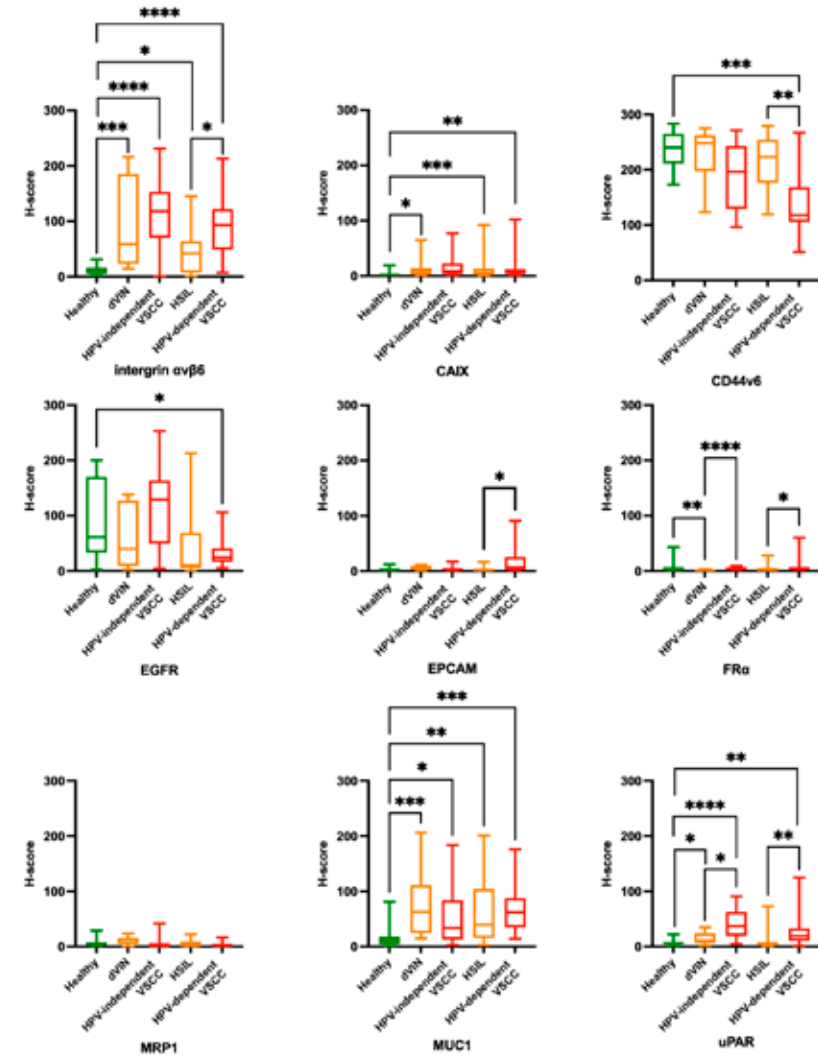
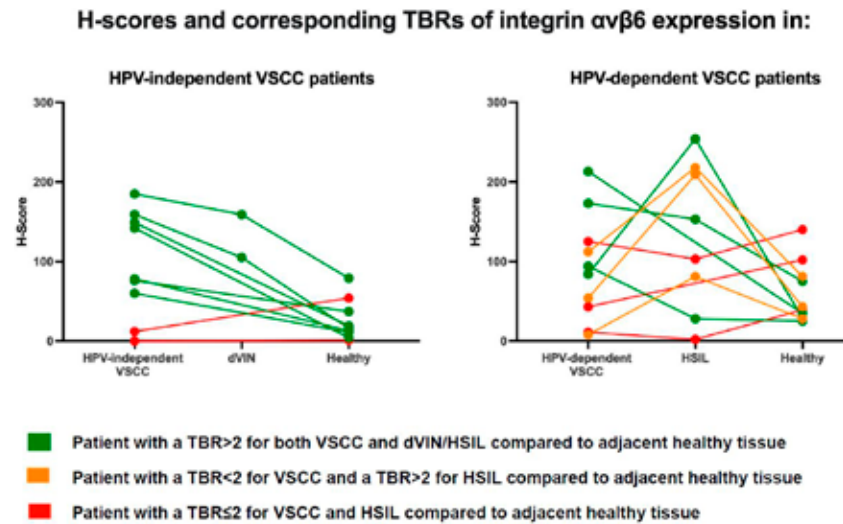


Figure 2 Boxplots representing median H-scores per vulvar tissue type (including 1st and 3rd percentiles) for integrin $\alpha v\beta 6$, CAIX, CD44V6, EGFR, EPCAM, FR α , MRP1, MUC1, UPAR. Statistical analyses were performed between different median H-scores: HV/dVIN, HV/HPV-independent VSCC, HV/HSIL, HV/HPV-dependent VSCC, dVIN/HPV-independent VSCC, HSIL/HPV-dependent VSCC.



ns = $p > 0.05$ (not shown), * = $p \leq 0.05$, ** = $p \leq 0.01$, *** = $p \leq 0.001$, **** = $p \leq 0.0001$. 10 dVIN, 16 HPV-independent VSCC, 15 HSIL, 13 HPV-dependent VSCC tissues and 15 healthy vulvar controls were included

Figure 3 Spaghetti plots of integrin $\alpha v \beta 6$ expression within vSCC patients. Lines in this plot represent patients, a dot is an average H-score of a vulvar tissue type within that patient's tissue section (for instance the average H-score of all a djacent HSIL tissue annotations). Left: HPV-independent vSCC patients, right: HPV-dependent vSCC patients. Based on H-scores, TBRs are calculated (H-score (pre)malignant tissue/H-score of healthy tissue=TBR). A green line indicates higher expression of $\alpha v \beta 6$ in (pre)malignant compared to the healthy tissue (TBR > 2); an orange line indicates a TBR < 2 for vSCC and a TBR > 2 for HSIL compared to healthy tissue; a red line indicates higher expression in healthy compared to (pre)malignant tissue (TBR \leq 1). Not all TBRs of vSCC patients are plotted, as not all tissue samples included normal (and/or premalignant) tissue adjacent to the tumor.



REFERENCES

- 1 Eva, L.J.; Sadler, L.; Fong, K.L.; Sahota, S.; Jones, R.W.; Bigby, S.M. Trends in HPV-dependent and HPV-independent vulvar cancers: The changing face of vulvar squamous cell carcinoma. *Gynecol. Oncol.* 2020, 157, 450–455, doi:10.1016/j.ygyno.2020.01.029.
- 2 Tan, A.; Bieber, A.K.; Stein, J.; Pomeranz, M.K. Diagnosis and management of vulvar cancer: A review. *J. Am. Acad. Dermatol.* 2019, 81, 1387–1396, doi:10.1016/j.jaad.2019.07.055.
- 3 Schuurman, M.; Einden, L.V.D.; Massuger, L.; Kiemeny, L.; van der Aa, M.; de Hullu, J. Trends in incidence and survival of Dutch women with vulvar squamous cell carcinoma. *Eur. J. Cancer* 2013, 49, 3872–3880, doi:10.1016/j.ejca.2013.08.003.
- 4 Thuijjs, N.B.; Van Beurden, M.; Bruggink, A.H.; Steenberg, R.D.M.; Berkhof, J.; Bleeker, M.C.G. Vulvar intraepithelial neoplasia: Incidence and long-term risk of vulvar squamous cell carcinoma. *Int. J. Cancer* 2021, 148, 90–98, doi:10.1002/ijc.33198.
- 5 Hinten, F.; Molijn, A.; Eckhardt, L.; Massuger, L.; Quint, W.; Bult, P.; Bulten, J.; Melchers, W.; de Hullu, J. Vulvar cancer: Two pathways with different localization and prognosis. *Gynecol. Oncol.* 2018, 149, 310–317, doi:10.1016/j.ygyno.2018.03.003.
- 6 McAlpine, J.N.; Kim, S.Y.; Akbari, A.; Eshragh, S.; Reuschenbach, M.; Doeberitz, M.V.K.; Prigge, E.S.; Jordan, S.; Singh, N.; Miller, D.M.; et al. HPV-independent Differentiated Vulvar Intraepithelial Neoplasia (dVIN) is Associated With an Aggressive Clinical Course. *Int. J. Gynecol. Pathol.* 2017, 36, 507–516, doi:10.1097/pgp.0000000000000375.
- 7 Oonk, M.H.; Planchamp, F.; Baldwin, P.; Bidzinski, M.; Brännström, M.; Landoni, F.; Mahner, S.; Mahantshetty, U.; Mirza, M.; Petersen, C.; et al. European Society of Gynaecological Oncology Guidelines for the Management of Patients With Vulvar Cancer. *Int. J. Gynecol. Cancer* 2017, 27, 832–837, doi:10.1097/igc.0000000000000975.
- 8 Dellinger, T.H.; Hakim, A.A.; Lee, S.J.; Wakabayashi, M.T.; Morgan, R.J.; Han, E.S. Surgical Management of Vulvar Cancer. *J. Natl. Compr. Cancer Netw.* 2016, 15, 121–128, doi:10.6004/jnccn.2017.0009.
- 9 Nooij, L.; Brand, F.; Gaarenstroom, K.; Creutzberg, C.; de Hullu, J.; van Poelgeest, M. Risk factors and treatment for recurrent vulvar squamous cell carcinoma. *Crit. Rev. Oncol.* 2016, 106, 1–13, doi:10.1016/j.critrevonc.2016.07.007.
- 10 Gaarenstroom, K.N.; Kenter, G.G.; Trimbos, J.B.; Agous, I.; Amant, F.; Peters, A.A.W.; Vergote, I. Postoperative complications after vulvectomy and inguinofemoral lymphadenectomy using separate groin incisions. *Int. J. Gynecol. Cancer* 2003, 13, 522–527, doi:10.1046/j.1525-1438.2003.13304.x.
- 11 Muigai, J.; Jacob, L.; Dinas, K.; Kostev, K.; Kalder, M. Potential delay in the diagnosis of vulvar cancer and associated risk factors in women treated in German gynecological practices. *Oncotarget* 2018, 9, 8725–8730, doi:10.18632/oncotarget.23848.
- 12 Micheletti, L.; Preti, M.; Cintolesi, V.; Corvetto, E.; Privitera, S.; Palmese, E.; Benedetto, C. Prognostic impact of reduced tumor-free margin distance on long-term survival in FIGO stage 1B/11 vulvar squamous cell carcinoma. *J. Gynecol. Oncol.* 2018, 29, e61, doi:10.3802/jgo.2018.29.e61.
- 13 Nooij, L.S.; van der Slot, M.A.; Dekkers, O.M.; Stijnen, T.; Gaarenstroom, K.N.; Creutzberg, C.L.; Smit, V.T.H.B.M.; Bosse, T.; Van Poelgeest, M.I.E. Tumour-free margins in vulvar squamous cell carcinoma: Does distance really matter? *Eur. J. Cancer* 2016, 65, 139–149, doi:10.1016/j.ejca.2016.07.006.
- 14 Vahrmeijer, A.L.; Hutteman, M.; Van Der Vorst, J.R.; Van De Velde, C.J.H.; Frangioni, J.V. Image-guided cancer surgery using near-infrared fluorescence. *Nat. Rev. Clin. Oncol.* 2013, 10, 507–518, doi:10.1038/nrclinonc.2013.123.
- 15 Rosenthal, E.L.; Warram, J.M.; de Boer, E.; Basilion, J.P.; Biel, M.A.; Bogyo, M.; Bouvet, M.; Brigman, B.E.; Colson, Y.L.; DeMeester, S.R.; et al. Successful Translation of Fluorescence Navigation During Oncologic Surgery: A Consensus Report. *J. Nucl. Med.* 2016, 57, 144–150, doi:10.2967/jnumed.115.158915.
- 16 Boonstra, M.C.; De Geus, S.W.; Prevoo, H.A.; Hawinkel, S.L.; Van De Velde, C.J.; Kuppen, P.J.; Vahrmeijer, A.L.; Sier, C.F. Selecting Targets for Tumor Imaging: An Overview of Cancer-Associated Membrane Proteins. *Biomarkers Cancer* 2016, 8, BIC.S38542–133, doi:10.4137/bic.s38542.
- 17 Hernot, S.; van Manen, L.; Debie, P.; Mieog, J.S.D.; Vahrmeijer, A.L. Latest developments in molecular tracers for fluorescence image-guided cancer surgery. *Lancet Oncol.* 2019, 20, e354–e367, doi:10.1016/s1470-2045(19)30317-1.
- 18 De Muynck, L.D.A.N.; Gaarenstroom, K.N.; Sier, C.F.M.; Van Duijvenvoorde, M.; Bosse, T.; Mieog, J.S.D.; De Kroon, C.D.; Vahrmeijer, A.L.; Peters, I.T.A. Novel Molecular Targets for Tumor-Specific Imaging of Epithelial Ovarian Cancer Metastases. *Cancers* 2020, 12, doi:10.3390/cancers12061562.
- 19 Hollandsworth, H.M.; Turner, M.A.; Hoffman, R.M.; Bouvet, M. A review of tumor-specific fluorescence-guided surgery for colorectal cancer. *Surg. Oncol.* 2021, 36, 84–90, doi:10.1016/j.suronc.2020.11.018.
- 20 Baart, V.M.; Van Duijn, C.; Van Egmond, S.L.; Dijkmeester, W.A.; Jansen, J.C.; Vahrmeijer, A.L.; Sier, C.F.M.; Cohen, D. EGFR and $\alpha v \beta 6$ as Promising Targets for Molecular Imaging of Cutaneous and Mucosal Squamous Cell Carcinoma of the Head and Neck Region. *Cancers* 2020, 12, 1474, doi:10.3390/cancers12061474.
- 21 Odenthal, J.; Rijpkema, M.; Bos, D.; Wagena, E.; Croes, H.; Grenman, R.; Boerman, O.; Takes, R.; Friedl, P. Targeting CD44v6 for fluorescence-guided surgery in head and neck squamous cell carcinoma. *Sci. Rep.* 2018, 8, 1–11, doi:10.1038/s41598-018-28059-9.
- 22 Huisman, B.; Burggraaf, J.; Vahrmeijer, A.; Schoones, J.; Rissmann, R.; Sier, C.; Van Poelgeest, M. Potential targets for tumor-specific imaging of vulvar squamous cell carcinoma: A systematic review of candidate biomarkers. *Gynecol. Oncol.* 2020, 156, 734–743, doi:10.1016/j.ygyno.2019.12.030.

- 23 Christensen, A.; Juhl, K.; Persson, M.; Charabi, B.W.; Mortensen, J.; Kiss, K.; Lelkaitis, G.; Rubek, N.; Von Buchwald, C.; Kjær, A. uPAR-targeted optical near-infrared (NIR) fluorescence imaging and PET for image-guided surgery in head and neck cancer: proof-of-concept in orthotopic xenograft model. *Oncotarget* 2016, 8, 15407–15419, doi:10.18632/oncotarget.14282.
- 24 Boonstra, M.; Van Driel, P.; Keereweer, S.; Prevoo, H.; Stammes, M.; Baart, V.; Löwik, C.; Mazar, A.; van de Velde, C.; Vahrmeijer, A.; et al. Preclinical uPAR-targeted multimodal imaging of locoregional oral cancer. *Oral Oncol.* 2017, 66, 1–8, doi:10.1016/j.oraloncology.2016.12.026.
- 25 Cheng, A.S.; Karnezis, A.N.; Jordan, S.; Singh, N.; McAlpine, J.N.; Gilks, C.B. p16 Immunostaining Allows for Accurate Subclassification of Vulvar Squamous Cell Carcinoma Into HPV-Associated and HPV-Independent Cases. *Int. J. Gynecol. Pathol.* 2016, 35, 385–393, doi:10.1097/pgp.000000000000263.
- 26 Kortekaas, K.E.; Bastiaannet, E.; van Doorn, H.C.; de Vos van Steenwijk, P.J.; Ewing-Graham, P.C.; Creutzberg, C.L.; Akdeniz, K.; Nooij, L.S.; van der Burg, S.H.; Bosse, T.; et al. Vulvar cancer subclassification by HPV and P53 status results in three clinically distinct subtypes. *Gynecol. Oncol.* 2020, 159, 649–656, doi:10.1016/j.ygyno.2020.09.024.
- 27 Dasgupta, S.; Ewing-Graham, P.C.; Swagemakers, S.M.; van der Spek, P.J.; van Doorn, H.C.; Hegt, V.N.; Koljenović, S.; van Kemenade, F.J. Precursor lesions of vulvar squamous cell carcinoma – histology and biomarkers: A systematic review. *Crit. Rev. Oncol.* 2020, 147, 102866, doi:10.1016/j.critrevonc.2020.102866.
- 28 Rakislova, N.; Alemany, L.; Clavero, O.; Saco, A.; Torné, A.; Del Pino, M.; Munmany, M.; Rodrigo-Calvo, M.; Guerrero, J.; Marimon, L.; et al. P53 Immunohistochemical Patterns in HPV-Independent Squamous Cell Carcinomas of the Vulva and the Associated Skin Lesions: A Study of 779 Cases. *Int. J. Mol. Sci.* 2020, 21, 8091, doi:10.3390/ijms21218091.
- 29 Bankhead, P.; Loughrey, M.B.; Fernández, J.A.; Dombrowski, Y.; McArt, D.G.; Dunne, P.D.; McQuaid, S.; Gray, R.T.; Murray, L.J.; Coleman, H.G.; et al. QuPath: Open source software for digital pathology image analysis. *Sci. Rep.* 2017, 7, 1–7, doi:10.1038/s41598-017-17204-5.
- 30 Berben, L.; Wildiers, H.; Marcelis, L.; Antoranz, A.; Bosio, F.; Hatse, S.; Floris, G. Computerised scoring protocol for identification and quantification of different immune cell populations in breast tumour regions by the use of QuPath software. *Histopathol.* 2020, 77, 79–91, doi:10.1111/his.14108.
- 31 Greene, C.; O'Doherty, E.; Sidi, F.A.; Bingham, V.; Fisher, N.C.; Humphries, M.P.; Craig, S.G.; Harewood, L.; McQuaid, S.; Lewis, C.; et al. The Potential of Digital Image Analysis to Determine Tumor Cell Content in Biobanked Formalin-Fixed, Paraffin-Embedded Tissue Samples. *Biopreservation Biobanking* 2021, 19, 324–331, doi:10.1089/bio.2020.0105.
- 32 Thike, A.A.; Chng, M.J.; Tan, P.H.; Fook-Chong, S. Immunohistochemical expression of hormone receptors in invasive breast carcinoma: correlation of results of H-score with pathological parameters. *Pathol.* 2001, 33, 21–25, doi:10.1080/00313020123290.
- 33 Van Oosten, M.; Crane, L.M.; Bart, J.; van Leeuwen, F.W.; van Dam, G.M. Selecting Potential Targetable Biomarkers for Imaging Purposes in Colorectal Cancer Using Target Selection Criteria (TASC): A Novel Target Identification Tool. *Transl. Oncol.* 2011, 4, 71–82, doi:10.1593/tlo.10220.
- 34 Hoogstins, C.E.; Weixler, B.; Boogerd, L.S.; Hoppener, D.J.; Prevoo, H.A.; Sier, C.; Burger, J.W.; Verhoef, C.; Bhairosingh, S.; Sarasqueta, A.F.; et al. In Search for Optimal Targets for Intraoperative Fluorescence Imaging of Peritoneal Metastasis From Colorectal Cancer. *Biomarkers Cancer* 2017, 9, 11792991772825,, doi:10.1177/1179299917728254.
- 35 Aleksandrov, A.; Meshulam, M.; Smith, A.V.; Chauvet, P.; Canis, M.; Bourdel, N. Fluorescence-guided management of deep endometriosis. *Fertil. Steril.* 2020, 114, 1116–1118, doi:10.1016/j.fertnstert.2020.07.026.
- 36 Chantima, W.; Thepthai, C.; Cheunsuchon, P.; Dharakul, T. EpCAM expression in squamous cell carcinoma of the uterine cervix detected by monoclonal antibody to the membrane-proximal part of EpCAM. *BMC Cancer* 2017, 17, 811, doi:10.1186/s12885-017-3798-z.
- 37 Bolognia, J.L. Aging skin. *Am. J. Med.* 1995, 98, S99–S103, doi:10.1016/s0002-9343(99)80066-7.
- 38 Koivisto, L.; Bi, J.; Häkkinen, L.; Larjava, H. Integrin $\alpha\beta6$: Structure, function and role in health and disease. *Int. J. Biochem. Cell Biol.* 2018, 99, 186–196, doi:10.1016/j.biocel.2018.04.013.
- 39 Desgrosellier, J.S.; Cheresh, D.A. Integrins in cancer: Biological implications and therapeutic opportunities. *Nat. Rev. Cancer* 2010, 10, 9–22, doi:10.1038/nrc2748.
- 40 Binmadi, N.; Elsis, A.; Elsis, N. Expression of cell adhesion molecule CD44 in mucoepidermoid carcinoma and its association with the tumor behavior. *Head Face Med.* 2016, 12, 1–5, doi:10.1186/s13005-016-0102-4.
- 41 Chen, J.; Ln, H. A Review of Prognostic Factors in Squamous Cell Carcinoma of the Vulva: Evidence from the Last Decade. *Semin. Diagn. Pathol.* 2020, doi:10.1053/j.semdp.2020.09.009.
- 42 Tummers, W.S.; Kimura, R.H.; Abou-Elkacem, L.; Beinat, C.; Vahrmeijer, A.L.; Swijnenburg, R.-J.; Willmann, J.K.; Gambhir, S.S. Development and Preclinical Validation of a Cysteine Knottin Peptide Targeting Integrin $\alpha\beta6$ for Near-infrared Fluorescent-guided Surgery in Pancreatic Cancer. *Clin. Cancer Res.* 2018, 24, 1667–1676, doi:10.1158/1078-0432.ccr-17-2491.
- 43 Hausner, S.H.; DiCara, D.; Marik, J.; Marshall, J.F.; Sutcliffe, J.L. Use of a peptide derived from foot-and-mouth disease virus for the noninvasive imaging of human Cancer: Generation and evaluation of 4-[18F] fluorobenzoyl A20FMDV2 for *in vivo* imaging of integrin $\alpha\beta6$ expression with positron emission tomography. *Cancer Res.* 2007, 67, 7833–7840, doi:10.1158/0008-5472.can-07-1026.
- 44 De Valk, K.S.; Deken, M.M.; Handgraaf, H.J.M.; Bhairosingh, S.S.; Bijlstra, O.D.; Van Esdonk, M.J.; Van Scheltinga, A.G.T.; Valentijn, A.R.P.; March, T.L.; Vuijk, J.; et al. First-in-Human Assessment of cRGD-ZW800-1, a Zwitterionic, Integrin-Targeted, Near-Infrared Fluorescent Peptide in Colon Carcinoma. *Clin. Cancer Res.* 2020, 26, 3990–3998, doi:10.1158/1078-0432.ccr-19-4156.
- 45 Saleem, A.; Helo, Y.; Win, Z.; Dale, R.; Cook, J.; Searle, G.E.; Wells, P. Integrin $\alpha\beta6$ Positron Emission Tomography Imaging in Lung Cancer Patients Treated With Pulmonary Radiation Therapy. *Int. J. Radiat. Oncol.* 2020, 107, 370–376, doi:10.1016/j.ijrobp.2020.02.014.
- 46 Sachindra, S.; Hellberg, T.; Exner, S.; Prasad, S.; Beindorff, N.; Rogalla, S.; Kimura, R.; Gambhir, S.S.; Wiedenmann, B.; Gröttinger, C. SPECT/CT Imaging, Biodistribution and Radiation Dosimetry of a 177Lu-DOTA-Integrin $\alpha\beta6$ Cystine Knot Peptide in a Pancreatic Cancer Xenograft Model. *Front. Oncol.* 2021, 11, doi:10.3389/fonc.2021.684713.
- 47 Liang, B.; Shahbaz, M.; Wang, Y.; Gao, H.; Fang, R.; Niu, Z.; Liu, S.; Wang, B.; Sun, Q.; Niu, W.; et al. Integrin $\beta6$ -Targeted Immunoliposomes Mediate Tumor-Specific Drug Delivery and Enhance Therapeutic Efficacy in Colon Carcinoma. *Clin. Cancer Res.* 2015, 21, 1183–1195, doi:10.1158/1078-0432.ccr-14-1194.
- 48 Niehues, H.; Bouwstra, J.A.; El Ghalbzouri, A.; Brandner, J.M.; Zeeuwen, P.L.J.M.; Van Den Bogaard, E.H. 3D skin models for 3R research: The potential of 3D reconstructed skin models to study skin barrier function. *Exp. Dermatol.* 2018, 27, 501–511, doi:10.1111/exd.13531.
- 49 Mathes, S.H.; Ruffner, H.; Graf-Hausner, U. The use of skin models in drug development. *Adv. Drug Deliv. Rev.* 2014, 69-70, 81–102, doi:10.1016/j.addr.2013.12.006.

CHAPTER 7

General discussion



As discussed in the introduction of this thesis, patient burden from vulvar (pre)cancers remains high despite evolving care.¹ This burden arises partly due to: I) problems in the diagnostics process, and II) as a result of the treatment regime. The diagnostic process is impeded by incorrect or delayed diagnosis. This is in part a result of the challenges accompanying a physician's visual and tactile assessment of vulvar diseases.² Additionally, invasively obtained biopsy material for pathologic review is limited and sometimes inconclusive. Delays may also occur when patients misconstrue symptoms due to lack of awareness or shame.^{3,4} Patient burden may also arise as a result of the treatment regime, side effects or insufficient impact of treatments.⁵⁻⁷ Luckily, the number of novel instruments has expanded, providing many new possibilities for value-based objective endpoints and biomarkers.⁸

In the present thesis, we have attempted to test several promising innovative instruments in a search for disease-specific biomarkers for vulvar (pre)cancers. A multimodal profiling approach (Figure 2, **Chapter 1**) guided this research, based on systems profiling of disease and drug effects in dermatology.⁹ The different investigated aspects include imaging, cellular and molecular characteristics and was complemented by patient reported outcomes and physician-based input. The focus of this thesis has specifically been on the molecular and imaging domains. It was assessed if the techniques included in these domains show the potential to improve the diagnostic process and/or the evaluation of therapeutic options for vulvar (pre)cancers. Over the longer term, the goal is to improve the burden for patients with vulvar (pre)cancers. This chapter summarizes and discusses the results and highlights perspectives for future research.

As previously discussed, FIGO staging and diagnosis of vulvar (pre)cancers still depends on clinical examination and histopathologic review of invasive biopsy material.¹⁰ In comparison to other more common cancer types, the literature concerning non-invasive imaging for identification and diagnosis of vulvar (pre)cancers is sparse and based mainly on case reports.¹¹⁻¹⁵ Vulvar lesions are easily accessible as they originates from the skin. Therefore, various non-invasive imaging tools were examined in patients with vulvar high grade squamous intraepithelial lesions (vHSIL) and lichen sclerosus, seeking for sensitive disease-specific biomarkers (**Chapter 2 and 3**). Using three different innovative non-invasive techniques, the vulvar skin was assessed at

different skin levels, from superficial up to 2mm in depth. Respectively dermatoscopy¹⁶, optical coherence tomography (OCT)¹⁷ and reflectance confocal microscopy (RCM)¹⁸ were examined. Dermatoscopy uses a lens with a build-in light source to magnify the skin surface in the transversal plane. OCT is comparable to ultrasound but uses laser light instead of sound waves for image acquisition. OCT creates images in the frontal plane, up to a depth of 1mm. RCM uses a diode laser as light source that illuminates the skin and gets reflected differently by various cell types. Reflection of cells is based on their refractive indices; this generates black-and-white images with a resolution almost comparable to conventional histology. RCM enables real time *in vivo* visualization of the epidermis down to the papillary dermis (2mm in depth) in the transversal plane.

It was demonstrated that the application of dermatoscopy, OCT and RCM was feasible and tolerable in vulvar high grade squamous intraepithelial lesion (vHSIL) and lichen sclerosus (LS) patients as well as in healthy controls. Of the three non-invasive innovative imaging tools dermatoscopy was considered the easiest to implement in clinical practice (**Chapter 2**). The execution is straightforward, the assessment time is short and interpretation comes with frequent use. Analysis of a set of dermatoscopic characteristics revealed that warty structures were only observed in vHSIL. In LS, sclerotic areas and arborizing vessels appeared as potential discriminative features. The dermatoscope is also lowest priced compared to the OCT and RCM. The prices of this instrument can be as low as 1.000 United States Dollars (USD), while the newest integrated systems including data capacity, may cost 10.000 USD. Dermatoscopy could ease diagnostics and follow-up and help as a guidance tool for biopsy sampling of suspected vulvar lesions. This technique could for example be of great advantage for imiquimod-treated HSIL patients, as their follow-up requires long-term surveillance of the entire genital tract because of the high probability of late recurrences.¹⁹ This is particularly important to diagnose malignant progression, which is currently a challenge for clinicians. Consequently, patients with other (pre) malignant vulvar diseases as dVIN and vSCC should be included in larger follow-up clinical trials. Several studies have confirmed that the diagnostic accuracy of pigmented lesions and the diagnostics of melanomas, is significantly better with dermatoscopy compared to conventional diagnostics if performed by an experienced user.¹⁶

We showed alignment is possible between some morphological disease features assessed and histopathology, although time-consuming. Primary focus was on the incorporated (automatic) OCT algorithms, measuring epidermal thickness and blood flow. It was concluded that these algorithms should first be adapted for the vulvar skin prior to potential implementation (Chapter 2). Although an OCT blood flow measurement on itself is currently unable to discriminate different vulvar diseases, it might be used as additional biomarker in a multimodal approach. It could hereby aid in the differentiation of healthy and diseased vulvar skin with comprised blood vessels like in inflamed tissue.

RCM images showed that healthy skin was characterized by a homogeneous, normal honeycomb patterned epidermis and a clear epidermal-dermal junction. Vulvar HSIL and LS lesions often displayed an atypical honeycomb pattern of the epidermis, combined with lymphocytic influx and the presence of melanophages. Distinct features specifically observed in LS included the presence of hyalinized vessels and sclerotic areas in the dermis (Chapter 3). Due to the explorative nature of this study and small sample size, no statistics were performed on these characteristics. RCM appears to have potential as optical biopsy tool but requires clinical validation in larger patient groups with long-term follow-up before implementation. Future studies should keep evaluating existing and emerging non-invasive imaging techniques developed for the discrimination of malignant progression of vulvar lesions. Preferably imaging tools are integrated in one device to acquire images at different skin depths.²⁰

Besides the advantage of being easily accessible from the outside, this vulvar cancer type originates from squamous cells, just like cutaneous squamous cell carcinoma (CSCC) does. This allows for knowledge transition between the dermatologic and gynecologic fields. For instance, in CSCC, epidermal homeostasis gets disrupted by interactions between epidermal tumor cells and the underlying stroma, allowing epidermal cells to invade into the stroma²¹. This process for CSCC is being studied in human-skin-equivalents (HSE's). HSE's are *in vitro* cultured skin models designed to mimic the characteristics of human skin as closely as possible. These models are used as tool to study biological processes in healthy and diseased skin.^{22,23} Moreover, HSE's can serve as a prediction model to determine the penetration profile of drugs across the skin.²⁴ As one of the aims of this thesis has been to improve new therapeutic options for vulvar (pre)cancers, HSE models have been developed that mimic healthy and malignant

vulvar skin (Chapter 4). Remnant skin specimen obtained at labial corrections were used to set up HSE models of the vulva. Vulvar keratinocytes were isolated, pre-treated and 'seeded' on a base of fibroblast cells in a petri dish. Comparison of the epidermal morphogenesis of normal vulvar tissue in these models showed great similarities with native healthy vulvar tissue. Immunohistochemical analysis using keratin-10 expression showed a physiological early cell differentiation program in the healthy models. The expression of keratin-17 is known to be absent in healthy epidermis and likewise not detectable in the models, stipulating the inactivated state of the keratinocytes. In conclusion, immunohistochemical results showed similar expression in the healthy HSE models compared to native vulvar tissue.

To allow pathophysiological characteristics to be easier transposed to clinical observations, tumorous HSE models were developed and compared to the healthy HSE models. For the set-up of VSCC models immortalized VSCC cell lines HTB117 and A431 were grown on a dermal scaffold of different fibroblasts. Both papillary- and reticular fibroblasts (RF) were used for dermal scaffolds, as these fibroblast types are generally present in healthy stroma. Also, dermal scaffolds with cancer-associated fibroblasts (CAF's) were generated, as this heterogenous cell is known to be part of the tumor microenvironment (TME) of different SCC's.^{21,25-27} All different tumorous HSE models showed typical SCC progression and revealed the interplay between VSCC cells and tumor stroma within VSCC development. CAF's in the CAF-based models expressed a consistent high level of α -SMA and COL11A1 after interaction with VSCC cells. This indicated that the phenotype of CAF is maintained, which might partially explain the profound invasive behavior observed in these models. A loss of RF markers and a gain of CAF marker expression was observed in the RF based models, indicating the apparent transition of a RF- into CAF phenotype. This shows that communication between VSCC cells and stromal fibroblasts could change a fibroblast's phenotype.²⁷ Recent studies already highlighted the importance of the immune TME involvement for VSCC's.^{28,29}

These models thus aid in gaining pathophysiological knowledge and can also be used for non-clinical drug evaluation. Non-clinical drug testing serves as a basis for the evaluation of potential risks and effectiveness of investigational drugs in humans.³⁰ If the novel vulvar tumor models are qualified and validated, they could offer great potential for research on drug action.³⁰⁻³³ The information obtained can be used to design trials that are

well-informed, addresses the pertinent questions and will most likely require smaller populations. This could alleviate the difficulties recruiting patients for clinical trials due to the low disease-incidence rates. The models could help improve the treatment of vulvar (pre)malignancies as hardly any significant new topical agent after imiquimod has been developed in the last decades for these diseases. Additionally, with the low number of leads on chemotherapeutic and targeted antibody treatments in the vulvar cancer niche, availability of these models could be an enormous step forward in early clinical drug development for vSCC.³⁴ A first step in testing drug response as part of this paradigm was done by adding chemotherapeutic agents carboplatin and paclitaxel to the medium of the vSCC models. A dose-dependent reduction of the relative tumor thickness was observed in the models (**Chapter 4**). Reduction of the epithelial cancer cells was most pronounced in the paclitaxel group. Remarkably, chemotherapeutic treatment did not seem to affect the expression intensity of α -SMA (CAF marker) in the vSCC models. This may corroborate the suggestion that CAF's can REPROGRAM tumor cell metabolism to maintain tumor cell survival and protect them from apoptosis induced by treatment. It further confirms the hypothesis of others reporting on 3D vSCC models created with CAF's and a self-established cell line of vulva cancer associated with lichen sclerosis.³⁵ The fact that CAF's remained *in situ* after chemotherapeutic treatment with carboplatin or paclitaxel is a major learning point, and emphasizes the need for drugs targeting stromal fibroblasts within the TME.

For an improved representation of the diversity of vulvar tumors and their TME, the organotypic 3D models could be personalized with isolated tumor cells of a patient. Research using patient-derived tumor organoid (PDO) models has shown to recapitulate the molecular and phenotypic heterogeneity of the patient tissue they were derived from.³⁶ Recent studies have shown the ability of these PDO's to predict patient drug response. For example, PDO models were used to predict responses for a chemotherapeutic in more than 80% metastatic colorectal cancer patients.³⁷ We suggest that personalized 3D vulvar models prove an attractive and scalable tool for drug screening, as they allow for expansion and biobanking. Having personalized targeted treatment options might greatly improve the flexibility and personalization of vulvar cancer care in clinical practice, as shown for e.g. psoriasis.⁹ Ideally, these personalized vulvar tumor models are used in a multimodal matter. Besides the use for drug evaluation of

existing treatments, the vulvar 3D models might be used for pathway- and drug analyses on somatic mutations for novel specific therapeutic strategies.^{38,39} Also, healthy and tumorous vulvar models can be used for molecular profiling for tumor-specific imaging. The latter includes all techniques used for real-time highlighting of tumors. One type of tumor-specific imaging is applied in the emerging field of fluorescent-guided surgery (FGS). FGS makes use of a contrast agent consisting of an antibody, small synthetic molecule, aptamer or a nanoparticle bound to a fluorescent label able to highlight the tumor. FGS real-time assists the surgeon with the identification of the tumor and the usage of near-infrared light allows for deeper tissue penetration. Ultimately, improved tumor margin detection using FGS could enhance precise surgery and limit morbidity. As this technique could potentially contribute to both improved diagnostics and treatment of vulvar (pre)cancers, it was further investigated in **Chapter 5 and 6** of this thesis.

A first step for implementation of targeted FGS, is the identification of markers that bind specific to vulvar carcinoma cells. A literature review was performed in **Chapter 5**, to identify potential tumor markers that could be used for FGS of differentiated vulvar intraepithelial neoplasia (dVIN), vHSIL and vSCC. A total of 627 articles were found, of which 222 met all eligibility criteria. Twelve vulvar carcinoma-specific tumor targets were identified and from these, 7 were considered most promising: EGFR, CD44V6, GLUT1, MRP1, MUC1, CXCR-4 and VEGF-A. However, most of these papers did not describe expression of these cell membrane located proteins in healthy vulvar tissue. Whilst this aspect is of key importance for the tumor-to-background ratio required to identify the aberrant tissue with FGS. Therefore, the expression of these targets should be tested in both healthy and (pre)malignant vulvar tissues. To investigate if the markers mentioned in literature are indeed candidates for FGS, the presence of these proteins has been examined by immunohistochemistry in healthy and diseased vulvar tissue samples (**Chapter 6**). Besides these literature-based markers, potential targets for FGS in other types of cancer were also included in this analysis. This resulted in the expression analysis of the integrin α v β 6 (α v β 6), CAIX, CD44V6, EGFR, EPCAM, FR α , MRP1, MUC1 and UPAR. The immunohistochemical presence of each marker was quantified using digital image analysis. Results showed that α v β 6 was significantly overexpressed in malignant cells compared to healthy vulvar cells. Tumor to background ratios for

$\alpha\beta6$ in premalignancies dVIN and HSIL were lower compared with vSCC, but still above a set threshold. Higher $\alpha\beta6$ expression was found in HSIL adjacent to HPV-dependent vSCC's compared with isolated HSIL, encouraging more effective removal of adjacent HSIL during vSCC surgery. The potential of $\alpha\beta6$ was also confirmed in a within-patient analyses of each individual tissue slide of a vSCC patient, including both healthy and malignant tissue. CAIX, EPCAM, MRP1 and FR α showed no or low expression in vulvar malignant tissues and were therefore excluded from further evaluation. CD44V6 and EGFR showed an overall high expression in all tissues, including normal squamous epithelium. MUC1 and UPAR were excluded from further evaluation due to their heterogenous or patchy expression pattern in vulvar malignant tissue.

Further validation of $\alpha\beta6$ as a potential target for FGS of vulvar (pre) cancers requires marker expression testing in vulvar animal- or 3D organotypic models. The vulvar models described in **Chapter 4** might be used to test promising targets. To do so, a contrast agent targeted against a promising target could be added to the medium of both healthy and tumorous *in vitro* vulvar models, whereafter expression rates are examined and compared. In this way, intravenous administration of a contrast agents is mimicked *in vitro*. Besides this imitation of intravenous administration, other application routes of contrast agents or drugs can be assessed. The effect of a contrast agent could be tested if incorporated into a cream or spray and applied to the surface of the vulvar skin of the air-liquid based 3D models. Another example: 5-ALA could topically be applied on the surface of the vulvar tumor models as non-targeted photodynamic therapy. This way, the models can help test for resistance to 5-ALA, a problem currently experienced in treatment of vulvar intraepithelial lesions with this drug.⁴⁰ Also targeted imaging can be combined with treatment. This requires conjugation of a tracer to a label compatible for treatment and imaging purposes. For example, with an $\alpha\beta6$ specific knotting peptide conjugated to e.g. FDA approved indocyanine green.^{41,42} This contrast agent might be used for both imaging of the targeted lesion and as treatment; by killing of tumor cells through the production of singlet oxygen species and photothermal heat upon near infrared irradiation.^{43,44} Besides for fluorescent imaging, targeted imaging agents can also be generated with e.g. nuclear- or activatable labels. This enables deployment of valuable targets for many state-of-the-art real time imaging techniques. Illustrated in the brain

tumor imaging niche, proving great progress in dual- or triple-modal imaging.⁴⁵ This multimodal approach makes use of e.g. FGS, MRI, CT, and/or photoacoustic imaging. A cocktail of labels coupled to a tracer targeting the same tumor target is used for this approach. The bundled merits of these techniques, like high spatiotemporal resolution, might overcome the challenges faced during single-modal imaging. Superiority of a multimodal approach in the gynecologic niche is illustrated by non-targeted dual-imaging of sentinel lymph nodes in patients with vSCC. A radioactive and fluorescent tracer (ICG-99mTc-nanocolloid) is used for improved visualization of affected lymph nodes.⁴⁶

In the clinic, molecular vSCC targets could also be used for a pre-treatment PET signal check to predict responses in patients. A clinical study using PD-L1-targeted 89Zr-atezolizumab imaging confirmed that clinical responses in patients with different types of cancer showed increased correlation with pretreatment PET signal compared to IHC or RNA-sequencing based predictive biomarkers.⁴⁷ In addition, the search for potential vSCC targets could be extrapolated to the TME or angiovascular environment of the tumor. Imaging of the TME using nuclear medicine-based targeted molecular imaging allows for sensitive visualization of dynamic changes in the TME.⁴⁸ A nice bridge to the apparently treatment-resistant CAF's observed in the TME of our vulvar tumors in the 3D models (**Chapter 4**). Personalized tumor targeted applications using molecular biomarkers therefore show great potential. Tumor targeting could help dynamic and quantitative visualization, but also play a role in patient stratification and treatment monitoring for targeted therapy.

Overall conclusions

In this thesis, multimodal research into vulvar (pre)cancers was described by focusing on three important cornerstones:

- 1 Application of novel non-invasive imaging instruments on healthy and diseased vulvar skin to improve diagnostics;
- 2 Establishment of *in vitro* healthy and vSCC 3D models aimed for future anticancer drug evaluation studies;
- 3 Investigation of promising targets for tumor-specific molecular real time imaging of vulvar (pre)cancers, to assist complete surgical excision.

First steps are taken into the clinical translation of these novel techniques for the management of patients with vulvar (pre)cancers. Future assessments on accuracy, sensitivity and specificity of these techniques should be performed. For the vulvar HSE models, endpoints should be evaluated for their predictive value on *in vivo* effects and translatability to humans.

REFERENCES

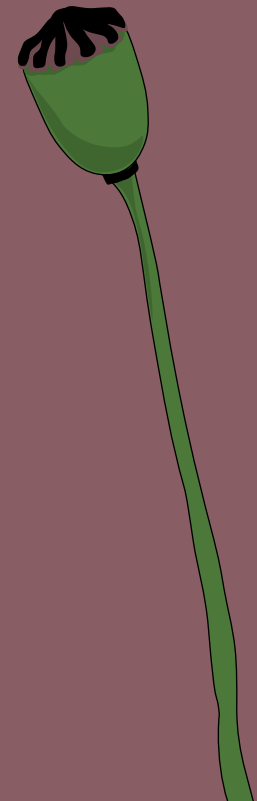
- Gaarenstroom, K. N. *et al.* Postoperative complications after vulvectomy and inguinofemoral lymphadenectomy using separate groin incisions. *Int. J. Gynecol. Cancer* 13, 522–527 (2003).
- Tan, A., Bieber, A. K., Stein, J. A. & Pomeranz, M. K. Diagnosis and management of vulvar cancer: A review. *J. Am. Acad. Dermatol.* 81, 1387–1396 (2019).
- Rüeggsegger, A. B., Senn, B. & Spirig, R. [‘Alone with the taboo’- The social support experienced by women with vulvar neoplasia: a qualitative study]. *Pflege* 31, 199–202 (2018).
- Bell, S. G., Kobernik, E. K., Haefner, H. K. & Welch, K. C. Association Between Vulvar Squamous Intraepithelial Lesions and Psychiatric Illness. *J. Low. Genit. Tract Dis.* 25, 53–56 (2021).
- Mullen, M. M. *et al.* Wound Complication Rates After Vulvar Excisions for Premalignant Lesions. *Obstet. Gynecol.* 133, 658–665 (2019).
- Grimm, D. *et al.* Sexual activity and function after surgical treatment in patients with (pre)invasive vulvar lesions. *Support. Care Cancer* 24, 419–428 (2016).
- Nooij, L. S. *et al.* Risk factors and treatment for recurrent vulvar squamous cell carcinoma. *Critical Reviews in Oncology/Hematology* (2016) doi:10.1016/j.critrevonc.2016.07.007.
- Kruizinga, M. D. *et al.* Development of Novel, Value-Based, Digital Endpoints for Clinical Trials: A Structured Approach Toward Fit-for-Purpose Validation. *Pharmacol. Rev.* 72, 899–909 (2020).
- Rissmann, R., Moerland, M. & van Doorn, M. B. A. Blueprint for mechanistic, data-rich early phase clinical pharmacology studies in dermatology. *Br. J. Clin. Pharmacol.* 86, 1011–1014 (2020).
- Virarkar, M. *et al.* Vulvar Cancer: 2021 Revised FIGO Staging System and the Role of Imaging. *Cancers (Basel)* 14, (2022).
- Cengiz, F. P., Emiroglu, N. & Hofmann Wellenhof, R. Dermoscopic and clinical features of pigmented skin lesions of the genital area. *An. Bras. Dermatol.* 90, 178–183 (2015).
- Kirillin, M., Motovilova, T. & Shakhova, N. Optical coherence tomography in gynecology: a narrative review. *J. Biomed. Opt.* 22, 1 (2017).
- Xu, L. *et al.* Study on the application and imaging characteristics of optical coherence tomography in vulva lesions. *Sci. Rep.* 12, (2022).
- Feng, L. *et al.* Imaging of Vulva Syringoma With Reflectance Confocal Microscopy. *Front. Med.* 8, (2021).
- Cinotti, E. *et al.* Dermoscopic and reflectance confocal microscopy features of two cases of vulvar basal cell carcinoma. *Dermatol. Pract. Concept.* 8, 68–71 (2018).
- Ring, C., Cox, N. & Lee, J. B. Dermatoscopy. *Clin. Dermatol.* 39, 635–642 (2021).
- Katkar, R. A., Tadinada, S. A., Amaechi, B. T. & Fried, D. Optical Coherence Tomography. *Dent. Clin. North Am.* 62, 421–434 (2018).
- Shahriari, N., Grant-Kels, J. M., Rabinovitz, H., Oliviero, M. & Scope, A. Reflectance confocal microscopy: Principles, basic terminology, clinical indications, limitations, and practical considerations. *J. Am. Acad. Dermatol.* 84, 1–14 (2021).
- Green, N., Adedipe, T., Dmytryshyn, J., Preti, M. & Selk, A. Management of Vulvar Cancer Precursors: A Survey of the International Society for the Study of Vulvovaginal Disease. *J. Low. Genit. Tract Dis.* 24, 387–391 (2020).
- Sahu, A. *et al.* Combined Handheld Reflectance Confocal Microscopy- Optical Coherence Tomography Probe for Detection and Depth Assessment of Basal Cell Carcinoma: A Prospective Pilot Study. *JAMA dermatology* 154, 1175 (2018).
- De Wever, O. & Mareel, M. Role of tissue stroma in cancer cell invasion. *J. Pathol.* 200, 429–447 (2003).
- Niehues, H. *et al.* 3D skin models for 3R research: The potential of 3D reconstructed skin models to study skin barrier function. *Experimental Dermatology* vol. 27 501–511 (2018).
- El Ghalbzouri, A., Siamari, R., Willemze, R. & Ponc, M. Leiden reconstructed human epidermal model as a tool for the evaluation of the skin corrosion and irritation potential according to the ECVAM guidelines. *Toxicol. In Vitro* 22, 1311–1320 (2008).
- Mathes, S. H., Ruffner, H. & Graf-Hausner, U. The use of skin models in drug development. *Advanced Drug Delivery Reviews* vols 69–70 81–102 (2014).
- Wu, P. *et al.* Adaptive Mechanisms of Tumor Therapy Resistance Driven by Tumor Microenvironment. *Front. Cell Dev. Biol.* 9, (2021).
- Janson, D., Rietveld, M., Mahé, C., Saintigny, G. & El Ghalbzouri, A. Differential effect of extracellular matrix derived from papillary and reticular fibroblasts on epidermal development in vitro. *Eur. J. Dermatol.* 27, 237–246 (2017).
- Hogervorst M, Rietveld M, de Gruijff F, El Ghalbzouri A. A shift from papillary to reticular fibroblasts enables tumour-stroma interaction and invasion. *Br. J. Cancer* 118, 1089–1097 (2018).
- Abdulrahman, Z., Kortekaas, K. E., De Vos Van Steenwijk, P. J., Van Der Burg, S. H. & Van Poelgeest, M. I. E. The immune microenvironment in vulvar (pre)cancer: review of literature and implications for immunotherapy. *Expert Opin. Biol. Ther.* 18, 1223–1233 (2018).
- Kortekaas, K. E. *et al.* High numbers of activated helper T cells are associated with better clinical outcome in early stage vulvar cancer, irrespective of HPV or P53 status. *J. Immunother. Cancer* 7, (2019).
- Wang, H. *et al.* 3D cell culture models: Drug pharmacokinetics, safety assessment, and regulatory consideration. *Clin. Transl. Sci.* 14, 1659–1680 (2021).
- Rouse, R. *et al.* Translating New Science Into the Drug Review Process: The US FDA’s Division of Applied Regulatory Science. *Ther. Innov. Regul. Sci.* 52, 244 (2018).
- Breslin, S. & O’Driscoll, L. Three-dimensional cell culture: the missing link in drug discovery. *Drug Discov. Today* 18, 240–249 (2013).
- Dame, K. & Ribeiro, A. J. S. Microengineered systems with iPSC-derived cardiac and hepatic cells to evaluate drug adverse effects. *Exp. Biol. Med.* 246, 317 (2021).

-
- 34 Search of: Completed Studies | Vulva Cancer- List Results- ClinicalTrials.gov. https://clinicaltrials.gov/ct2/results?cond=Vulva+Cancer&Search=Apply&recrs=e&age_v=&gndr=&type=&rslt=
 - 35 Dongre, H. *et al.* Establishment of a novel cancer cell line derived from vulvar carcinoma associated with lichen sclerosus exhibiting a fibroblast-dependent tumorigenic potential. *Exp. Cell Res.* 386, 111684 (2020).
 - 36 Tuveson, D. & Clevers, H. Cancer modeling meets human organoid technology. *Science* 364, 952–955 (2019).
 - 37 Ooft, S. N. *et al.* Patient-derived organoids can predict response to chemotherapy in metastatic colorectal cancer patients. *Sci. Transl. Med.* 11, (2019).
 - 38 Zięba, S., Chechlińska, M., Kowalik, A. & Kowalewska, M. Genes, pathways and vulvar carcinoma- New insights from next-generation sequencing studies. *Gynecol. Oncol.* 158, 498–506 (2020).
 - 39 McWhirter, R. E., Marthick, J. R., Boyle, J. A. & Dickinson, J. L. Genetic and epigenetic variation in vulvar cancer: current research and future clinical practice. *Aust. N. Z. J. Obstet. Gynaecol.* 54, 406–411 (2014).
 - 40 Mossakowska, B. J. *et al.* Mechanisms of Resistance to Photodynamic Therapy (PDT) in Vulvar Cancer. *Int. J. Mol. Sci.* 2022, Vol. 23, Page 4117 23, 4117 (2022).
 - 41 Tummers, W. S. *et al.* Development and preclinical validation of a cysteine knottin peptide targeting integrin avb6 for near-infrared fluorescent-guided surgery in pancreatic cancer. *Clin. Cancer Res.* 24, 1667–1676 (2018).
 - 42 van Manen, L. *et al.* A practical guide for the use of indocyanine green and methylene blue in fluorescence-guided abdominal surgery. *J. Surg. Oncol.* 118, 283 (2018).
 - 43 Sevieri, M. *et al.* Indocyanine Green Nanoparticles: Are They Compelling for Cancer Treatment? *Front. Chem.* 8, 535 (2020).
 - 44 Kuo, W. S. *et al.* Gold nanomaterials conjugated with indocyanine green for dual-modality photodynamic and photothermal therapy. *Biomaterials* 33, 3270–3278 (2012).
 - 45 Zhang, L. *et al.* Multifunctional nanotheranostics for near infrared optical imaging-guided treatment of brain tumors. *Adv. Drug Deliv. Rev.* 190, 114536 (2022).
 - 46 Deken, M. M. *et al.* Near-infrared fluorescence imaging compared to standard sentinel lymph node detection with blue dye in patients with vulvar cancer- a randomized controlled trial. *Gynecol. Oncol.* 159, 672–680 (2020).
 - 47 Bensch, F. *et al.* 89Zr-atezolizumab imaging as a non-invasive approach to assess clinical response to PD-L1 blockade in cancer. *Nat. Med.* 24, 1852–1858 (2018).
 - 48 Li, D., Li, X., Zhao, J. & Tan, F. Advances in nuclear medicine-based molecular imaging in head and neck squamous cell carcinoma. *J. Transl. Med.* 2022 201 20, 1–15 (2022).

APPENDICES

CHAPTER 8

Nederlandse samenvatting



De vulva is het uitwendige deel van het vrouwelijke geslachtsorgaan. Hiermee bestaat de vulva uit de schaamlippen, opening van de vagina, de uitgang van de urinebuis en de clitoris. Naast normale variatie van de vulva en de invloed van het biologische ouderdomsproces, kan de vulva ook veranderen door kwaadaardige aandoeningen. Zo kan er schaamlipkanker ontstaan, de officiële term daarvoor is vulvacarcinoom. In dit proefschrift richten alle onderzoeken zich op het vulvacarcinoom en ziekten van de vulva die kunnen leiden tot een vulvacarcinoom (voorstadia).

In 2019 kregen 433 vrouwen de diagnose vulvacarcinoom in Nederland. Wereldwijd is de incidentie ongeveer 2,6 per 100.000 vrouwen. Het is met deze incidentie een vrij zeldzame kankersoort. Desondanks zien we dat het aantal nieuwe vulvacarcinoom patiënten de afgelopen jaren toeneemt. Met name jongere vrouwen krijgen steeds vaker deze ziekte, terwijl dit type kanker voornamelijk voorkomt bij vrouwen ouder dan 60 jaar. Gelukkig is de overlevingskans relatief groot als een vulvacarcinoom op tijd wordt opgemerkt. Wanneer er een verdenking is op een vulvacarcinoom, bijvoorbeeld door een waargenomen verdikking of wondje van de vulva, wordt van de verdachte plek een ‘hapje’ van de huid genomen. Dit weefsel wordt vervolgens onder de microscoop bekeken, om te controleren om wat voor ziekte het precies gaat. Het kan bijvoorbeeld ook om een voorstadium van vulvacarcinoom gaan, die afwijkingen van de huid kunnen er vergelijkbaar uitzien. Bij een voorstadium van vulvacarcinoom zijn er onder de microscoop onrustige of afwijkende cellen te zien. Een voorstadium is nog geen kanker, maar het kan wel kanker worden. Dit kan gebeuren als deze voorstadia te laat ontdekt worden of niet voldoende behandeld zijn. Voor zover bekend, zijn er twee soorten voorstadia die kunnen leiden tot een vulvacarcinoom. Het kleinste deel van de vulvacarcinomen ontstaat uit het voorstadium vulvaire hooggradige squameuze intraepitheliale lesie (VHSIL). VHSIL ontstaat meestal door de aanwezigheid van het humaan papillomavirus (HPV). Vrouwen met VHSIL hebben ongeveer 10% kans om vulvacarcinoom te ontwikkelen als ze geen behandeling krijgen. Het tweede voorstadium heet gedifferentieerde vulvaire intraepitheliale neoplasie (DVIN). In ongeveer 30% van de gevallen leidt DVIN tot vulvacarcinoom. De oorzaak van het ontstaan van DVIN is onbekend. Het is wel bekend dat dit voorstadium kan ontstaan bij vrouwen die al jaren last hebben van lichen sclerosus (LS). LS is een goedaardige inflammatoire aandoening, waarbij de huid van de schaamlippen wit kan verkleuren en waardoor de schaamlippen soms zelfs

verdwijnen. De bovengenoemde patiënten kunnen klachten ervaren van de vulva, waaronder: jeuk, pijn of een branderig gevoel.

De eerste keuze behandeling voor vulvacarcinoom is het chirurgisch verwijderen van de aandoening. Deze operatie wordt eventueel gevolgd door chemotherapie of radiotherapie, afhankelijk van de ernst van het vulvacarcinoom. Het voorstadium HSIL kan behandeld worden met lasertherapie of met een zalf (imiquimod), terwijl het voorstadium DVIN meestal ook chirurgisch verwijderd wordt. LS is een chronische huidaandoening van de vulva en gaat niet meer weg. LS wordt wel behandeld met hormoonzalf, om klachten te verminderen en het risico op progressie naar DVIN of vulvacarcinoom te verkleinen.

Helaas herkennen zowel patiënten als medisch specialisten deze aandoeningen van de vulva niet altijd direct. Hierdoor zit vertraging tussen het ontstaan van een (voorstadium) vulvacarcinoom en het herkennen van de ziekte. Verder komen (voorstadium) vulvacarcinomen nog te vaak terug na het wegsnijden, doordat niet alle kwaadaardige cellen zijn opgemerkt en verwijderd. Dit zorgt hierdoor voor een grote ziektelast bij de patiënten. Bovendien blijkt het nog steeds een taboe om deze klachten bespreekbaar te maken.

De studies beschreven in dit proefschrift zijn opgezet om (voorstadium) vulvacarcinoom beter te leren herkennen en onderzoek naar nieuwe behandelingen te bevorderen. Er is gebruik gemaakt van een multimodale aanpak om de vulva vanuit verschillende domeinen te karakteriseren. De domeinen bestudeerd zijn: door de patiënt gerapporteerde uitkomsten (bv. vulvaire pijn en jeuk), door een arts gerapporteerde klinische scores, beeldvorming (bv. dermatoscopie), cel eigenschappen (bv. analyse onder de microscoop) en moleculaire analyses (bv. immuunhistochemie). In dit proefschrift lag de nadruk specifiek op de moleculaire en beeldvormende domeinen. Met deze veelzijdige aanpak zijn we in staat diverse vulvaire biomarkers per groep gezonde vrouwen of patiënten te onderzoeken. Een goede biomarker zou idealiter aan de volgende criteria voldoen: onderscheidend zijn voor gezonde en aangedane huid, stabiel gemeten kunnen worden over tijd, een behandelingseffect registreren en de techniek waarmee de biomarker wordt verkregen moet goed getolereerd worden door vrouwen.

Op basis van de verschillende beoordeelde innovatieve technieken werd dit proefschrift opgedeeld in drie delen:

- **DEEL I** gaat in op de toepassing van innovatieve beeldvormingstechnieken op gezonde en zieke huid van de vulva, opzoek naar biomarkers om diagnostiek en behandeling te verbeteren (**hoofdstuk 2+3**);
- **DEEL II** schetst de ontwikkeling van gezonde vulva- en vulvacarcinoom 3D huidmodellen, voor onderzoek naar (nieuwe) behandelingen van vulvacarcinoom (**hoofdstuk 4**);
- **DEEL III** beschrijft de zoektocht naar potentiële targets voor tumor specifieke beeldvorming van vulvacarcinoom (**hoofdstuk 5+6**).

DEEL EEN: TOEPASSING VAN INNOVATIEVE BEELD-VORMINGSTECHNIEKEN OP GEZONDE EN ZIEKE HUID VAN DE VULVA

In een klinische studie zijn nieuwe innovatieve beeldvormingstechnieken toegepast op gezonde en aangedane huid van de vulva. De toegepaste beeldvormingstechnieken heten: dermatoscopie, optische coherentie tomografie (OCT) en de confocale laser microscopie. We onderzochten hiervoor de huid van vulva's van 10 gezonde vrouwen, 5 vrouwen met VHSIL en 10 vrouwen met LS. We hoopten ook patiënten met vulvacarcinoom mee te laten doen aan deze studie, maar deze groep patiënten bleek lastig te rekruteren. Deelnemers kwamen op dag één van de studie voor drie rondes met huidmetingen. Ter controle werden er biopten (hapje weefsel) van de vulva afgenomen aan het einde van dag 1. Het bioptweefsel geldt als 'gouden standaard' om de diagnose te stellen. Dit gebeurde door een gespecialiseerde patholoog het biopt onder de microscoop te laten beoordelen. Na deze studieperiode startte alleen de groep met LS-patiënten op dag 8 met een standaard toegepaste behandeling met hormoonzalf voor 4 weken. Zij kwamen voor aanvullende huidmetingen op dag 21 en 36 terug. Verder werden er op de laatste studiedag (dag 36) bij de LS-patiënten extra biopten afgenomen, als referentie na de behandelperiode. Alle huidmetingen werden bij VHSIL en LS uitgevoerd op lesionale en niet-lesionale vulvaire huid. Bij de gezonde vrouwen werd enkel gezonde huid gemeten.

De data van deze klinische studie is beschreven in **hoofdstuk 2 en 3** van dit proefschrift.

In **hoofdstuk 2** twee staat de toepassing van dermatoscopie en OCT op de vulva beschreven bij VHSIL- en LS-patiënten en bij gezonde vrouwen. De dermatoscoop is een vergrootglas voor de huid, voorzien van een lichtbron.

Hierdoor kun je dieper in de oppervlakte van de huid kijken en zie je structuren die je met het blote oog niet kan zien. Uit de analyse van een reeks dermatoscopische opnames bleek dat wratachtige structuren alleen werden waargenomen bij VHSIL. Bij LS bleken sclerotische gebieden en arboriserende vaten potentiële discriminerende kenmerken. De dermatoscoop was gemakkelijk in gebruik, de uitvoer duurde 1-2 minuten per patiënt en het apparaat werd goed verdragen door de vrouwen in de studie. Verder werd de OCT toegepast op de huid van de vulva. Bij deze methode reflecteren huidcellen op een bepaalde manier het licht waarmee ze worden aangestraald, waarbij beelden (dwarsdoorsnedes) worden gevormd. De methode is te vergelijken met echografie, waarbij geluid wordt gebruikt in plaats van licht. Structurele OCT-beelden konden voor VHSIL en LS worden afgestemd op de histologie voor kenmerken als hyperkeratose en dermale-epidermale junctie. Een nieuwe bevinding in deze studie was de verhoogde bloedstroom, gemeten door het ingebouwde algoritme van de OCT, in LS-patiënten (gemiddeld \pm SD 0,053 \pm 0,029) in vergelijking met gezonde controles (0,040 \pm 0,012, $p=0,0024$). Daarnaast lieten de resultaten zien dat het ingebouwde OCT-algoritme voor epidermale diktebepaling momenteel nog niet bruikbaar is op de huid van de vulva.

In **hoofdstuk 3** wordt de toepassing van de beeldvormingstechniek 'confocale laser microscopie' beschreven op de vulvaire huid. De confocale laser microscoop bestaat uit een computerscherm die verbonden is aan een draaibare arm waar de laser aanhangt om de opnames van de huid te maken. Deze opnames zijn gebaseerd op het laserlicht dat door diverse celltypen verschillend terug reflecteert en weer opgevangen wordt door het systeem. Het systeem zet deze reflectie vervolgens om in een zwart-wit beeld van de cellen. Je kunt met deze techniek dus 'door de huid' heen kijken, zonder de huid te beschadigen. Het is nog niet eerder beschreven in de literatuur dat deze techniek bij zoveel vrouwen op de vulvaire huid is getest. Dat maakte dit onderzoek uniek. Een groot deel van het manuscript wat verslag legt over deze techniek is daarom gewijd aan uitleg over de toepassing op de vulva, voorzien van illustraties. Bij het bekijken van de opnames werd de gezonde huid gekenmerkt door een homogene, normale epidermis met honingraatpatroon en duidelijke epidermale-dermale juncties. VHSIL en LS laesies vertoonden vaak een atypisch honingraatpatroon van de epidermis en lymfocyttaire influx met aanwezigheid van melanofagen

(immuuncellen). Specifieke kenmerken van LS waren de aanwezigheid van gehyaliniseerde vaten en sclerotische gebieden in de dermis. Vanwege de exploratieve aard van deze studie en de kleine hoeveelheid onderzochte vrouwen, werd er geen statistiek uitgevoerd op deze resultaten. Wij vroegen de vrouwen achteraf hoe zij de toepassing van het apparaat hadden ervaren. Bijna alle vrouwen hadden geen last van het apparaat, wel vonden sommige vrouwen de opname lang duren. Validatie van deze resultaten op grote schaal zou van reflectie confocale microscopie een klinisch hulpmiddel kunnen maken om vulvaire afwijkingen op niet-invasieve wijze te identificeren.

DEEL TWEE: DE ONTWIKKELING VAN GEZONDE VULVA- EN VULVACARCINOOM 3D HUIDMODELLEN

Om meer te weten te komen over vulvacarcinomen en nieuwe behandelingen te ontwikkelen voor dit type kanker, is het belangrijk dat we ‘levende’ vulvacarcinomen na kunnen bootsen. Hiervoor zijn zogenaamde modellen nodig van het vulvacarcinoom. Deze modellen zijn belangrijk om de stap kleiner te maken tussen het testen van nieuwe chemische stoffen op dood weefsel in het laboratorium en de daadwerkelijke toediening aan patiënten. Deze chemische stoffen kunnen bijvoorbeeld nieuwe medicijnen zijn of een nieuw antilichaam gekoppeld aan een fluorescente stof voor toepassing van beeldgeleide chirurgie (zoals beschreven in **hoofdstuk 5+6**). Daarnaast kunnen dit soort modellen de onderzoeker meer inzicht geven in nog niet bekende eigenschappen van een vulvacarcinoom. Vaak worden dieren gebruikt voor als basis voor deze modellen. Echter, voor het vulvacarcinoom is het opstellen van een representatief diermodel lastig gebleken. Dit komt met name doordat de vulva een relatief klein en delicaat gebied is en de vulva van een dier niet altijd overeenkomt met de menselijke vulva. Daarnaast zijn diermodellen in het algemeen prijzig, tijdsintensief en is de data niet altijd goed te ‘vertalen’ naar de menselijke situatie. Wij gingen daarom een samenwerking aan met een groep onderzoekers uit het LUMC, die ervaring hebben met het opkweken van ‘levende’ 3D-huidmodellen in een petrischaal. In onze studie onderzochten wij of we deze 3D-huidmodellen ook kunnen opzetten met gezonde vulvaire huid en met vulvacarcinoomcellen. Deze modellen behandelden we met

verschillende concentraties van chemotherapie, om te zien of we de tumor kunnen behandelen in de petrischaal.

Voor het opzetten van gezonde huidmodellen van de vulva, zoals beschreven in **hoofdstuk 4**, was huid van de schaamlippen nodig. Dit weefsel werd verkregen als restant van schaamlipcorrecties. De levende cellen van deze stukjes schaamlip werden voorbereid en ‘gezaaid’ op een bodem van fibroblast cellen in een petrischaal. Fibroblasten zijn normaal ook aanwezig onder de bovenste laag van de huid (bindweefsel) en zorgen voor stevigheid. Door al deze cellen te voeden met vloeibare voeding (medium), was het mogelijk ze op te kweken tot 3D huidmodellen. Karakteristieken van de huidmodellen van de schaamlippen werden vergeleken met normale huid van de schaamlippen. Deze karakteristieken werden getest op eiwit niveau met immunohistochemie en op RNA-niveau met PCR testen. Er waren veel overeenkomsten zichtbaar tussen echte en model-huid van de vulva. Naast gezonde huidmodellen van de vulva, wilden wij ook vulvacarcinoom modellen opzetten. Hiervoor maakten wij gebruik van vulvacarcinoom cellijnen. Deze cellijnen zijn afkomstig van verschillende vulvacarcinomen patiënten, waarbij de cellen onsterfelijk zijn gemaakt. Dit vergemakkelijkt langdurig onderzoek, wat vereist is voor het meerdaags kweken in een petrischaal. Daarnaast lieten de vulvacarcinoom modellen veel overeenkomsten zien met echte vulvacarcinomen. Bovendien is een start gemaakt met het behandelen van de vulvacarcinomen opgekweekt in een petrischaal. Het toevoegen van medicijnen in het medium van de huidmodellen zou overeenkomsten moeten vertonen met toediening van medicijnen via een infuus in de bloedbaan. Hiervoor werd gekozen te starten met chemotherapie, namelijk met carboplatin en paclitaxel. Lage en hoge concentraties van deze chemotherapie werden toegevoegd in het medium waarin de vulvacarcinomen groeiden. Bij de vulvacarcinomen die behandeld waren met een lage concentratie chemotherapeuticum zagen we dat de kankercellen werden afgebroken en alle nog normale cellen bleven leven. Bij hoge concentraties chemotherapeuticum zagen we dat alle cellen doodgingen, ook de goede cellen die de bodem van het huidmodel vormden. Deze resultaten tonen de potentie aan van in vitro 3D vulva modellen als instrumenten voor verder onderzoek naar bijvoorbeeld pathofysiologie en geneesmiddelenontwikkeling op dit gebied.

DEEL DRIE: DE ZOEKTOCHT NAAR POTENTIËLE TARGETS VOOR TUMOR SPECIFIEKE BEELDVORMING VAN VULVACARCINOOM

Beeldgeleide chirurgie is een techniek die gebruikt kan worden om anatomische structuren tijdens een operatie op te laten lichten. Het kan hierbij zowel gaan om structuren die behouden moeten blijven als structuren die je beter wilt onderscheiden, omdat ze in het geheel verwijderd moeten worden. In deze laatste categorie valt ons onderzoek. Momenteel bepaalt de gynaecoloog tijdens de operatie tot waar de kankercellen reiken, door het verdachte weefsel goed te bekijken en eraan te voelen. Deze beoordeling is subjectief en variabel. Met toepassing van beeldgeleide chirurgie hopen wij in de toekomst te voorkomen dat een vulvacarcinoom incompleet wordt verwijderd tijdens een operatie. Wij richten ons hiervoor op het zoeken naar markers die specifiek op vulvacarcinoom cellen voorkomen en niet of minder op gezonde cellen van de vulva. Wij kunnen vervolgens een tracer gebruiken die aan deze marker bindt, waaraan een label gekoppeld is. Deze combinatie van tracer en label heet een probe en kan worden opgebouwd uit verschillende onderdelen. Wij focussen op het gebruik van een probe met een antilichaam gekoppeld aan een fluorescent label. Vervolgens kan het verdachte gebied worden aangestraald met een lichtbron en bekeken via een speciaal camerasysteem dat fluorescent licht kan detecteren. Op deze manier licht het vulvacarcinoom op ten opzichte van de naastgelegen weefsels. Dit kan live worden toegepast op de operatiekamer, zonder het operatieveld te beïnvloeden.

Voor de toepassing van deze techniek is het heel belangrijk een tumor-specifieke marker te vinden. Hierbij is het belangrijk dat de marker talrijk aanwezig is op tumorcellen en in veel mindere mate op gezonde cellen van de vulva. Deze zoektocht naar tumor-specifieke markers is beschreven in het laatste gedeelte van dit proefschrift.

In **hoofdstuk 5** hebben we alle bestaande literatuur doorzocht om potentiële tumormarkers te identificeren, die we kunnen gebruiken voor beeldgeleide chirurgie van vulvacarcinomen. In totaal werden 627 artikelen doorgenomen, waarvan 222 artikelen voldeden aan alle toelatingscriteria. Twaalf vulvacarcinoom-specifieke tumormarkers werden geïdentificeerd en van deze werden 7 als meest veelbelovend beschouwd, namelijk: EGFR, CD44V6, GLUT1, MRP1, MUC1, CXCR-4 en VEGF-A. De meeste van deze

artikelen onderzochten de aanwezigheid van de marker in (voorstadium) vulvacarcinoom weefsel en niet in gezond vulva weefsel. Om te onderzoeken of deze markers geschikt zijn voor beeldgeleide chirurgie, zal de aanwezigheid van deze markers dus opnieuw onderzocht moeten worden, waarbij ook gezond weefsel als controle wordt meegenomen.

In **hoofdstuk 6** wordt de expressie van verschillende markers getest in weefsel van voorstadia HSIL en DVIN en vulvacarcinoom patiënten en in weefsel van gezonde vulva's (weefsel verkregen van correctie van schaamlippen). Markers werden geselecteerd op basis van de resultaten van het literatuuronderzoek uit hoofdstuk 1 en ervaringen met markers binnen soortgelijk onderzoek bij andere kankersoorten. Uiteindelijk werden de markers avb6, CAIX, CD44V6, EGFR, EPCAM, FRa, MRP1, MUC1 en UPAR getest. De techniek die hiervoor gebruikt wordt heet 'immunohistochemie'. Hiermee kan je op een dun plakje weefsel, specifiek een marker testen op aan- of afwezigheid. De aanwezigheid van elke marker werd gekwantificeerd met behulp van digitale beeldanalyse. Uit de analyse van deze resultaten bleek dat avb6 overmatig aanwezig was in kwaadaardige cellen t.o.v. gezonde vulva cellen. Hiermee maakt avb6 de meest robuuste discriminatie mogelijk van vulvacarcinomen grenzend aan gezond weefsel. In de toekomst moet dit onderzoek op grotere schaal herhaald worden om deze gegevens te valideren. Een vervolgstap is vervolgens om de aan- afwezigheid van de marker te testen in dier- of huidmodellen waar het vulvacarcinoom wordt nagebootst met levende cellen. Daarna kan gekeken worden of toepassing van beeldgeleide chirurgie voor vulvacarcinoom in de patiënt bijdraagt aan verbeterde behandeling.

PERSPECTIEVEN

Ontwikkeling van medicijnen met behulp van vulvacarcinoom 3D huidmodellen

Geneesmiddelenonderzoek in het laboratorium of in dieren, dient als basis voor de evaluatie van potentiële risico's en effectiviteit van nieuwe geneesmiddelen bij mensen. Omdat de vereiste laboratorium modellen voor medicijntesten voor vulvacarcinoom ontbreken, hebben wij 3D huidmodellen ontwikkeld met menselijke gezonde en tumorcellen van de vulva (hoofdstuk 4). Deze nieuwe modellen moeten nu verder worden gekwalificeerd en gevalideerd. Hierna bieden ze de mogelijkheid om de processen in het lichaam waaraan een nieuw geneesmiddel wordt onderworpen

(farmacokinetiek) na te bootsen voor onderzoek. Voor een betere weergave van de diversiteit van tumoren kunnen de 3D-modellen worden gepersonaliseerd met geïsoleerde tumorcellen van een patiënt. Recente studies hebben aangetoond dat deze gepersonaliseerde modellen de geneesmiddelenrespons van patiënten kunnen voorspellen. Idealiter wordt in de toekomst een klein stukje vulvacarcinoom verwijderd en voor meerdere doeleinden gebruikt. Een deel van de cellen kan gebruikt worden om de gepersonaliseerde 3D-modellen te maken, terwijl een ander deel wordt gebruikt om tumor specifieke biologische kenmerken te onderzoeken. Met deze kennis kan een tumor specifieke probe ontwikkeld worden voor fluorescentie geleide chirurgie (**hoofdstuk 5+6**). Een andere mogelijkheid is screening van het afgenomen weefsel op DNA-niveau, om nieuwe specifieke therapeutische strategieën te ontwikkelen. Ten slotte kan het resterende weefsel helpen bij het identificeren van het infiltratiepatroon van immuuncellen in de tumor voor immunotherapeutische strategieën.

Naast het gebruik van vSCC 3D-modellen voor de ontwikkeling van geneesmiddelen, leren ze ons ook veel over de fysiologisch relevante cellulaire micro-omgeving van de tumor. Als voorbeeld hiervan hebben wij door de modellen het belang gezien van contact tussen tumorcellen van de buitenste huidlaag en de onderliggende lederhuid (hoofdstuk 4). Communicatie tussen deze cellen zou het fenotype van gezonde lederhuid cellen kunnen veranderen naar kanker geassocieerde cellen. Dit is belangrijke informatie, omdat we zagen dat chemotherapie deze kanker geassocieerde cellen niet kon doodmaken. Dit wijst op de noodzaak voor geneesmiddelen die gericht zijn op deze kanker geassocieerde cellen in combinatie met de primaire tumorcellen.

Klinische perspectieven voor niet-invasieve beeldvormingstechnieken

De diagnose vulvacarcinoom is nog steeds afhankelijk van klinische inspectie en histopathologisch onderzoek van biopsiemateriaal. Daarom onderzochten wij nieuwe non-invasieve beeldvormingstechnieken die diagnostiek en management van (voorstadia) vulvacarcinoom kunnen optimaliseren. Wij achten van de drie niet-invasieve beeldvormingstechnieken de dermatoscopie het gemakkelijkst implementeerbaar in de klinische praktijk. Dermatoscopie zou de diagnostiek en follow-up kunnen vereenvoudigen en helpen als hulpmiddel bij het nemen van biopten van verdachte vulvaire laesies. Dit zou bijvoorbeeld van groot voordeel kunnen zijn

voor HSIL-patiënten, aangezien voor hun follow-up langdurige bewaking van het gehele genitale gebied nodig is, gezien de mogelijkheid op terugkeer van de ziekte. Om dermatoscopie vSHIL en lichen sclerosus te valideren, moeten patiënten met andere vulvaire aandoeningen als DVIN en vulvacarcinoom worden opgenomen in vervolgstudies. Alleen op deze manier kan de potentie van de dermatoscoop worden onderzocht om de ontwikkeling van gezond naar tumorweefsel te discrimineren. Er zou vervolgens een software algoritme voor de dermatoscoop kunnen worden ontwikkeld, om deze progressie naar tumorweefsel automatisch te kunnen detecteren.

Daarnaast concludeerden wij in dit proefschrift dat confocale laser microscopie een veelbelovende, goed verdragen beeldvormingstechniek is voor diepgaande weefselanalyse van vulvaire (pre)kanker. Wij waren echter de eersten die met dit apparaat systematisch weefselkenmerken analyseerden voor deze aandoeningen. Er is daarom meer klinisch onderzoek nodig met dit apparaat, in grotere patiëntengroepen en met langdurige follow-up, voordat het kan worden toegepast in de kliniek. Toekomstige studies moeten andere veelbelovende niet-invasieve technieken blijven evalueren die zijn ontwikkeld voor de discriminatie van weefsel. Bijvoorbeeld technieken als Multiphoton Tomografie (nabij-infrarood licht voor multiphotonabsorptie) of Raman Spectroscopie (licht valt op moleculen en geeft interactie). De snelle vooruitgang op het gebied van niet-invasieve huidbeeldvorming geeft aan dat weefsevaluatie in de nabije toekomst minder afhankelijk kan worden enkel klinische inspectie en histopathologisch onderzoek.

Toekomst voor tumor-specifieke beeldvorming van het vulvacarcinoom

Momenteel worden MRI en PET/CT gebruikt om tumoruitbreiding naar dieper gelegen weefsels en lymfeklierbetrokkenheid in beeld te brengen. Helaas hebben deze traditionele beeldvormingsmethoden een aantal nadelen die moeten worden opgelost. Een van die nadelen is dat ze geen live beeld geven aan de medisch specialist. Dit is wel het geval bij tumor specifieke beeldvorming, zoals beschreven in **hoofdstuk 5+6**. In deze hoofdstukken lag de nadruk op selectie van tumor-specifieke markers voor fluorescentiegeleide beeldvorming met nabij-infrarode fluorescerende labels. Terwijl een tumor specifieke tracer ook gekoppeld kan worden aan een nucleair of activeerbaar label. Dit maakt brede inzet van veelbelovende tumor-specifieke targets voor allerlei beeldvormingstechnieken mogelijk. Ter illustratie: in de niche van de beeldvorming van hersentumoren is

grote vooruitgang geboekt op het gebied van duo- of drievoudige beeldvorming. Hiervoor wordt een cocktail van labels aan dezelfde tracer gekoppeld en kan de tumor met verschillende technieken, zoals MRI, CT en fluorescente beeldvorming, in beeld gebracht worden. De gebundelde voordelen van deze technieken, zouden de uitdagingen van de beeldvorming met een enkele techniek kunnen overwinnen.

CONCLUSIES

In dit proefschrift werd divers onderzoek naar (voorstadium) vulvacarcinoom beschreven, onderverdeeld in drie delen:

- I Toepassing van nieuwe niet-invasieve beeldvormingstechnieken op gezonde en zieke huid van de vulva, om de diagnostiek te verbeteren;
- II Succesvol opzetten van gezonde en vulvacarcinoom 3D modellen, om medicijnonderzoek in de toekomst te vergemakkelijken;
- III Ontdekking van een potentiële marker op (voorstadium) vulvacarcinoom cellen, als target voor live tumor specifieke beeldvorming voor completere chirurgische verwijdering.

De resultaten van dit proefschrift toonden aan dat deze technieken veelbelovend zijn om (voorstadium) vulvacarcinoom beter in beeld te brengen en te behandelen. De eerste stappen zijn gezet in de klinische vertaling van deze nieuwe technieken voor de behandeling van deze patiënten.

CURRICULUM VITAE

Bertha Woutrina (Bertine) Huisman was born on the 13th of May 1992 in Ermelo, the Netherlands. After graduating at the Guido de Brès secondary school in Amersfoort in 2010, she started with Biomedical Sciences at Science Park of the AMC in September of the same year. She went 5 months abroad to Salt Lake City (Utah, USA) for her minor and successfully completed different anatomical courses. During this minor she applied for 'de zij-instroom' of the Medical School at Leiden University and was allowed to start this track in 2013, after completion of her Bachelor of Sciences. As she ideally wanted to end up with a career that bridged the clinics and research, she started the Master Biomedical Sciences at the Leiden University in 2014. For these masters she worked on two graduation projects titled 'Unravelling the role of placental thrombomodulin downregulation in the pathogenesis of pre-eclampsia' and 'Near-infrared fluorescence imaging in frozen-thawed cortical ovarian tissue to exclude breast cancer metastases'. In April 2018 she graduated the Master of Biomedical Sciences and in June 2018 she became a Medical Doctor. Bertine started her professional carrier as PhD student and research physician at the gynaecology group of the Centre for Human Drug Research and the Leiden University Medical Centre. Under supervision of M. van Poelgeest, C. Sier, prof. R. Rissmann and prof. J. Burggraaf she worked on her thesis. As part of her research training, she was educated as a clinical pharmacologist. In the summer of 2022, she married Albert de Glint with whom she happily lives together in Roelofarendsveen. By the end of that year she started a residency at the gynecology & obstetrics department of the IJsselland Ziekenhuis.

PUBLICATION LIST

B.W. Huisman*, L. Pagan*, R.G.C. Naafs, W. ten Voorde, R. Rissmann, J.M.J. Piek, J. Damman, M.J. Juachon, M. Osse, T. Niemeyer-van der Kolk, C.L.M. van Hees, M.I.E. van Poelgeest. Dermatoscopy and optical coherence tomography in vulvar HSIL and lichen sclerosis: results of a prospective observational trial. *J of Lower Genital Tract Disease* Jan 2023. doi: 10.1097/JGT.0000000000000731

B.W. Huisman, L. Pagan, M. Ulrich, R. Rissmann, J. Damman, J.M.J. Piek, T. Niemeyer-van der Kolk and M.I.E. van Poelgeest. Reflectance confocal microscopy as a non-invasive imaging tool in vulvar high grade squamous intraepithelial lesions and lichen sclerosis: a descriptive morphological study in patients and healthy volunteers. Submitted to *BJOG* in September 2022. Submitted to *Experimental Dermatology* in December 2022

B.W. Huisman*, S. Wu*, M.H. Rietveld, R. Rissmann, M.H. Vermeer, M.I.E. van Poelgeest, A. El Ghalbzouri. Development of healthy and tumorous vulvar organotypic 3D models as a novel tool to study tumour-stroma interaction and drug efficacy. Submitted to *Cancers* in January 2023.

Huisman BW, Burggraaf J, Vahrmeijer AL, Schoones JW, Rissmann RA, Sier CFM, van Poelgeest MIE. Potential targets for tumor-specific imaging of vulvar squamous cell carcinoma: A systematic review of candidate biomarkers. *Gynecol Oncol*. 2020 Mar;156(3):734-743.

Huisman BW, Cankat M, Bosse T, Vahrmeijer AL, Rissmann R, Burggraaf J, Sier CFM, van Poelgeest MIE. Integrin $\alpha v \beta 6$ as a Target for Tumor-Specific Imaging of Vulvar Squamous Cell Carcinoma and Adjacent Premalignant Lesions. *Cancers (Basel)*. 2021 Nov 29;13(23):6006.

Huisman BW, Nené LEH, Linders FLL, Gambrah TK, van der Kolk TN, de Kam ML, Bavinck JNB, Burggraaf J, Feiss G, Rissmann R. No effect of topical digoxin and furosemide for patients with actinic keratosis. *J Eur Acad Dermatol Venereol*. 2023 Feb;37(2):e172-e174.

W. de Laat, L. Pagan, R.K. Malcolm, M. Wiegerinck, V. Nickolson, **B.W. Huisman**, R. Stuurman, M. van Esdonk, N. Klarenbeek. First-in-human study to assess the pharmacokinetics, tolerability and safety of single-dose oxybutynin hydrochloride administered via a microprocessor-controlled intravaginal ring. *Drug Delivery*. 2023 Jan. doi:10.1080/10717544.2023.2180113

Grievink HW, Smit V, **Huisman BW**, Gal P, Yavuz Y, Klerks C, Binder CJ, Bot I, Kuiper J, Foks AC, Moerland M. Cardiovascular risk factors: The effects of ageing and smoking on the immune system, an observational clinical study. *Front Immunol*. 2022 Sep 15;13:968815.

In 't Veld AE, Jansen MAA, **Huisman BW**, Schoonakker M, de Kam ML, Moes DJAR, van Poelgeest MIE, Burggraaf J, Moerland M. Monitoring of Ex Vivo Cyclosporin A Activity in Healthy Volunteers Using T Cell Function Assays in Relation to Whole Blood and Cellular Pharmacokinetics. *Pharmaceutics*. 2022 Sep 16;14(9):1958.

Pagan L, Ederveen RAM, **Huisman BW**, Schoones JW, Zwittink RD, Schuren FHJ, Rissmann R, Piek MJM, van Poelgeest MIE. The Human Vulvar Microbiome: A Systematic Review. *Microorganisms*. 2021 Dec 12;9(12):2568.

Peters IT, van der Steen MA, **Huisman BW**, Hilders CG, Smit VT, Vahrmeijer AL, Sier CF, Trimbos JB, Kuppen PJ. Morphological and phenotypical features of ovarian metastases in breast cancer patients. *BMC Cancer*. 2017 Mar 21;17(1):206.

**Both authors contributed equally*

